

**Recombinant Antibody Fusion Proteins for Depletion of Autoreactive B  
Lymphocytes**

**Dissertation**

der Fakultät für Biologie  
der Eberhard-Karls-Universität Tübingen

zur Erlangung des Grades eines Doktors  
der Naturwissenschaften

vorgelegt von

S. Marcel Zocher

aus Korbach

2002

Tag der mündlichen Prüfung: 30.09.2002

Dekan: Prof. Dr. Hans-Ulrich Schnitzler

1. Berichterstatter: Prof. Dr. Patrick A. Baeuerle

2. Berichterstatter: Prof. Dr. Hans-Georg Rammensee

# ***Table of Contents***

<b>1. Index</b>	<b>4</b>
<b>2. Introduction</b>	<b>12</b>
2.1. Autoimmune diseases	12
2.2. Humoral autoimmunity	12
2.3. An example of a complex autoimmune disease: Multiple sclerosis	15
2.4. Experimental autoimmune encephalomyelitis (EAE), a model for MS	16
2.5. Myelin oligodendrocyte glycoprotein (MOG) as a model auto-antigen	18
2.6. Antibody-based therapeutic approaches	20
2.7. Objectives	22
<b>3. Summary</b>	<b>27</b>
<b>4. Material and Methods</b>	<b>28</b>
4.1. Molecular biology	28
4.1.1. Isolation of RNA from MOG-transfected fibroblasts	28
4.1.2. Reverse transcription	28

4.1.3. Amplification of MOG-coding cDNA fragments _____	29
4.1.4. Polymerase chain reaction (PCR) _____	29
4.1.5. Construction of MOGxCD3 encoding expression vector _____	29
4.1.6. Construction of MOG-Fc encoding expression vector _____	30
4.1.7. Isolation of RNA from HD69-transfected CHO cells _____	30
4.1.8. Reverse transcription _____	30
4.1.9. Amplification of IgG1-coding cDNA fragments _____	31
4.1.10. Polymerase chain reaction (PCR) _____	31
4.1.11. PCR product purification _____	31
4.1.12. Ligation of PCR products into pCR-Script Amp vector _____	31
4.1.13. Transformation _____	31
4.1.14. Preparation of plasmid DNA/ MiniPreps _____	32
4.1.15. Preparation of plasmid DNA/ MaxiPreps _____	32
4.1.16. Construction of expression vector coding for MOG-Fc fusion protein ____	32
4.2. Cell culture and biochemical analysis _____	33
4.2.1. Expression and purification of MOGxCD3 fusion protein _____	33
4.2.1.1. Stable transfection of CHO cells _____	33
4.2.1.2. Purification of expressed MOGxCD3 fusion protein _____	34
4.2.1.3. Protein analysis MOGxCD3 _____	36
4.2.1.3.1. SDS-PAGE _____	36
4.2.1.3.2. Western blotting _____	36
4.2.2. Expression and purification of MOG-Fc Fusion Protein _____	37
4.2.2.1. Stable transfection of CHO cells _____	37
4.2.2.2. Purification of expressed MOG-Fc fusion protein _____	37

4.2.2.3. Protein analysis MOG-Fc _____	38
4.2.2.3.1. SDS-PAGE _____	38
4.2.2.3.2. Western blotting _____	38
4.2.3. Binding of auto-antigen fusion protein to auto-antibody _____	39
4.2.3.1. Source of auto-antibodies _____	39
4.2.3.2. Sandwich-ELISA for detection of MOG-Fc fusion protein _____	39
4.2.3.3. Sandwich-ELISA for detection of MOGxCD3 fusion protein _____	40
4.3. Binding of auto-antigen fusion proteins to immune effector cells _____	40
4.3.1. Isolation of PBMCs _____	40
4.3.2. Isolation of CD3 <sup>+</sup> cells _____	41
4.3.3. Binding assay of MOGxCD3 to CD3 <sup>+</sup> PBMCs _____	41
4.3.4. Binding assay of MOG-Fc to Fc $\gamma$ R <sup>+</sup> cell line p388.D1 _____	41
4.4. Antibody-dependent cellular cytotoxicity _____	41
4.4.1. Establishment of cell-surface $\alpha$ MOG-positive hybridoma cell line _____	41
4.4.2. FACS-based ADCC assay _____	42
4.5. Binding analysis of MOG-Fc fusion protein to mouse splenocytes _____	42
4.6. <i>Ex vivo</i> elimination of B cells by MOG-Fc _____	43
4.7. <i>In vivo</i> depletion of B cells in TH mice by MOG-Fc _____	43
4.8. Transfer of transgenic B cells into recipient wild-type mice _____	44
4.9. Detection of $\alpha$ MOG-Fc immune responses in ELISA _____	44

4.10. Immunomodulatory effects of MOG-Fc treatment in EAE _____	45
4.10.1. Induction of EAE _____	45
4.10.2. Clinical evaluation of EAE _____	45
4.11. Determination of T cell fine specificity against MOG M36 epitope _____	46
4.11.1. Peptide synthesis _____	46
4.11.2. T-cell proliferation assay _____	46
4.11.3. Peptide competition assay _____	46
4.11.4. Cloning of mutated MOG-Fc constructs _____	47
4.11.5. Selective binding of mutated MOG-Fc to autoreactive B cells _____	47
4.12. Treatment of mice _____	48
<b>5. Results _____</b>	<b>49</b>
5.1. Design, expression and biochemical characterization of fusion proteins _____	49
5.1.1. Choice of expression vector _____	49
5.1.2. Design and characterization of MOG-Fc _____	50
5.1.3. Design and characterization of MOGxCD3 _____	55
5.2. Binding of MOG fusion proteins to effector cells _____	59
5.2.1. Binding of MOG-Fc to Fc receptor positive cell line _____	59
5.2.2. Binding of MOGxCD3 to primary human T cells _____	60
5.3. Assessment of <i>in vitro</i> cytotoxicity _____	62

5.3.1. Investigation of cytotoxicity mediated by MOG-Fc	64
5.3.2. Investigation of cytotoxicity mediated by MOGxCD3	69
5.4. Investigation of MOG-Fc <i>in vivo</i> using a transgenic mouse model	73
5.4.1. Cell binding activity	73
5.4.2. <i>In vivo</i> effect of MOG-reactive B cells in transgenic and wild-type mice	76
5.4.2.1. Antibody responses in mice treated with MOG-Fc	76
5.4.2.2. <i>Ex vivo</i> cytotoxic activity of MOG-Fc	79
5.4.2.3. Effect on the B-cell population in TH mice	81
5.4.2.4. Effect on autoreactive B cells and antibody titers in a transfer model	82
5.5. Effect of MOG-Fc treatment in EAE	86
5.6. Fine specificity of the T-cell response in SJL/J mice	89
5.6.1. Alanine scan of M36 epitope	89
5.7. Generation of mutated MOG-Fc proteins (R-MOG, S-MOG)	91
5.8. Treatment of PLPs-immunized animals transferred with TH B cells	94
<b>6. Discussion</b>	<b>97</b>
6.1. <i>In vitro</i> properties of MOGxCD3 fusion protein	97
6.2. Rationale for construction of Fc fusion protein	99

6.3. Investigation of targeting autoreactive B cells with Fc fusion protein	101
6.4. Effect of MOG-Fc treatment in EAE	104
6.5. Perspectives	106
<b>7. Acknowledgements</b>	<b>114</b>
<b>8. Publications</b>	<b>115</b>
<b>9. Abbreviations</b>	<b>116</b>
<b>10. Reference List</b>	<b>118</b>
<b>11. Curriculum vitae</b>	<b>137</b>





## 2. Summary

For most autoimmune diseases known, treatment options are very limited. In fact, there is not a single autoimmune indication where a disease-specific treatment regimen has been described. It was the aim of this work to investigate novel strategies for specific depletion of autoreactive B cells as the root cause of many autoimmune diseases.

The first part of this thesis describes the generation of recombinant proteins that were engineered to induce re-directed lysis of autoreactive target cells mediated via immune effector cells. Two such proteins were designed, expressed and characterized. One fusion protein, designated MOGxCD3, had the function of recruiting T cells to eliminate autoreactive hybridoma cells. The other, named MOG-Fc, was engineered for the recruitment of Fc $\gamma$ R<sup>+</sup> effector cells. The generation, purification, biochemical characterization, and *in vitro* investigation of cytotoxicity is shown. Both recombinant proteins were found to be functional and showed a specific redirected lysis of MOG-reactive B cells *in vitro*.

In the second part, the properties of the fusion protein MOG-Fc generated for recruitment of Fc $\gamma$ R positive effector cells were investigated using a transgenic mouse model possessing high numbers of autoreactive B cells. As a model system, the MOG-Ig transgenic TH mouse was chosen. This system permitted to examine the *in vivo* activity of the MOG-Fc fusion protein on autoreactive B cells and antibody titers in a non-pathological situation. Likewise, toxic effects of the recombinant fusion protein could be monitored in TH mice, due to the fact that these mice possessed high numbers of autoreactive B cells, but typically do not show a pathological phenotype<sup>11</sup>.

In a third part, the immunomodulatory properties of the generated Fc fusion protein were examined in experimental autoimmune encephalomyelitis (EAE), a model of multiple sclerosis thought to be mediated by inflammatory T cells, where demyelinating MOG-specific autoantibodies are suggested to play an exacerbating role. It was discovered that treatment delayed the onset of disease in the M36-induced EAE model, but was followed by a rapidly progressive disease course, which was clinically more severe than in the untreated control groups. Modifications of the immunodominant epitope contained within the fusion protein had no influence on disease progression.

Taken together, this work shows that single-chain fusion proteins can be engineered to target B cells specific for the autoantigen MOG for depletion via immune-effector mechanisms. This was achieved by coupling the MOG extracellular domain to a C-terminally attached effector domain consisting of either an Fc part of human IgG1 or a single-chain variable domain (scFv) directed against CD3ε. These proteins induced the efficient depletion of MOG-specific B cells *in vitro*, *ex vivo* and *in vivo*, and thus represent a novel approach for recombinant proteins targeting autoreactive B cells in antibody-mediated autoimmunity. Due to the exacerbating potential of the autoantigen fragment, their use as a therapeutic option in autoimmune conditions requires further development.

### **3. Introduction**

#### **3.1. Autoimmune diseases**

The immune system has evolved as a highly effective defensive shield against invading pathogens, such as viruses, bacteria, fungi, protozoa and tumor cells. To combat infection, innate immunity as well as acquired humoral and cellular immune responses act in concert to protect the host organism. It is the recognition of non-self that lies at the heart of immunology. However, the protection afforded by the detection of harmful pathogens comes at a price. All lymphocytes have the intrinsic capability to recognize any given antigen, and mechanisms are in place that ensure the deletion, silencing or inactivation of cell clones against self antigens. Since this is not a perfect process, some of these autoreactive clones eventually escape deletion, but they are usually rendered anergic when they encounter their antigen in the periphery, or remain in a state of immunological ignorance. Autoimmune responses are a natural consequence of the open repertoire of both T-cell and B-cell receptors, which allows them to recognize any antigen, irrespective of its self- or non-self origin. In rare instances, such autoreactive clones are reactivated from their "indifferent", or ignorant state, and mount an adaptive immune response against self tissues. When these responses are sustained and cause lasting tissue damage, they become medically significant and are classified as autoimmune diseases.

#### **3.2. Humoral autoimmunity**

In most instances studied, the aetiology of human autoimmune disease has remained elusive, even though molecular mimicry by microbial pathogens and MHC class II genotype may play

a role in predisposition to disease development<sup>1</sup>. It is now recognized that each autoimmune disease possesses a characteristic pathology mediated mainly by B cells (immunopathogenesis of type II and III), T cells (type IV), or a combination thereof. In the case of type II autoimmunity, IgM or IgG antibodies to cell surface or matrix antigens lead to tissue damage<sup>2</sup>. Classical examples of such pathological manifestations are pemphigus vulgaris, myasthenia gravis or Grave's disease.

Grave's disease is caused by the production of antibodies specific for the receptor for thyroid-stimulating hormone (TSH). These autoantibodies are agonists for the TSH receptor, thereby stimulating the production of thyroid hormones. Thus, Grave's disease manifests itself as a disease of disrupted feedback regulation of thyroid hormone production, resulting in hyperthyroidism<sup>3</sup>.

In myasthenia gravis, the acetylcholine receptor is the target of autoimmune attack<sup>4</sup>. Neuromuscular transmission is blocked by antibodies predominantly against the alpha-chain of the receptor, which is thought to result in internalization and degradation of acetylcholine receptors found in the neuromuscular junction. Patients present with progressive weakness and do eventually die because of their disease.

Pemphigus vulgaris (PV) is a disease of the skin, where the stratified epithelial cells of the skin lose their ability to adhere to one another<sup>5</sup>. This acantholysis of keratinocytes leads to separation of the suprabasal epidermal layer, resulting in severe and potentially fatal blister formation in skin and oral mucosa. Loss of adhesion is thought to be mediated by antibodies against desmosomal cadherins, such as desmoglein 3 (Dsg 3) and Dsg 1. Even though therapy of PV with corticosteroids has proven to reduce mortality from 90 to 10%, long-term effects are severe and can be fatal<sup>6</sup>.

A large number of autoantigens has been identified to date, and the mode of action of many pathogenic antibody responses directed against these target structures is known and relatively well-understood. However, the event that may ultimately *initiate* an autoimmune response in humans is still a matter of speculation. This explains why treatment options to most autoimmune diseases are extremely dissatisfactory: they are not addressing the root cause of the disease, but induce global suppression of the immune system as a whole. General immunosuppression does lead to a short-term clinical improvement in the autoimmune condition, but it also goes hand-in-hand with severe side effects, such as increased susceptibility to infection or even the development of malignancies<sup>7</sup>. Thus, there is an urgent demand for more specific, non-hormonal therapeutic approaches for antibody-mediated autoimmune diseases.

The aim of this work was to devise new ways to eradicate those cells of the immune system that can be held accountable for the production of autoreactive antibodies, that is, the autoreactive B cells. This goal should be accomplished by combining within a single-chain protein a known autoantigen with a cytotoxic effector mechanism. Only those B cells harboring a B-cell receptor reactive against the autoantigen on their cell surface would bind this fusion protein, which should lead to a highly specific elimination of only the autoreactive B-cell compartment, sparing B cells with other specificities. In fact, the number of autoreactive B cells is so low that, even in individuals affected with autoimmune disease, their presence can be monitored only indirectly via detection of secreted immunoglobulin or, in some cases, by extremely sensitive assays, such as ELISPOT<sup>8</sup>. This poses a challenge to the investigation of B-cell specific therapies, since the cellular compartment that needs to be addressed cannot be readily detected in conventional experimental systems.

A core requirement for a suitable model system to investigate immunotherapeutic strategies is the presence of large numbers of autoreactive B cells. These B lymphocytes should be easily traceable, thereby allowing the assessment of B-cell specific interventions. While transgenic approaches introducing immunoglobulin genes coding for anti-self B-cell receptors seem at first glance a straightforward strategy, special consideration has to be given to the investigated target antigen. As a matter of fact, in most of the targeted transgenic mouse models studied so far, the regulatory potential of the immune system was able to cope even with large numbers of transgenic autoreactive B cells, resulting in their efficient deletion or inactivation by different means<sup>9</sup>. Thus, there are only very few cases where the transgenic expression of autoreactive antibody results in the generation of a fully functional, autoreactive B-cell population<sup>10</sup>. One such system is the so-called “TH mouse”<sup>11</sup>, a transgenic mouse model system with B cells reactive against the autoantigen myelin oligodendrocyte glycoprotein (MOG). MOG was discovered due to its pivotal role in the induction of experimental autoimmune encephalomyelitis (EAE), a model for multiple sclerosis.

### **3.3. An example of a complex autoimmune disease: Multiple sclerosis**

Multiple sclerosis (MS) is a chronic inflammatory disease of the central nervous system (CNS). In contrast to mainly antibody-mediated afflictions, the pathology observed in MS is thought to be centrally driven by T-helper 1 (Th1) cells. MS is the most common neurological disease of young adults of Northern European descent, the onset of clinical symptoms usually appearing between age 20 and 40<sup>12;13</sup>. The disease is more prevalent in women than in men, who outnumber men with the disease at a 2:1 ratio. The cause of MS is unknown, but genetic factors are important. The concordance rate among monozygotic twins is 30%, a 10-fold

increase over dizygotic twins or first-degree relatives<sup>14;15</sup>. An important genetic factor are HLA class II genes, with HLA DR2 carrying a 4-fold increased risk for Northern European caucasoids<sup>16</sup>. The clinical picture of MS typically involves an initial course, manifested by relapse and remission for several years. In about half of the cases, the disease progresses to a more chronic phase. Patients present with symptoms entirely attributable to pathology of the central nervous system, which may include disturbances in visual acuity, motor disturbances affecting walking and use of hands, incoordination, incontinence, spasticity and problems including loss of touch, pain, and temperature. Cognitive function is not impaired in MS<sup>13</sup>. The central nervous system shows a classic picture of inflammation extending into the myelin sheath, as characterized by infiltration of lymphocytes, localized myelin destruction and loss of oligodendrocytes. Intrathecal Ig synthesis, demonstrated by the presence of oligoclonal bands in the cerebral spinal fluid of MS patients, further argues for an immune-mediated mechanism of the disease. Due to the presence of macrophages and lymphocytes in MS lesions, and the association of MS with MHC genotype, MS is believed to be an autoimmune disease involving immunopathological reactions against myelin proteins. Indeed, immunization of experimental animals with CNS antigens leads to the development of an MS-like disease designated experimental autoimmune encephalomyelitis (EAE).

### **3.4. Experimental autoimmune encephalomyelitis (EAE), a model for MS**

EAE shares many characteristic features with multiple sclerosis, such as histopathology, dependence on genetic factors and clinical symptoms<sup>17</sup>. Following immunization with CNS antigen in the periphery, an autoimmune response is initiated towards myelin antigens that involves migration of autoreactive T lymphocytes into the CNS<sup>18</sup>, where they act in concert with humoral autoimmunity to induce inflammation, loss of blood-brain-barrier (BBB)



integrity, migration of macrophages and, consequently, destruction of myelin leading to neurological deficits<sup>19;20</sup>. Indeed, passive transfer of EAE by activated encephalitogenic T cells specific for myelin basic protein (MBP) has reinforced the concept that myelin-specific T cells may be involved in the initiation of inflammatory responses in the CNS<sup>21</sup>.

Even though the major myelin constituent MBP induces clinical disease upon immunization in CFA, it does not induce the demyelinating plaques in primates or rats, which are so very characteristic of MS lesions<sup>22</sup>. Besides MBP, several other CNS autoantigens were investigated for their encephalitogenic potential, including proteolipid protein (PLP), myelin-associated glycoprotein (MAG), myelin oligodendrocytic basic protein (MOBP) or myelin oligodendrocyte glycoprotein (MOG). Remarkably, MOG is the only CNS antigen to elicit both encephalitogenic T cells as well as demyelinating plaques in nonhuman primates<sup>23;24</sup>, thus reproducing the complex pathology seen in MS. In fact, demyelination was found to be associated with the presence of MOG-specific antibodies in CNS lesions of MOG-induced EAE in the marmoset and also in acute multiple sclerosis lesions<sup>25</sup>. The observation that intravenous injection of anti-MOG immunoglobulin leads to an exacerbated chronic-relapsing disease course, after primary EAE induction via transfer of MBP-specific T cells, supports the notion that humoral autoimmunity may play a role as an exacerbating factor in disease progression<sup>26</sup>. However, the unusual potency of MOG as an encephalitogen, which induces both highly pathogenic T cells as well as demyelinating autoantibodies, clearly indicate that MOG-induced EAE is not the most suitable system to investigate therapeutic strategies aimed at targeting solely the B-cell response in antibody-mediated autoimmunity. Therefore, the emphasis of this work was placed on the choice of MOG as a model target auto-antigen to investigate B-cell depletion strategies in the absence of an inflammatory context, as encountered in EAE.

### **3.5. Myelin oligodendrocyte glycoprotein (MOG) as a model auto-antigen**

Myelin oligodendrocyte glycoprotein (MOG) is a transmembrane protein exclusively found on the outermost sheath of CNS myelin, making up only 0.05% of total myelin protein content. In contrast to other proteins of the central nervous system, such as the major constituents proteolipid protein (PLP) or myelin basic protein (MBP)<sup>27</sup>, MOG is not expressed in the thymus. Therefore, MOG-specific T- or B-cell clones are not subject to clonal deletion and, due to the absence of MOG in the periphery, they are not anergized or inactivated in peripheral tissues. Thus, autoreactive B-cell clones can be maintained in the periphery in a fully functional state, provided that the intact blood-brain-barrier (BBB) prevents their entry into the CNS. In fact, gene targeting of a rearranged anti-MOG heavy chain VDJ segment to replace the endogenous J region resulted in transgenic mice (TH) almost exclusively expressing anti-MOG heavy chains in their B-cell repertoire (see Fig. 1 illustrating the gene replacement strategy)<sup>11</sup>. Here, TH stands for “transgenic heavy chain”. Together with endogenous light chains, these transgenic Ig heavy chains assemble to form fully functional B-cell receptors, resulting in a high proportion of MOG-reactive B cells and also high anti-MOG autoantibody titers<sup>11</sup>. Not surprisingly, TH mice are predisposed to develop CNS autoimmunity, like experimental autoimmune encephalomyelitis (EAE). However, autoreactive B cells and autoantibody titers are only conditionally pathogenic upon challenge with CNS antigen emulsified in complete Freund's adjuvant (CFA), not affecting healthy animals. B cells develop normally in this model, since endogenous constant regions are still present and allow for class switching, whereas endogenous light chains endow the TH mice with the ability to respond to pathogens with an effective humoral immune response. Taken together, the features of i) high numbers of autoreactive B cells in the periphery, ii) high autoantibody titers and iii) normal B-cell development, make the TH mouse an ideal

model system to study strategies aimed at specifically targeting autoreactive B cells. This work was aimed at devising such a strategy through recombinant fusion proteins encompassing an antibody-based effector domain. The rationale is grounded in the experience gained by using antibodies as immunotherapeutic modalities.

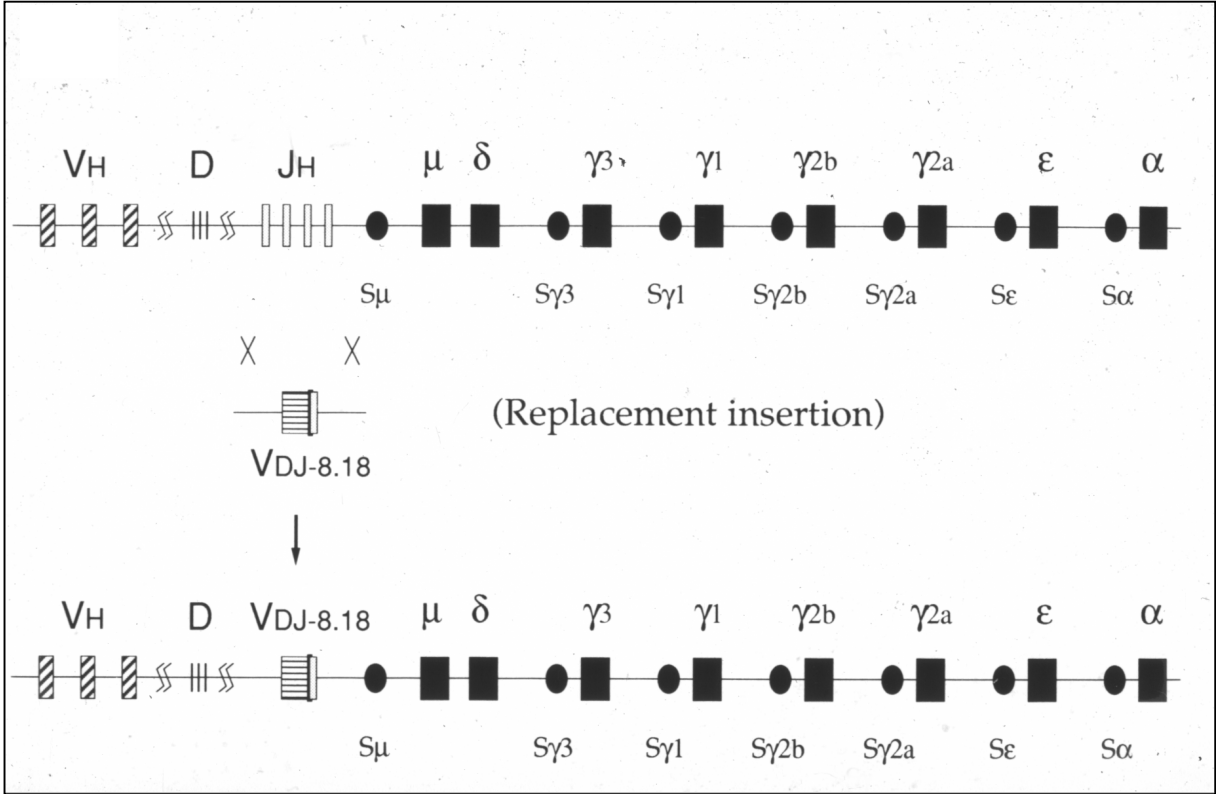


**Fig. 1.** Site-directed replacement of the JH locus with the TH MOG gene. Structure of the wild-type IgH locus and the targeted insertion. Illustration kindly provided by Antonio Iglesias (after Litzenburger 1998).

### **3.6. Antibody-based therapeutic approaches**

Antibodies are prototypic adaptor molecules. The intact humoral immune system has the capacity to generate antibodies that can bind just about any molecular target structure. In its role in defense against pathogens, an antibody has the function to mediate contact between a pathogen's target surface and an effector mechanism. This effector mechanism may consist of cellular components of the immune system, such as natural killer cells (NK) or macrophages (MO), or a cascade of enzymes like the complement system. In doing so, humoral immunity constitutes an essential part of the immune system, and antibodies cooperate with cellular immunity to fight off invading viruses or bacteria very effectively.

Naturally, the situation is quite different when the pathogenic moiety is not a microbe, but a cellular component of the host. One such example is found in the grave consequences caused by cancer cells. Once a malignant clone is growing to a tumor, it has undergone multiple rounds of selection and found a way to escape those immunological checkpoints that usually prevent uncontrolled proliferation of transformed cells. The immune system has devised an intricate recognition network to eliminate diseased cells. Major anti-tumor effector mechanisms are provided by natural killer cells (NK) and CD8<sup>+</sup> cytotoxic T cells (CTLs). Both effector cell populations are controlled by MHC class I. NK cells lyse only those targets with low or absent levels of cell-surface MHC class I, while CTLs recognize tumor-associated antigens (TAA) presented in the context of surface MHC class I and destroy the tumor cell. A variety of mechanisms have been described by which tumors may escape immune recognition, including down-regulation of MHC class I molecules on the cells' surface, alteration of the cytokine milieu within the tumor to render TAA-specific T cells anergic, expression of molecules such as CD95L that may induce premature lymphocyte cell death<sup>28-</sup>

<sup>30</sup>, or establishment of a tissue architecture that limits the penetration of lymphocytes<sup>31;32</sup>. In these situations, the immune system is at a loss and will not be able to cope on its own with the danger posed from transformed self cells. It is the desire of tumor immunotherapy to make tumor cells again visible to the immune system, thereby inducing their ultimate destruction. The approaches are numerous and include vaccination with tumor antigens in adjuvant<sup>33;34</sup>, DC vaccines<sup>35</sup>, completely synthetic vaccines based on tumor-specific T-cell epitopes<sup>36</sup>, *ex vivo* transduction of irradiated tumor cells with recombinant adeno-associated viruses carrying genes coding for co-stimulatory molecules<sup>37</sup> and also vaccination approaches with a variety of bacteria engineered to express tumor antigens when they are taken up by phagocytic cells<sup>38</sup>.

Despite the enormous efforts undertaken in order to break tolerance mainly on the T-cell level by vaccination approaches, there is only one single approach that has so far proven efficacious in humans with a high success rate. These are recombinant antibodies. In fact, several products are currently approved for use in patients and on the market (table 1)<sup>39</sup>. One of these is the chimeric IgG1-antibody Rituxan, directed against the CD20 antigen on B cells<sup>40;41</sup>. Rituxan has been approved for follicular Non-Hodgkin's lymphoma (NHL). By a mechanism relying to a large part on antibody-dependent cellular cytotoxicity (ADCC)<sup>42</sup>, this molecule induces highly efficient killing of malignant cells in B-cell lymphomas. The CD20 antigen is expressed on essentially all B cells found in the periphery. Therefore, anti-CD20 treatment results in the depletion of the whole B-cell pool. While this is certainly an acceptable situation in oncology, the requirements for an approach targeting B cells in chronic autoimmune afflictions need to be more stringent.

**Table 1. The emerging antibody therapeutics.**

<b>Antibody</b>	<b>Indication</b>	<b>Target</b>	<b>Company</b>	<b>Status</b>
<i>All rodent</i>				
PanoRex	Colon carcinoma	EpCam, EGP-2	Glaxo Wellcome	Approved Germany
Orthoclone (OKT-3)	Transplantation rejection	CD3	Johnson & Johnson	Approved US
<i>Chimeric</i>				
ReoPro	High-risk angioplasty	GP1Ib, IIIa	Centocor/Lilly	Approved US
Rituxan	Non-Hodgkin's lymphoma	CD20	IDEC/Genentech	Approved US
Remicade	Crohn's disease	TNF- $\alpha$	Centocor/Schering Plough	Approved US
Simulect	Transplantation rejection	CD25	Novartis	Approved US
<i>Humanized</i>				
Synagis	RSV infection	RSV F protein	MedImmune	Approved US
Zenapax	Transplantation rejection	CD3	Protein Design Laboratories/Roche	Approved US
Herceptin	Breast cancer	HER-2	Genentech/Roche	Phase 3*
CMA676	Acute myeloid leukemia	CD33	Celltech	Phase 3
Anti-IgE	Asthma	IgE	Genentech	Phase 3
<i>Human</i>				
Anti-TNF- $\alpha$	Rheumatoid arthritis	TNF- $\alpha$	CAT/BASF	Phase 2
Anti-TGF- $\beta$	Proliferative vitreoretinopathy	TGF- $\beta$	CAT	Phase 1/2

\*Recommended for approval by US Food and Drug Administration (Rockville, MD). EGP-2 = epithelial glycoprotein-2; RSV = respiratory syncytial virus; TNF- $\alpha$  = tumor necrosis factor- $\alpha$ ; TGF- $\beta$  = transforming growth factor- $\beta$ .

### 3.7. Objectives

The aim of the work presented here was the establishment of a novel principle for the specific targeting of autoreactive B cells through recombinant antibody-based fusion proteins. Using TCR-specific F(ab')<sub>2</sub> antibody fragments chemically coupled to TNP (2,4,6-trinitrophenyl), the bridging of T-cell and B-cell receptors was demonstrated previously<sup>43</sup>, thus forcing

interactions between CTLs and TNP-specific B cells. Building upon this concept, novel proteins can be envisioned to combine a B-cell targeting domain with an antibody effector mechanism within a single protein chain. The choice of this effector mechanism was an important consideration.

A number of mechanisms exist that may lead to target cell destruction through exogenously supplied antibodies. These consist of i) antibody-dependent cellular cytotoxicity (ADCC), ii) specific signal-inducing properties, iii) complement-dependent cytotoxicity (CDC) and iv) induction of an anti-anti-idiotypic response.

ADCC is a major mechanism involved in target cell lysis for therapeutic antibodies such as Rituxan<sup>42</sup> and can be monitored in cell culture systems. Antibodies bound to the target cell induce the recruitment of FcR-positive effector cells like natural killer cells (NK), macrophages (MO), monocytes and granulocytes. Those effector cells recognize their target cells when they are “decorated” with bound antibodies, which triggers the release of cytotoxic granules through high-avidity binding of Fc receptors to multiple immunoglobulin constant parts, and leads to destruction of the target cell. The cytotoxic potential of an antibody can be quantitated by release of <sup>51</sup>Cr from cells or a number of fluorescent dyes, e.g. propidium iodide, that stain only those cells that have undergone various stages of apoptotic or necrotic forms of cell death. The Fc part of human IgG1 has proven to be most suitable for the induction of ADCC when compared to Fc parts of other IgG isotypes<sup>42</sup>.

Complement-mediated lysis is yet another mechanism that may lead to antibody-dependent cell death. The most potent inducers of the complement cascade are IgM antibodies, based on their pentameric structure. Whereas at least two IgG antibodies are required to initiate the binding of C1q, the initiator of the classical pathway of complement, a single IgM molecule

can recruit C1q and set off the complement cascade. The role of complement fixation by antibodies is a central mechanism in the host defense against pathogens. However, its role in the destruction of tumor cells *in vivo* is largely unresolved, due to the expression of complement inhibitory proteins on mammalian cells. Likewise, most common inbred mouse strains have very low levels of complement as compared to other mammals. Complete lack of complement activity has been reported for many mouse strains, attributed to the absence of C5. For example, total hemolytic CH50 titers of <160 are observed for the SJL/J and C57BL/6 mouse strains, in comparison to 6,666 for humans and 10,324 for guinea pig<sup>44</sup>. In fact, the sera of these mice produce less than 22% maximum lysis at optimal serum concentrations in standard sheep erythrocyte lysis assays. This limits the value of the mouse as an experimental model to investigate the contribution of CDC to antibody-mediated cell lysis.

Induction of the anti-idiotypic network and modulation of signal transduction through cell-surface receptors are other mechanisms by which antibodies may initiate cell death of target cells. After antibody treatment, patients may respond with an anti-idiotypic antibody (ab2) and, consequently, with an anti-anti-idiotypic response (ab3). These ab3 responses may support the action of the supplied therapeutic antibody, since they will again recognize the primary antigen. In fact, vaccination strategies with anti-idiotypic antibodies directed against the idiotype specific for the epithelial cell antigen EpCAM are currently in clinical trials for adjuvant therapy of colon carcinoma<sup>45-47</sup>. However, the true effect of the anti-anti-idiotypic response in supporting the action of an exogenously supplied primary antibody is still unclear.

Reports about rituximab indicate that binding to the CD20 differentiation antigen induces a pro-apoptotic signal<sup>41</sup>. This signal-inducing effect of the antibody may add to its cell-mediated cytotoxic properties. Similar properties were discovered for trastuzumab, a



monoclonal antibody directed against the HER2/neu surface protein. The HER2/neu glycoprotein is over-expressed on 25-30% of breast carcinoma cells in women with metastatic breast cancer. HER2/neu is a putative receptor tyrosine kinase involved in the survival and growth of carcinoma cells, and trastuzumab is thought to interfere with signaling through this receptor<sup>48</sup>.

Despite more than 15 years of experience in antibody therapy, the mechanisms that are truly essential for a clinical response in patients have largely remained unidentified until recently. A recent report has investigated the role of Fc receptor engagement in the therapeutic effect of trastuzumab and rituxan in a mouse tumor model<sup>42</sup>. The investigators were able to show that the anti-tumor effect of these monoclonal antibodies largely depends on immune activation through the Fc receptor. The therapeutic effect of rituxan was essentially abolished in Fc $\gamma$ RIII knockout mice, while trastuzumab retained about 40% of its activity as compared to wild-type mice. This result indicates that ADCC is *the* major mechanism to therapeutic antibody efficacy in the mouse model. Equally intriguing is the finding that monoclonal antibody therapy is more potent in mice lacking the inhibitory receptor Fc $\gamma$ RIIB. Thus, approaches that selectively engage activating receptors without affecting inhibitory Fc receptors could increase the potency of an antibody-based drug.

Considering the findings outlined above, a strategy was devised for the construction of fusion proteins harnessing the most promising cytotoxic effector functions. In a first recombinant protein, the human IgG1 Fc region was fused in a C-terminal position to the human MOG protein. The idea was to target autoreactive B cells through the MOG domain, while at the same time recruiting Fc receptor positive immune effector cells through the IgG1 Fc domain. Due to the bispecific nature of the protein, it was hoped that engagement of Fc receptors would lead to the specific elimination of autoreactive target B cells. In a second approach, a

bispecific protein was generated that included human MOG in an N-terminal position fused to a murine single-chain Fv antibody (scFv) directed against the epsilon chain of the human CD3 T-cell receptor complex. It was envisioned that these antibody fusion proteins would bind to the MOG-reactive B-cell receptor (BCR) and recruit T cells to eliminate anti-MOG<sup>+</sup> autoreactive B lymphocytes. The single-chain Fv format has an additional appeal in its ability to potentially trigger T cells in the absence of the engagement of inhibitory receptors. The T-cell recruiting fusion protein could only be tested *in vitro*, since its parental anti-CD3 monoclonal antibody recognizes only human CD3 epsilon and does not cross-react with the TCR complex of other species with the exception of chimpanzees. This is in contrast to the human IgG1 Fc part in the first fusion protein, which is known to cross-react with murine Fc receptors and can be used in experimental mouse systems<sup>50</sup>. Here, two novel proteins were generated, one with the validated IgG1-Fc constant region, the other with a scFv domain directed against CD3 on human T cells. These novel bispecific proteins were evaluated for their potential to specifically eliminate autoreactive,  $\alpha$ MOG<sup>+</sup> B cells.

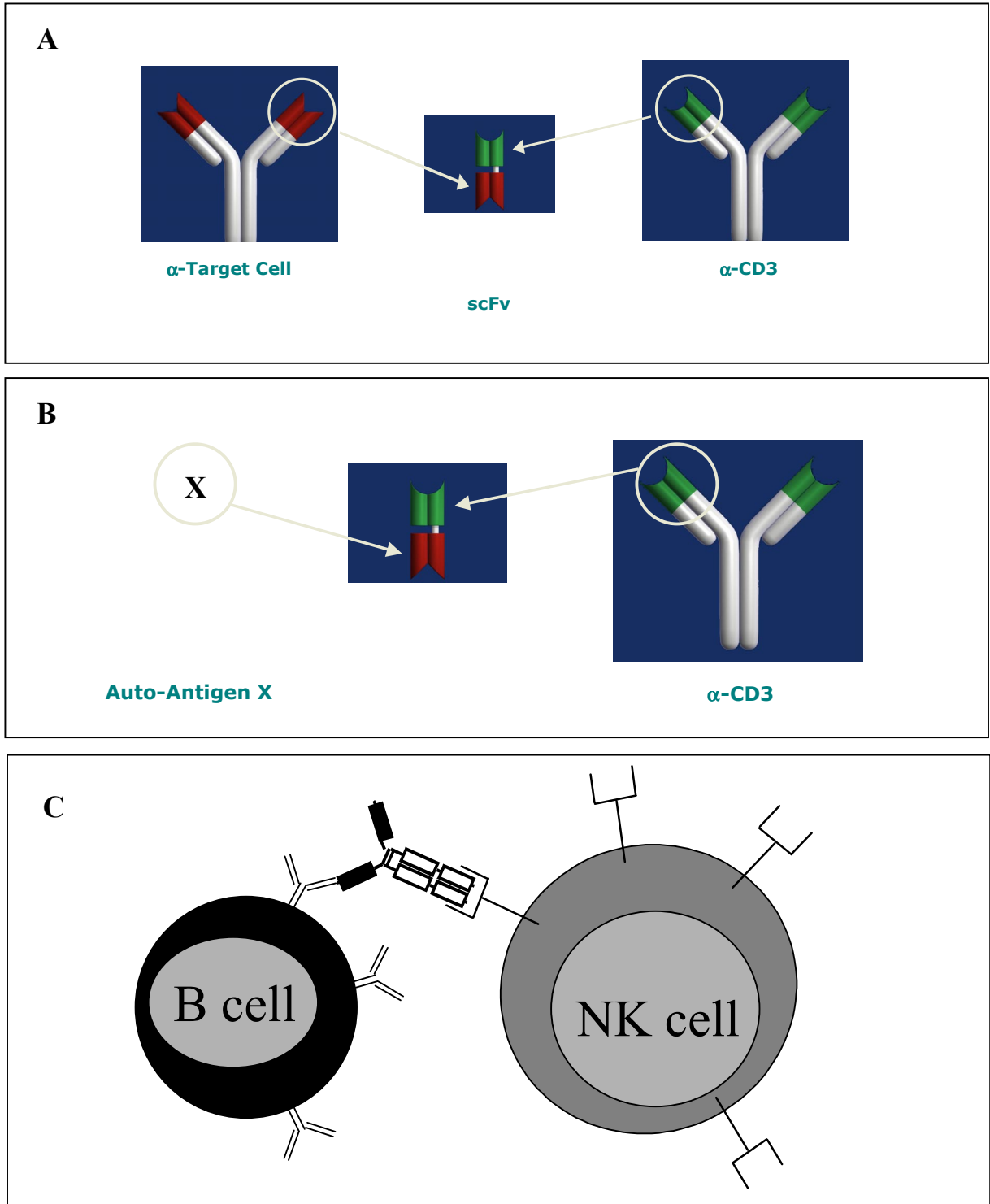


**Fig. 2.** Working principle of bispecific antibody fusion proteins. **A.** Construction of a single-chain Fv (scFv) antibody by combination of 2 antibody variable regions. Example shows scFv Ab targeting T cells via CD3. **B.** Targeting autoreactive B cells. *ScFv antibody fusion protein* for recruitment of T cells to B cells reactive against a putative auto-antigen X. Adapted from Micromet AG, 2002. **C.** Illustration of concept for induction of re-directed lysis through a *bispecific Fc fusion protein*. B cells are targeted via autoantigen domain of fusion protein (black) for depletion through Fc $\gamma$ R+ effector cells, such as NK cells.

## **4. Material and Methods**

### **4.1. Molecular biology**

For expression of auto-antigen effector domain constructs, pEF-dhfr  $\alpha$ (CD19xCD3)<sup>49</sup> was modified by removing the region coding for the single-chain  $\alpha$ CD19 antibody. As described below, the remaining  $\alpha$ CD3 expression cassette was used for insertion of cDNA coding for the auto-antigenic domain of the human MOG protein and provides an ideal system for further cloning of auto-antigen x  $\alpha$ CD3 fusion proteins.

#### **4.1.1. Isolation of RNA from MOG-transfected fibroblasts**

Total RNA was isolated from MOG-transfected fibroblasts (kindly provided by Chris Lington, MPI Neurobiology Martinsried) using the Qiagen RNEasy RNA Extraction Kit according to the manufacturer's suggestions. RNA was dissolved in H<sub>2</sub>O and stored at  $-80^{\circ}\text{C}$ .

#### **4.1.2. Reverse transcription**

Using isolated RNA from 4.2.1. as a template, cDNA was synthesized as follows:

2  $\mu\text{g}$  total RNA were added to 0.5  $\mu\text{g}$  Oligo-dT primer in a total reaction volume of 12  $\mu\text{l}$ . The reaction mixture was incubated at  $70^{\circ}\text{C}$  for 10 min. Then, 4  $\mu\text{l}$  5x First Strand Buffer (Gibco BRL), 2  $\mu\text{l}$  0.1 M DTT and 1  $\mu\text{l}$  10 mM dNTPs were added. Incubation was performed at  $42^{\circ}\text{C}$  for 2 min, after which 200 U of Superscript II Reverse Transcriptase (RT) (Gibco BRL) were added. The reaction mixture was incubated for 50 min. at  $42^{\circ}\text{C}$ . Then, RT was inactivated due to a 15 min incubation step at  $70^{\circ}\text{C}$ . Isolated cDNA was stored at  $-20^{\circ}\text{C}$ .

#### **4.1.3. Amplification of MOG-coding cDNA fragments**

In order to obtain cDNA coding for the extracellular domain of the human MOG protein (MOG-ex), the following primers were chosen:

Primer 1 (MOG-Ex 5'): 5'-TAGAATTCATGGCAAGCTTATCGAGACCC-3'

Primer 2 (MOG-Ex 3'): 5'-CATCCGGATCCAGGGCTCACCCAGTAGA-3'

Primers were designed as to allow amplification of the first 462 bases of the region coding for both leader sequence and extracellular domain of the human MOG protein, while introducing EcoRI and BspEI restriction sites at 5' and 3' ends of the amplified fragment, respectively. This leads to a final product of 474bp of length.

#### **4.1.4. Polymerase chain reaction (PCR)**

For PCR, 50 pmol/ each of appropriate primer, 1  $\mu$ l dNTPs 10 mM, 4  $\mu$ l cDNA, 5  $\mu$ l Pfu-buffer 5x (Stratagene) and 5 U Pfu-Polymerase (Stratagene) were added to a final volume of 50  $\mu$ l in H<sub>2</sub>O, and specific cDNA was amplified by PCR.

#### **4.1.5. Construction of MOGxCD3 encoding expression vector**

In order to obtain the desired construct, expression vector  $\alpha$ (CD19xCD3) pEF-dhfr was subjected to restriction with EcoRI and BspEI, leading to removal of the fragment coding for anti-CD19. The remaining vector-anti CD3 portion was gel-extracted (gel extraction kit, Qiagen). Equally, MOG-ex was partially digested with BsaWI and EcoRI, and the corresponding fragment of 474bp of length was isolated via gel-extraction as described above. BsaWI restriction was chosen due to this enzyme's insensitivity to dam-methylation at the original BspEI restriction site. DNA was eluted in 30  $\mu$ l Tris pH 8.5 and stored at -20°C. Ligation of isolated DNA fragments was performed with equal volumes of extracted DNA

and 5 U of T4 DNA Ligase in a total volume of 20  $\mu$ l in 1x T4 buffer (Roche Biochemicals). Ligation was allowed to proceed for 30 min. at room temperature (RT). Of each ligation reaction, 3  $\mu$ l were used to transform *E. coli* XL-1 Blue as described above. Colonies were picked and subjected to MiniPrep analysis. Following analytical restriction enzyme digestion, appropriate clones were sequenced (Sequiseive, Vaterstetten). Correct clones were grown in 300 ml LB-Amp medium, and plasmid DNA was isolated using the Qiagen plasmid prep kit as described above. Again, integrity of isolated DNA was verified via restriction enzyme analysis.

#### **4.1.6. Construction of MOG-Fc encoding expression vector**

#### **4.1.7. Isolation of RNA from HD69-transfected CHO cells**

Total RNA was isolated from HD69-transfected CHO cells<sup>51</sup> using the Qiagen RNEasy RNA Extraction Kit according to the manufacturer's suggestions. RNA was dissolved in H<sub>2</sub>O and stored at  $-80^{\circ}\text{C}$ .

#### **4.1.8. Reverse transcription**

Using isolated RNA from 2.1. as a template, cDNA was synthesized as follows:

2  $\mu$ g total RNA were added to 0.5  $\mu$ g Oligo-dT primer in a total reaction volume of 12  $\mu$ l. The reaction mixture was incubated at  $70^{\circ}\text{C}$  for 10 min. Then, 4  $\mu$ l 5x First Strand Buffer (Gibco BRL), 2  $\mu$ l 0.1 M DTT and 1  $\mu$ l 10 mM dNTPs were added. Incubation was performed at  $42^{\circ}\text{C}$  for 2 min, after which 200 U of Superscript II Reverse Transcriptase (RT) (Gibco BRL) were added. The reaction mixture was incubated for 50 min. at  $42^{\circ}\text{C}$ . Then, RT was inactivated due to a 15 min incubation step at  $70^{\circ}\text{C}$ . Isolated cDNA was stored at  $-20^{\circ}\text{C}$ .

#### **4.1.9. Amplification of IgG1-coding cDNA fragments**

In order to obtain cDNA coding for the Fc-domain of the human IgG1 antibody backbone, the following primers were chosen:

Primer 3 (IgG1-Fc 5′): 5′-TATCCGGAGAGCCCACCTCTTGTGACAAAAC-3′

Primer 4 (IgG1-Fc 3′): 5′-GTGTGCGACTCATTACCCGGAGACAGGG-3′

Primers were designed as to allow amplification of the 699 bases coding for the Fc part of the human IgG1 backbone, while introducing BspEI and SalI restriction sites at 5′ and 3′ ends of the amplified fragment, respectively. This leads to a final product of 711 bp in length.

#### **4.1.10. Polymerase chain reaction (PCR)**

For PCR, 50 pmol each of appropriate primer, 1 μl dNTPs 10 mM, 4 μl cDNA, 5 μl Pfu-buffer 5x (Stratagene) and 5 U Pfu-Polymerase (Stratagene) were added to a final volume of 50 μl in H<sub>2</sub>O, and specific cDNA was amplified by PCR.

#### **4.1.11. PCR product purification**

DNA was recovered from PCR reaction mixture according to the manufacturer's suggestions (Roche Applied Biosciences).

#### **4.1.12. Ligation of PCR products into pCR-Script Amp vector**

Blunt-ended PCR products generated by Pfu DNA polymerase were ligated into pCR-Script Amp vector (Stratagene #211188).

#### **4.1.13. Transformation**

Plasmids were transformed into competent *E. coli* strain XL-1 Blue using 4  $\mu$ l of ligation product added to 50  $\mu$ l of *E. coli*. The mixture was incubated on ice for 10 min., 1 min. at 42°C, and then again on ice for 2 min. Thereafter, 150  $\mu$ l LB-medium were added and expression of ampicillin resistance genes was induced due to 45 min at 37°C while shaking. Reaction mixtures were plated on LB-Amp Agarose plates (50  $\mu$ g ampicillin/ml) and incubated at 37°C for 16 h.

#### **4.1.14. Preparation of plasmid DNA/ MiniPreps**

Colonies were picked and grown in LB-Amp medium (100  $\mu$ g/ ml) for 8-12h. Bacteria were spun down, and plasmid DNA was isolated according to manufacturer's suggestions (Plasmid Mini-Kit, Qiagen). DNA was subjected to restriction enzyme analysis, and suitable clones were sequenced (SequiServe, Vaterstetten).

#### **4.1.15. Preparation of plasmid DNA/ MaxiPreps**

Correct clones were grown in 300 ml LB-Amp medium, and plasmid DNA was isolated using plasmid maxi kit (Qiagen).

#### **4.1.16. Construction of expression vector coding for MOG-Fc fusion protein**

In order to obtain the desired construct, expression vector  $\alpha$ (CD19xCD3) pEF-dhfr was subjected to restriction with EcoRI and Sall, leading to removal of the fragment coding for  $\alpha$ (CD19xCD3). The remaining linearized vector was gel-extracted (gel extraction kit, Qiagen). Equally, MOG-ex was partially digested with BsaWI and EcoRI, and the corresponding fragment of 474bp of length was isolated via gel-extraction as described above. BsaWI restriction was chosen due to this enzyme's insensitivity to dam-methylation at the original BspEI re-striction site. DNA was eluted in 30  $\mu$ l Tris pH 8.5 and stored at -20°C.



Ligation of isolated DNA fragments was performed with equal volumes of extracted DNA and 5 U of T4 DNA Ligase in a total volume of 20  $\mu$ l in 1x T4 buffer (Roche Biochemicals). Ligation was allowed to proceed for 30 min. at room temperature (RT). Of each ligation reaction, 3  $\mu$ l were used to transform E. coli XL-1 Blue as described above. Colonies were picked and subjected to MiniPrep analysis. Following analytical restriction enzyme digestion, appropriate clones were sequenced (Sequiseive, Vaterstetten). Correct clones were grown in 300  $\mu$ l LB-Amp medium, and plasmid DNA was isolated using the Qiagen plasmid prep kit as described above. Again, integrity of isolated DNA was verified via restriction enzyme analysis.

## **4.2. Cell culture and biochemical analysis**

### **4.2.1. Expression and purification of MOG $\times$ CD3 fusion protein**

#### **4.2.1.1. Stable transfection of CHO cells**

CHO cells were plated at  $3 \times 10^5$ /well in tissue culture 6-well plates and incubated at 37°C overnight. 3  $\mu$ g of DNA were pipetted in sterile Eppendorf tubes, supplemented with 100  $\mu$ l MEM- $\alpha$  medium (Gibco BRL) and 10  $\mu$ l SuperFect transfection reagent (Qiagen) and incubated for 10 min. at RT. 600  $\mu$ l of MEM- $\alpha$  medium were added, and the reaction mixture was transferred to CHO cells. Following a 2 h-incubation at 37°C, the supernatant was aspirated, cells were washed once with PBS, and 2 ml MEM- $\alpha$  medium (10% FCS, HT-supplement 1:100) were added to each well. Transfection efficiency was determined to be 10% via standard  $\beta$ -galactosidase control transfection. After 24h at 37°C, transfected cells were transferred to 10 ml cell culture bottles (Nunclone  $\Delta$ , Nalge Nunc International) and selected for expression of the dhfr marker via growth in non-supplemented MEM- $\alpha$  medium plus 10% di-

alysed FCS. Following two passages of confluent cells at 1:5 splitting ratios, transfectants were further selected by addition of 20 nM MTX to the selection medium. Cells were passaged 3 times, whereafter MTX concentration was increased to 100 nM. Following a further 3 passages, MTX was added to a final concentration of 500 nM.

#### **4.2.1.2. Purification of expressed MOG $\times$ CD3 fusion protein**

Stably transfected CHO-cells were transferred to 500 ml roller-bottles (Nalge Nunc International) in 250 ml MEM- $\alpha$ , 500 nM methotrexate (MTX) and 5% dialysed FCS. The following day, another volume of medium was added without FCS to obtain a final concentration of 2.5% FCS. Cells were grown for 1 day post confluency. Cells were separated from the supernatant by centrifugation at 4500 rpm, 30 min. in a Rotanta 46 centrifuge (Hettich), and recombinant protein was purified from cell culture supernatant as follows:

The MOG $\times$ CD3 protein was isolated in a three-step purification process including cation exchange chromatography, immobilized metal affinity chromatography (IMAC) and gel filtration.

The final product had a molecular weight of approximately 45 kDa under native conditions as determined by gel filtration in PBS. This corresponds to a monomeric form of the MOG $\times$ CD3.

The purity of the isolated protein was >95% as determined by SDS-PAGE. Under the conditions applied, the molecule appeared at approximately 45 kD in its monomeric form.

The final yield of purified protein was approximately 2.4 mg / 1 cell culture supernatant.

The GradiFrac System (Pharmacia) was used for chromatography. All chemicals were of research grade and purchased from Sigma (Deisenhofen) or Merck (Darmstadt).

Cation exchange was performed on a HiTrap SP Sepharose column (Pharmacia) that was equilibrated with buffer A1 (20 mM MES, pH 5.5). Cell culture supernatant was diluted 2:1 with buffer A1 and applied to the column (10 ml) with a flow rate of 4 ml/min. Unbound sample was washed out with buffer A1 and the bound protein was eluted with 100% buffer B1 (20 mM MES, pH 5.5, 1 M NaCl). Eluted protein fractions were pooled for further purification.

IMAC was performed, using a HisTrap column (Pharmacia) that was loaded with NiSO<sub>4</sub> according to the manufacturer's protocol. The column was equilibrated with buffer A2 (20 mM NaPP, pH 7.5, 0.4 M NaCl), and the sample was diluted 2:1 with buffer A2 to obtain a pH of 7. The sample was applied to the column (2 ml) with a flow rate of 1 ml/min and the column was washed with buffer A2 to remove unbound sample. Bound protein was eluted using a linear gradient of buffer B2 (20 mM NaPP pH 7.5, 0.4 M NaCl, 0.5 M Imidazol) (0-100% buffer B2 in 10 column volumes). Eluted protein fractions were pooled for further purification.

Gel filtration chromatography was performed on a Sephadex S200 HiPrep column (Pharmacia) equilibrated with PBS (Gibco). Eluted protein samples (flow rate 1 ml/min) were subjected to SDS-Page and Western blotting for MOG $\times$ CD3 detection. The column was previously calibrated for molecular weight determination (molecular weight marker kit, Sigma MW GF-200).

Protein concentrations were determined using protein assay dye concentrate (BioRad) and IgG (BioRad) as standard protein.

SDS-PAGE under non-reducing conditions was performed with precast 4-12% Bis-Tris gels (NOVEX). Sample preparation and application were according to the manufacturer's protocol. The molecular weight was determined with SeeBlue protein standard (NOVEX). The gel was stained with colloidal Coomassie (NOVEX protocol).

#### **4.2.1.3. Protein analysis MOG $\times$ CD3**

##### **4.2.1.3.1. SDS-PAGE**

For each peak detected, corresponding fractions were pooled and analyzed for purity via SDS-PAGE, followed by coomassie staining. Of each pool, 5  $\mu$ l were run on a Bis-Tris Gel 4-12% (NuPage), using MOPS/SDS as running buffer.

##### **4.2.1.3.2. Western blotting**

Fractions were subjected to SDS-PAGE as described above. Protein was blotted to reinforced nitrocellulose membrane (Optitran BA-S 83, Schleicher & Schuell) at 200 mA for 1 h (blotting buffer: 48 mM Tris, 39 mM Glycin, 0.01 % SDS). Recombinant fusion protein was detected with the anti-MOG monoclonal antibody 8.18-C5 at 5  $\mu$ g/ml in PBS; bound anti-MOG ab was detected via anti-mouse IgG antibody, AP-conjugated at 1:10000 in PBS (Sigma A-2429). The membrane was stained with BCIP/NBT (Sigma B-5655).

## **4.2.2. Expression and Purification of MOG-Fc fusion protein**

### **4.2.2.1. Stable transfection of CHO cells**

CHO cells were plated at  $3 \times 10^5$ / well in tissue culture 6-well plates and incubated at 37°C overnight. 3 µg of DNA were pipetted in sterile Eppendorf tubes, supplemented with 100 µl MEM-α medium (Gibco BRL) and 10 µl SuperFect transfection reagent (Qiagen) and incubated for 10 min. at RT. 600 µl of MEM-α medium were added, and the reaction mixture was transferred to CHO cells. Following a 2 h-incubation at 37°C, the supernatant was aspirated, cells were washed once with PBS, and 2 ml MEM-α medium (10% FCS, HT-supplement 1:100) were added to each well. Transfection efficiency was determined to be 10% via standard β-galactosidase control transfection. After 24 h at 37°C, transfected cells were transferred to 10 ml cell culture bottles (Nunclone Δ, Nalge Nunc International) and selected for expression of the dhfr vector via growth in non-supplemented MEM-α medium plus 10% dialysed FCS. Following two passages of confluent cells at 1:5 splitting ratios, transfectants were further selected by addition of 20 nM MTX to the selection medium. Cells were passaged 3 times, whereafter MTX concentration was increased to 100 nM. Following a further three passages, MTX was added to a final concentration of 500 nM.

### **4.2.2.2. Purification of expressed MOG-Fc fusion protein**

Stably transfected CHO-cells were transferred to 500 ml roller-bottles (Nalge Nunc International) in 250 ml MEM-α, 500 nM MTX and 5% dialysed FCS. The following day, another volume of medium was added without FCS to obtain a final concentration of 2.5% FCS. Cells were grown for 1 day post confluency. Cells were separated from the supernatant by centrifugation at 4500 rpm, 30 min. in a Rotanta 46 centrifuge (Hettich), and recombinant protein was purified using a 1-step purification procedure via Protein A affinity chromatography

(HiTrap Protein A column, Pharmacia) on the GradiFrac System (Pharmacia). The column was equilibrated with 10 ml of buffer A (20 mM Tris pH 7.2), and 500 ml of cell culture supernatant were passed through the column. Flow rate was 2 ml/ min. Bound Protein was eluted with 20 mM citrate, pH 3, using a linear gradient. Fusion protein yield amounted to 10 mg/l. Protein was > 95% pure as assessed by Coomassie staining.

#### **4.2.2.3. Protein analysis MOG-Fc**

##### **4.2.2.3.1. SDS-PAGE**

For each peak detected, corresponding fractions were pooled and analyzed for purity via SDS-PAGE, followed by coomassie staining. Of each pool, 5 µl were run on a Bis-Tris Gel 4-12% (NuPage), using MOPS/SDS as running buffer.

##### **4.2.2.3.2. Western blotting**

Fractions were subjected to SDS-PAGE as described above. Protein was blotted to reinforced nitrocellulose membrane (Optitran BA-S 83, Schleicher & Schuell) at 200 mA for 1h (blotting buffer: 48 mM Tris, 39 mM Glycin, 0.01 % SDS). Recombinant fusion protein was detected with anti-MOG monoclonal antibody (8.18-C5, kindly provided by Chris Linington, MPI Neurobiology, Martinsried) at 5 µg/ ml in PBS; bound anti-MOG ab was detected via anti-mouse IgG antibody, AP-conjugated at 1:10000 in PBS (Sigma A-2429). For detection of the human IgG1-Fc domain, recombinant protein was blotted as described above, and the Fc domain was stained with  $\alpha$ -human IgG1 ab, Fc-specific, coupled to alkaline phosphatase (AP), at 1:10000 in PBS (Sigma A-9544). The membrane was stained with BCIP/NBT (Sigma B-5655).

### **4.2.3. Binding of auto-antigen fusion protein to auto-antibody**

#### **4.2.3.1. Source of auto-antibodies**

The hybridoma 8.18-C5<sup>52</sup> was cultivated in serum-free medium (Gibco). Cells were separated from supernatant by centrifugation, and mouse anti-MOG monoclonal IgG1 antibodies were purified using a 1-step purification procedure via Protein G affinity chromatography (HiTrap Protein G column, Pharmacia) on the GradiFrac System (Pharmacia). Column was equilibrated with 10 ml of buffer A (20 mM Tris-HCl, pH 7.2), and 500 ml of cell culture supernatant were passed through the column. Flow rate was 2 ml/min. Bound protein was eluted with 20 mM citrate, pH 3, using a linear gradient. Antibody yield amounted to 4.5 mg/l. Protein was > 95% pure as assessed by Coomassie staining

#### **4.2.3.2. Sandwich-ELISA for detection of MOG-Fc fusion protein**

Isolated  $\alpha$ MOG ab 8.18-C5 was used to detect purified MOG-Fc fusion protein and to verify existence of 1) functional extracellular domain of MOG protein and 2) Fc effector domain in the recombinant protein. MaxiSorp 96-well plates (Nalge Nunc International) were coated with  $\alpha$ -MOG at 5  $\mu$ g/ml overnight at 4°C. Plates were blocked with 1% BSA for 1 h at RT, washed with PBS/ 0.05% Tween 20. Plates were incubated with various dilutions of MOG-Fc fusion protein in PBS for 1 h at RT, and bound fusion protein was detected using  $\alpha$ -human IgG1 ab, Fc-specific and AP-conjugated (Sigma A-9544) at 1: 10,000. Alkaline phosphatase-conjugated antibody was stained with pNPP (Sigma N-2770) and quantitated on the SpectraFluor ELISA reader (Tecan).

#### **4.2.3.3. Sandwich-ELISA for detection of MOGxCD3 fusion protein**

Isolated  $\alpha$ MOG ab 8.18-C5 was used to detect purified MOGxCD3 fusion protein and to verify existence of 1) functional extracellular domain of MOG protein and 2) anti-CD3 effector domain in the recombinant protein. MaxiSorp 96-well plates (Nalge Nunc International) were coated with  $\alpha$ MOG at 5  $\mu$ g/ml overnight at 4°C. Plates were blocked with 1% BSA for 1h at RT, washed with PBS/0.05% Tween 20. Plates were incubated with various dilutions of MOGxCD3 fusion protein in PBS for 1 h at RT, and bound fusion protein was detected using  $\alpha$ MT101ab (Davids Biotechnology, DabioPrep 2 Batch 2), an antibody specifically developed against the CD19xCD3 scFv described above. Bound chicken ab was detected using AP-coupled donkey- $\alpha$ -chicken ab at 1:10000 (Dianova 703-055-155). Alkaline phosphatase-conjugated antibody was stained with pNPP (Sigma N-2770) and quantitated on the SpectraFluor ELISA reader (Tecan).

### **4.3. Binding of auto-antigen fusion proteins to immune effector cells**

#### **4.3.1. Isolation of PBMCs**

Buffy coats were diluted 1:2 in PBS and separated in Ficoll gradient of density 1.077 (Sero-med Cat.No. L 6115). Lymphocytes were separated and washed twice with PBS. Erythrocytes were lysed with lysis buffer (8.29 g NH<sub>4</sub>Cl cell culture tested (Sigma A-0171), 1.0 g KHCO<sub>3</sub> 0.037 g EDTA, cell culture tested (Sigma E-6511); H<sub>2</sub>O ad. 1 l).

Thrombocytes were separated during 20 min of centrifugation at 100 x g. Remaining Lymphocytes were transferred to cell culture bottles and stored at 37°C/ 5% CO<sub>2</sub>.



#### **4.3.2. Isolation of CD3+ cells**

Human T-cell enrichment columns (R&D Systems Cat. No. HTCC-500/525) were used for isolation of T-cells according to manufacturer's suggestions.

#### **4.3.3. Binding assay of MOG $\times$ CD3 to CD3+ PBMCs**

To explore the binding of the MOG $\times$ CD3 fusion protein to CD3+ cells, 200,000 CD3+ cells were added to each well of a V-bottom microtiter plate (Greiner Labortechnik). Recombinant MOG $\times$ CD3 protein was added to obtain final concentrations of 0.032 up to 100  $\mu$ g/ml in a total volume of 50  $\mu$ l per well. Bound fusion protein was detected via binding of 8.18-C5 diluted 1:1000 in FACS-buffer (PBS 1x, 0.05% NaN<sub>3</sub>, 1% FCS), whereafter bound mouse monoclonal ab was stained with  $\alpha$ -mouse IgG-FITC (Sigma F-6257) at 1:40 dilution.

#### **4.3.4. Binding assay of MOG-Fc to Fc $\gamma$ R+ cell line p388.D1**

Binding of MOG-Fc to a murine macrophage cell line was investigated in FACS. The monocyte/macrophage cell line p388.D1<sup>53</sup> expressing murine Fc receptors was incubated with MOG-Fc. Bound MOG-Fc was detected via FITC-labeled anti-human Fc $\gamma$  antibody by flow cytometry. Binding was quantitated and expressed as mean fluorescence intensity (MFI).

### **4.4. Antibody-dependent cellular cytotoxicity**

#### **4.4.1. Establishment of cell-surface $\alpha$ MOG-positive hybridoma cell line**

8.18-C5 hybridoma cell line<sup>52</sup> (kindly provided by C. Linington, MPI Neurobiology, Martinsried) was adapted to serum-free medium (Hybridoma SFM, Gibco). Cells were passaged 1:5 every third day, and cultured in 100% SFM for a period of 4-5 months.

Thereafter, MOG-reactivity in the hybridoma pool was assessed by FACS-analysis, using biotinylated MOG protein for staining.

#### **4.4.2. FACS-based ADCC assay**

A FACS-based assay<sup>54;55</sup> was performed using freshly isolated human PBMCs as effector cells (ECs) for the MOG-Fc fusion protein and isolated human T cells for the MOG $\times$ CD3 fusion protein (see above). ECs and 8.18-C5 target cells were incubated overnight at 37°C/5% CO<sub>2</sub> at an E:T ratio of 10:1 and serial dilutions of fusion protein added in a constant volume of 20 $\mu$ l to 180 $\mu$ l cell suspension. Cells were stained with FITC-labeled goat-anti-mouse IgG antibody (Pharmingen 12064D) and propidium iodide. The live target cell population was measured as percentage of the whole cell population analyzed. Unspecific background (bg) was measured in the absence of protein. Cytotoxicity (CT) was calculated as  $CT = 100 \times (1 - (\text{live target cells in sample} / \text{live target cells in control}))$ . Background staining of human PBMCs incubated alone was subtracted. Values greater 100% were due to slight proliferation of PBMCs. To verify that reduction in the number of live target cells was due to cell lysis as opposed to a growth inhibitory effect, target and effector cells were incubated with the optimal dose of MOG-Fc (10  $\mu$ g/ml) as described above, and PI-positive dead target cells measured in FACS and expressed as percentage of total target cells detected. Cell lysis (CL) was calculated as  $CL = 100 \times (\text{dead target cells}) / (\text{total number of target cells})$ . Error bars represent standard deviation values (S.D.) from triplicates.

#### **4.5. Binding analysis of MOG-Fc fusion protein to mouse splenocytes**

Mice were sacrificed and the spleen was removed. Single-cell suspensions were generated by passage through a sterilized tissue-culture sieve in DMEM medium. Erythrocytes were removed by incubation in erythrocyte lysis buffer (8.29 g NH<sub>4</sub>Cl cell culture tested (Sigma A-

0171), 1.0 g  $\text{KHCO}_3$  0.037 g EDTA, cell culture tested (Sigma E-6511);  $\text{H}_2\text{O}$  ad. 1L) for 10 min. on ice. Cells were washed with PBS/ 1% FCS/ 0.05%  $\text{NaN}_3$  and stained with the appropriate combination of antibodies as described. Cells were incubated with fusion protein, and bound MOG-Fc was detected with goat anti-human IgG FITC antibody (ICN 67-217). FACS analysis was carried out on a FACS Calibur (Becton Dickinson) using CellQuest software.

#### **4.6. *Ex vivo* elimination of B cells by MOG-Fc**

Splenocytes from TH mice (SJL/J background) were prepared. Single-cell suspensions were incubated with MOG-Fc (10  $\mu\text{g}/\text{ml}$ ) for 16 h at  $37^\circ\text{C}$ / 5%  $\text{CO}_2$  in DMEM/10% FCS in 5 ml cell culture polypropylene vials (Becton-Dickinson) at a density of  $4 \times 10^6$  cells/ml. Lymphocyte analysis was carried out by FACS using antibodies against  $\text{IgM}^a$ , IgD, Thy1 and CD19 (all BD Pharmingen). All tests were performed in triplicates.

#### **4.7. *In vivo* depletion of B cells in TH mice by MOG-Fc**

Female TH SJL/J-mice were treated twice with 100  $\mu\text{g}$  of MOG-Fc in 500  $\mu\text{l}$  PBS through i.p. injection (n=5). Blood was collected each day after treatment, PBLs were prepared, and lymphocytes were analyzed via FACS (FACSCalibur, Becton-Dickinson).  $\text{MOG}^+$  B cells were quantitated and normalized as percentage of total  $\text{B220}^+$  B cells detected in the lymphocyte gate. Biotinylated rMOG concentrations were chosen as to induce complete competitive inhibition of MOG-Fc binding. The experiment was repeated with TH mice on BL/6 background and yielded comparable results.

#### **4.8. Transfer of transgenic B cells into recipient wild-type mice**

Spleen cells of TH mice were stimulated with LPS (Sigma, 10 mg/ml) for 3 days. Non-B cells were then separated through incubation with biotinylated anti-CD43 Abs followed by sorting with Streptavidin-coupled magnetic beads (Dynabeads® M-280, Dynal, Oslo, Norway). 15 mice were injected i.v. with  $1.6 \times 10^7$  purified B cells. The next 3 days each 5 mice received a daily i.p. injection of either 100 µg recombinant MOG-Fc protein or 100 µg human IgG1 Ab, or PBS, respectively. Three days after the last i.p. injection, peripheral blood was taken from each mouse and the levels of transferred B cells as well as of the anti-MOG Ab-titer was determined in FACS and ELISA experiments, respectively. To this time point, six days after the B cell transfer, most LPS-stimulated TH B cells expressed low levels of MOG-binding, surface IgG, detected by double staining with biotinylated MOG, followed by streptavidin-phycoerythrin and with goat anti-mouse IgG (Fc-specific) (BD-Pharmingen).

#### **4.9. Detection of αMOG-Fc immune responses in ELISA**

Specific Abs were detected in ELISA assays as follows: microtiter plates coated with recombinant MOG protein or recombinant human IgG1<sup>51</sup> at a concentration of 10 µg/ml were incubated with individual sera at three different dilutions (1:10, 1:100 or 1:1000), and bound Abs were detected with alkaline phosphatase-labeled goat anti-mouse IgM or goat anti-mouse IgG Abs (BD-Pharmingen). Values for IgM correspond to the 1:100 dilution and values for IgG correspond to the 1:1000 dilution. The levels of serum MOG-Fc protein were determined in ELISA by coating plates with purified anti-MOG mAb 8.18-C5 (10 µg/ml) and developing bound protein with biotin-conjugated, monoclonal anti-human IgG (Fc-specific, clone HP-6017, Sigma, St. Louis, USA), followed by streptavidin-alkaline phosphatase and p-nitrophenyl phosphate (Sigma) incubation.

## **4.10. Immunomodulatory effects of MOG-Fc treatment in EAE**

### **4.10.1. Induction of EAE**

For conventional immunization, the antigen solution was mixed with equal volumes of complete Freund's adjuvant (CFA). This mixture was forced through a 24G tube (Hamilton) fixed between two syringes until a hard emulsion was obtained. After anesthesia with ether, mice were given injections of a total of 100 µg of antigen in a volume of 200 µl of emulsion. Female SJL/J mice (Charles River) were injected in the flanks and footpads. 300 ng of pertussis toxin in PBS were injected intraperitoneally on the day of immunization and again 48 hours later.

### **4.10.2. Clinical evaluation of EAE**

Weight was measured daily and clinical disease was assessed after immunization with the encephalitogen. The animals were scored for clinical signs of EAE according to the following scale:

0	no signs of disease
1	loss of tail tone
2	partial paralysis of one or both hindlimbs
3	complete paralysis of one or both hindlimbs
4	complete paralysis of one or both hindlimbs, paralysis of fore limbs
5	moribund or dead

## **4.11. Determination of T cell fine specificity against MOG M36 epitope**

### **4.11.1. Peptide synthesis**

The M36 region contained within the MOG extracellular domain was synthesized as a 15-mer peptide (EuroGentech). A set of singly substituted peptides was generated, each peptide carrying a single amino acid substitution to alanine from position 1 to position 15 (alanine scan).

### **4.11.2. T-cell proliferation assay**

Proliferation response of M36-specific T-cell-line (kindly provided by A. Iglesias, MPI Neurobiology Martinsried) to ala-substituted peptides was tested via standard <sup>3</sup>H-thymidine incorporation assay. Briefly, T-cells were cultured for a period of 14 days post re-stimulation with wild-type peptide. For assessment of proliferation, T cells were transferred to restimulation medium (DMEM complete, 5% FCS). Wild-type SJL/J splenocytes were prepared by standard protocol (see 4.5.) and irradiated with 4000 rad for use as APCs. The assay was set up in flat-bottom 96-well tissue culture plates. APCs and T cells were seeded at 10:1 (10<sup>6</sup>:10<sup>5</sup> per well) and incubated with 10µg/ ml of peptide at 37°C/ 5% CO<sub>2</sub>. After 48 hours, the cells were pulsed with <sup>3</sup>H-thymidine (1µCi/ ml). Thymidine incorporation was investigated 16 hours later.

### **4.11.3. Peptide competition assay**

Thymidine incorporation assay was performed to investigate the ability of the mutated peptides to function as T-cell antagonists, thus excluding interactions solely mediated through decreased binding to MHC II<sup>56;57</sup>. APCs were pre-pulsed with 10 µg/ ml of wt M36 peptide

for 2h at 37°C/ 5% CO<sub>2</sub>. Cells were then washed with restimulation medium and incubated with 10µg/ ml of the substituted M36 variants. Proliferation was assessed as described in 4.11.2.

#### **4.11.4. Cloning of mutated MOG-Fc constructs**

Site-directed mutagenesis was performed by standard protocol. Briefly, primers were synthesized covering the 5' and 3' terminal sequence (5': A, 3': D) of the region encoding the MOG extracellular domain. For mutagenesis, primers were chosen to include the desired nucleotide exchanges flanked by 15 to 20 bases to both the 3' and 5' end (forward primer (5'): C, backward primer (3'): B). Primers A and B were used in PCR to generate fragment I., primers C and D generated fragment II, each using MOG-Fc as a template. Following gel extraction, fragments I. and II. were used as templates to synthesize mutated MOG-Fc with primers A and D. This resulted in mutated constructs encoding MOG-Fc carrying a single amino acid substitution to alanine at position 10 of the M36 region (R-MOG), and another variant carrying a single substitution to alanine at position 13 (S-MOG). Transfection of CHO cells, selection of stable transfectants and purification of protein were carried out exactly as described for the wild-type MOG-Fc protein.

#### **4.11.5. Selective binding of mutated MOG-Fc to autoreactive B cells**

Whole lymphocytes from transgenic knock-in mice were prepared from spleen as described elsewhere<sup>11</sup>. Cells were incubated with fusion protein, and bound MOG-Fc was detected with goat-anti-human IgG FITC antibody (ICN 67-217). The subsequent incubation with anti-IgM, anti-B220, and anti-CD5 Abs was performed on ice for 20 min.

#### **4.12. Treatment of mice**

Female SJL/J mice were immunized with PLPs peptide on day 0. TH B cells were transferred 24 hours later via intravenous injection through the tail (see section 4.8.). On day 7 post-immunization, mice were treated with 100 µg of MOG-Fc protein ("wild-type"), 100 µg R-MOG and 100 µg S-MOG. Treatment was repeated on days 8 and 9. Mice were scored for clinical signs of EAE throughout the experiment, and weight changes were recorded daily.



## **5. Results**

### **5.1. Design, expression and biochemical characterization of fusion proteins**

Bispecific fusion proteins targeting autoreactive B cells must conform to a number of theoretical considerations. Informed choices had to be made regarding the selected expression system and the purification protocol. The structural integrity of the recombinant proteins was investigated by SDS-PAGE, Western blotting and ELISA analysis.

#### **5.1.1. Choice of expression vector**

The expression vector pEFdhfr was chosen in conjunction with dhfr-deficient chinese hamster ovary (CHO) cells as a suitable eucaryotic expression system. In pEFdhfr (Fig. 3), the expression of the construct of interest is driven by the promoter of the human elongation factor alpha. This promoter is known to be a very strong promoter in virtually all eukaryotic cells, thereby making this expression system a powerful tool for high protein expression without limitations regarding the selected eukaryotic host cell line<sup>49</sup>. The construct of interest is cloned into the multiple cloning site (MCS) using one or more of the restriction sites encoded in the MCS (EcoR1, Xba1, Sma1, Sal1). The expression of the construct of interest is linked to the expression of the selection marker dihydrofolate reductase (DHFR) via the internal ribosomal entry site (IRES). This arrangement assures that almost all stably transfected cells will express the construct, as both genes depend on the promoter of EF $\alpha$ . A strong polyadenylation signal for both genes is provided by the SV40 polyadenylation site, and the pUC18 backbone of the plasmid provides a well-characterized plasmid backbone with

ampicillin resistance for cloning purposes. This vector was used for the expression of the constructs encoding the two fusion proteins MOG-Fc and MOGxCD3.

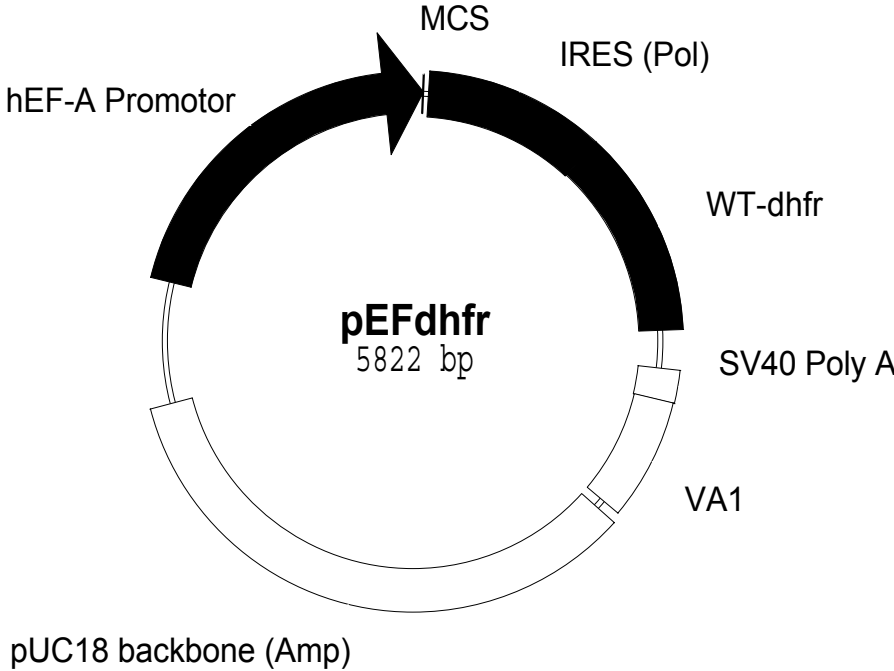


**Fig. 3.** Expression vector pEF-dhfr for transfection of dhfr-deficient chinese hamster ovary cells (CHO). MCS: multiple cloning site. IRES: internal ribosomal entry site. Dhfr: dehydrofolate reductase. SV40 Poly A: simian virus 40 polyadenylation sequence. PUC18: ampicillin resistance. HEF-A promotor: promotor of human elongation factor alpha

**A**

**MOG-Fc construct**

1173 bp



**B**

**MOGxCD3 construct**

1241 bp



**Fig. 4.** Generation of fusion protein constructs. **A.** Domain arrangement of MOG-Fc construct. **B.** Domain arrangement of MOGxCD3 construct. MOG-ex: extracellular domain of human myelin oligodendrocyte glycoprotein.

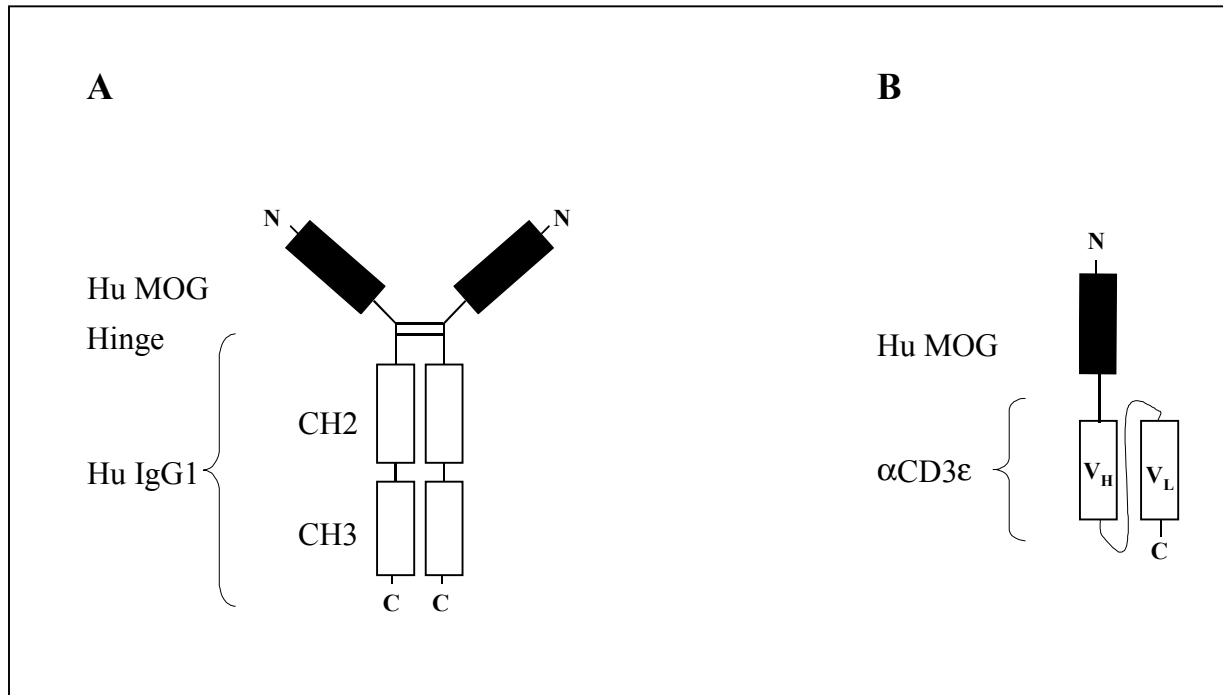


**Fig. 5.** Structure of fusion proteins **A.** Design of MOG-Fc. The constant CH3 and CH2 domains of human IgG1 (Hu IgG1) (open boxes), including the hinge region with two disulfide bonds, were fused to the extracellular domain of human myelin oligodendrocyte glycoprotein (Hu MOG) (filled boxes). **B.** Design of MOG $\times$ CD3. The extracellular domain of human MOG was connected to a C-terminally attached scFv antibody directed against the  $\epsilon$  chain of the human CD3 complex. N, N termini; C, C termini.

### 5.1.2. Design and characterization of MOG-Fc

The N-terminal 154 amino acids of the extracellular domain of human pro-MOG were fused to the C-terminal 233 amino acids of human IgG1 encompassing the hinge, CH2 and CH3 domains (see Fig. 4 for domain arrangement). The basic architecture of the fusion protein is shown in Figure 5A. Placing the fusion junction at the flexible hinge is known to facilitate proper folding of domains and helps to preserve the function of both parts of the molecule<sup>58,59</sup>. The pEFdhfr expression vector for MOG-Fc was constructed as described in the experimental protocol. Chinese hamster ovary (CHO) cells were transfected with the vector and selected for stable expression of the selection marker dhfr for a period of approximately two months. Glycosylation patterns of proteins expressed in CHO cells are very similar to those of human origin, which provides for maintenance of binding capacity to B cells as well as effector cells and also reduces the likelihood of immune responses to the fusion protein itself. Moreover, Fc fusion proteins can be expressed in CHO cells in much the same manner and efficacy as whole immunoglobulins. Purification of the molecule can be then be performed in a single-step protein A affinity chromatography. The ease of this type of purification, together with efficient mammalian cell expression, are significant advantages of such a bispecific Ig-chimera containing the Fc region over other fusion protein formats.

After completion of the selection procedure, stably transfected cells were used to seed a panel of 500 ml cell-culture roller bottles. It was discovered that culture systems allowing adherent growth of CHO cells (NalgeNunc International) produced the most consistent results. CHO cells were cultured 3 days post-confluency, which amounted to approximately 8-10 days in total culture time. MOG-Fc was purified from cell culture supernatant using a single protein A affinity chromatography step. Average yield was on the order of 5 – 10 mg of secreted

recombinant protein per liter of cell-culture supernatant. All of the MOG-Fc fusion protein purified from culture supernatant appeared to be in a dimerized form, as was evident upon SDS-PAGE analysis (Fig. 6, left panel) and by Western blotting using an anti-MOG monoclonal antibody (Fig. 6, right panel). Under reducing conditions, the affinity-purified MOG-Fc had an apparent molecular weight of 49 kDa (Figs. 3, lanes labeled +DTT), which is in accordance with the calculated molecular weight of 42 kDa and an expected complex-type N-glycosylation. A single band with an apparent molecular weight of 98 kDa was seen upon SDS-PAGE in the absence of reducing agent. Under these conditions, no monomeric MOG-Fc was detectable by SDS-PAGE or Western blotting (Figs. 6).

The integrity of the MOG-Fc protein was further confirmed in a sandwich ELISA using the anti-MOG monoclonal antibody 8.18-C5 for capturing and an alkaline phosphatase (AP)-conjugated anti-human-IgG antibody for subsequent detection (Fig. 7). Titration of the purified MOG-Fc protein resulted in a dose-dependent signal, showing that both antigen (MOG) as well as effector (IgG1-Fc) domains of the recombinant protein were present. Also, binding to the anti-MOG monoclonal antibody 8.18-C5 provided evidence that the B-cell targeting domain at the N-terminus of the fusion protein was correctly folded and capable of binding MOG-reactive immunoglobulin, as would be encountered in membrane-bound form on MOG-reactive B cells.

Taken together, size analysis by SDS-PAGE, Western blotting and binding to anti-MOG and anti-human Fc antibodies in ELISA suggested that MOG-Fc of the correct size and antigenicity was produced by CHO cells. Thus, all structural requirements of the MOG-Fc fusion protein were met.

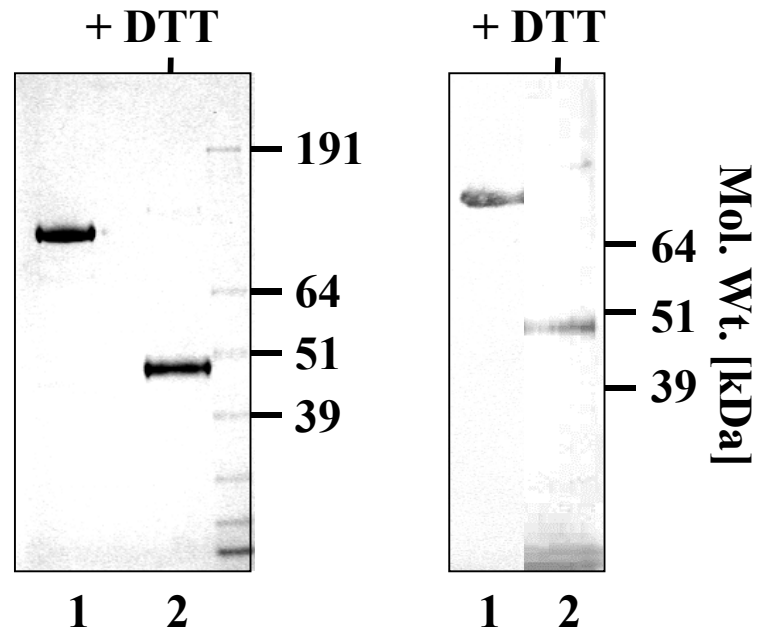


**Fig. 6.** Design, expression, purification and characterization of MOG-Fc. MOG-Fc was expressed in CHO cells and affinity-purified by protein A sepharose chromatography. Left: SDS-PAGE analysis of purified MOG-Fc in the absence (lane 1) and presence (lane 2) of the reducing agent dithiothreitol (DTT). Right: Western blot analysis of MOG-Fc in the absence (lane 1) and presence (lane 2) of DTT. After transfer of MOG-Fc from SDS gel to nitrocellulose filter, MOG-Fc was detected by the MOG-specific monoclonal antibody 8.18-C5 and an AP-conjugated secondary goat-anti-mouse antibody. The position of molecular weight standards is shown on the left and their size given as kilo Dalton (kDa).

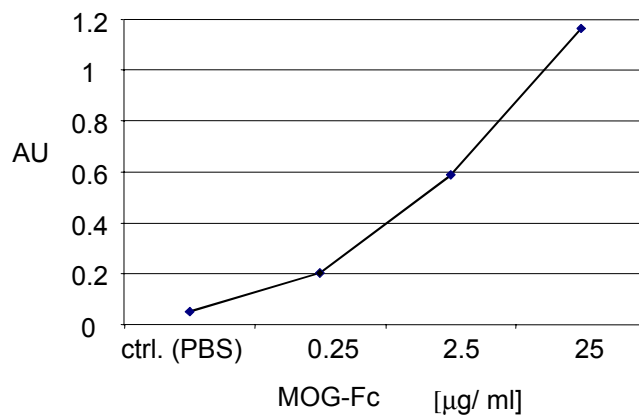


**Fig. 7.** Detection of MOG-Fc fusion protein in ELISA. ELISA plates were coated with anti-MOG antibody 8.18-C5 to capture the fusion protein by its MOG domain. Bound MOG-Fc fusion protein was detected with an AP-conjugated anti-human Fc antibody.

### 5.1.3. Design and characterization of MOGxCD3

For the construction of a MOG fusion protein with specificity for human T cells, expression vector pEF-dhfr was used. The construct consisted of the MOG extracellular domain at the N-terminus fused to the heavy chain variable region of an anti-human CD3 epsilon-specific Fv fragment (see Fig. 4, 5)<sup>49</sup>. A flexible glycine-serine linker with 15 amino acids in length was used to connect the two anti-CD3 V<sub>H</sub> and V<sub>L</sub> variable domains. A stretch of 6 histidines was fused at the outer C-terminus to allow affinity purification over nickel-chelating columns. Following stable transfection into dhfr-deficient CHO cells, the secreted protein was purified by 3-step chromatography, consisting of cation exchange, metal chelate chromatography and gel filtration. Identity and size of the purified recombinant protein were investigated via SDS-PAGE analysis followed by Western blotting.

After gel filtration, a single band was visible in SDS-PAGE, corresponding to the predicted size of the MOGxCD3 fusion protein (Fig. 8A, lane 5). Western blotting with 8.18-C5 anti-MOG monoclonal antibody revealed a single band with MOG reactivity (Fig. 8B) of the size observed in SDS-PAGE. Thus, both protein size and anti-MOG immunoreactivity were as expected.

In order to test whether both the MOG targeting moiety and the CD3 effector domain were present in the MOGxCD3 fusion protein, an ELISA was established using anti-MOG monoclonal antibody for capture followed by detection by an anti-Fv antibody specific for the anti-CD3 scFv. As shown in Fig. 9, incubation with MOGxCD3 resulted in a dose-dependent signal. Thus, MOGxCD3 was produced as an intact molecule consisting of both effector and targeting domains, and therefore had the potential to bridge MOG-reactive B-cell receptors and human T cells via CD3 epsilon. Furthermore, the binding of 8.18-C5 anti-MOG antibody



to the fusion protein indicated that the MOG targeting moiety was correctly folded, since 8.18-C5 detects a conformation-dependent epitope of the MOG extracellular domain<sup>52</sup>.

In conclusion, biochemical analysis revealed that two fusion proteins of the desired size and immunoreactivity were generated. These two proteins met all requirements they were designed for: MOG reactivity was found with both MOG-Fc as well as MOGxCD3, indicating that the MOG extracellular domain was correctly folded. Both proteins were readily secreted into the cell culture supernatant, which shows that the MOG-specific leader sequence can efficiently direct export of MOG antibody fusion proteins to the extracellular compartment. MOG-Fc was produced as a disulfide-linked dimer, whereas MOGxCD3 was detected solely as a monomeric protein upon gel filtration.

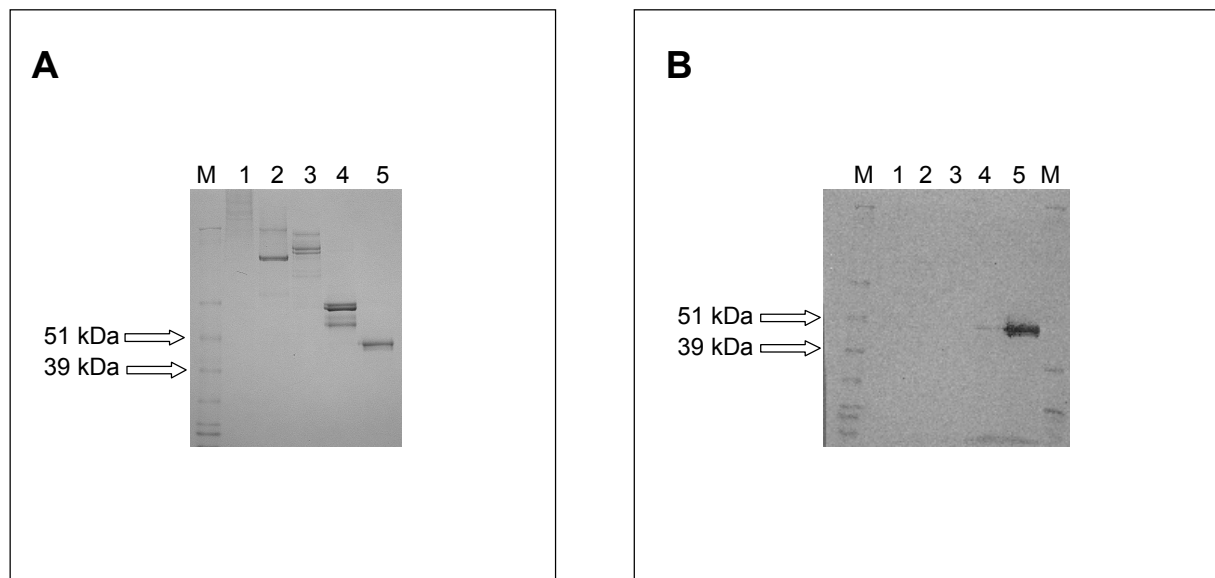


**Fig. 8.** Design, expression, purification and characterization of MOGxCD3. MOGxCD3 was expressed in CHO cells and affinity-purified by 3-step chromatography. **A.** 5 Gel filtration peaks are shown, separated by SDS-PAGE and analyzed by Coomassie blue staining. Peak number 5 contains monomeric MOGxCD3 protein of a molecular mass of approximately 47kDa **B.** After transfer of MOGxCD3 from SDS gel to nitrocellulose filter, MOGxCD3 was detected by the MOG-specific monoclonal antibody 8.18-C5 and an AP-conjugated secondary goat-anti-mouse antibody. The position of molecular weight standards is shown on the left and their size given as kilo Dalton (kDa).

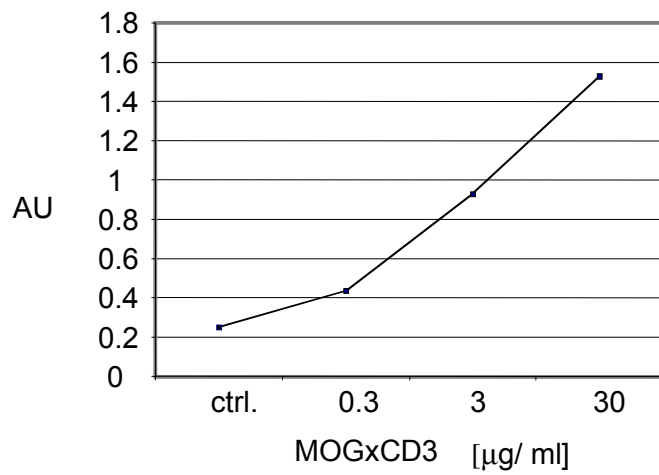


**Fig. 9.** Detection of MOGxCD3 fusion protein in ELISA. ELISA plates were coated with anti-MOG antibody 8.18-C5 to capture the fusion protein by its MOG domain. Bound MOG-Fc fusion protein was detected with an AP-labelled chicken-anti-scFv polyclonal antibody.

## **5.2. Binding of MOG fusion proteins to effector cells**

Biochemical analysis showed that the structural requirements were fulfilled by both recombinant proteins. Furthermore, ELISA data proved that the MOG domain was correctly folded and functionally intact, and that proteins containing both effector and MOG domain on a single polypeptide chain were generated. The ability of the Fc part in MOG-Fc to bind to Fc-receptor positive cells, as well as the capability of the anti-CD3 scFv in MOGxCD3 to bind to human T cells was examined in the following experiments.

### **5.2.1. Binding of MOG-Fc to Fc receptor-positive cell line**

The murine monocyte-macrophage cell line p388.D1 was employed as FcR-positive cell line<sup>53</sup>. The p388.D1 cells were incubated with various dilutions of the MOG-Fc protein. Binding of the Fc fusion protein was investigated in FACS analysis via FITC-labeled anti-human Fc $\gamma$  antibody. As shown in Fig. 10, bound MOG-Fc was detected in a dose-dependent manner. MFI values observed for MOG-Fc were similar to those obtained with another human IgG1 serving as isotype control (not shown). The Fc effector domain of the fusion protein was intact, properly dimerized and thus capable of binding to FcR<sup>+</sup> cells. This suggested that the MOG-Fc protein was truly of a bispecific nature, capable of binding to both effector as well as target cells.

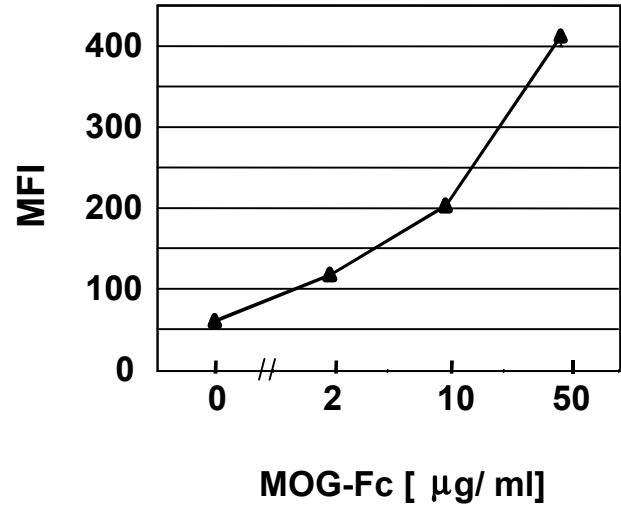
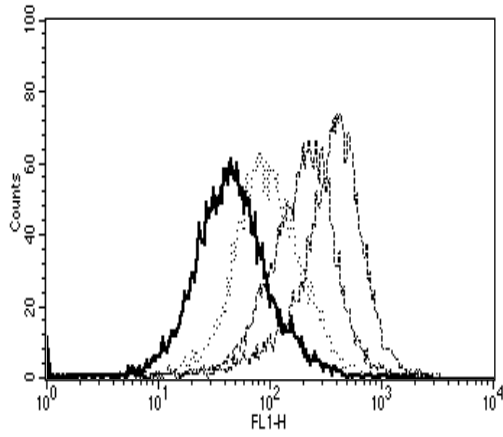


**Fig. 10.** Binding of MOG-Fc to a murine macrophage cell line. The monocyte/macrophage cell line p388.D1 expressing murine Fc receptors was incubated with MOG-Fc. Bound MOG-Fc was detected via FITC-labeled anti-human Fc $\gamma$  antibody by flow cytometry (left panel). Binding was quantitated and is expressed as mean fluorescence intensity (MFI) (right panel).

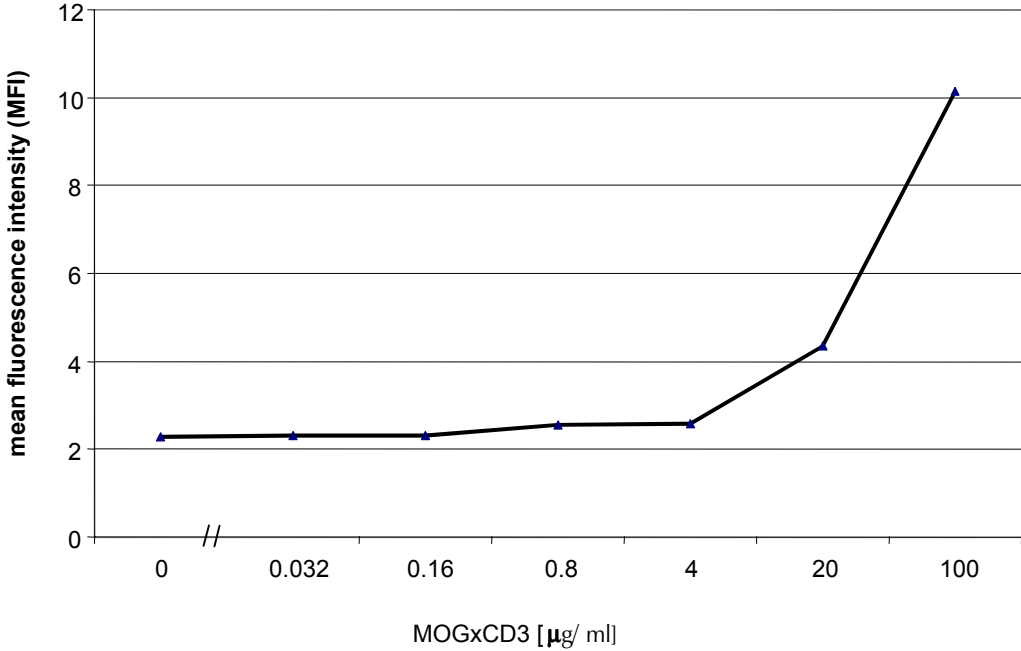
### 5.2.2. Binding of MOG $\times$ CD3 to primary human T cells

Single-chain antibody fragments can suffer a complete loss in binding activity when fused to other protein domains. This is due to the fact that the unnaturally linked heavy and light chain variable domains have to firmly assemble to form a binding groove for their respective antigen. In a complete antibody, the constant domains of the Fab part serve dimerization via a disulfide bridge in the C<sub>H1</sub> region, allowing correct assembly of the separate variable domains from heavy and light chains.

To investigate whether the MOG $\times$ CD3 construct was still able to bind to CD3 $\epsilon$  on human T cells, a FACS-based binding assay was used. Human CD3-positive cells were isolated from buffy coats as described in the material and methods section. Following incubation with varying concentrations of the MOG $\times$ CD3 fusion protein, recombinant protein bound to CD3-positive cells was detected with anti-MOG monoclonal antibody. FACS analysis revealed a dose-dependent signal at protein concentrations between 4 and 100  $\mu$ g/ml (Fig. 11). This result was not necessarily expected, since fusion partners other than scFvs have never been investigated with this C-terminal anti-CD3 antibody fragment. Thus, the MOG $\times$ CD3 protein was able to bind to human T cells as well as the anti-MOG B-cell receptor, a prerequisite for receptor bridging between T cells and autoreactive B cells.

Taken together, *in vitro* analysis indicated that MOG-Fc and MOG $\times$ CD3 fusion proteins of the correct size and structure were generated with the desired binding properties of the MOG targeting, Fc $\gamma$ - as well as anti-CD3 effector domains. These proteins had the potential to bridge the receptors of autoreactive B cells with those of effector cells, which may lead to re-

directed lysis of the putative target B cell. Consequently, a test for functional activity was developed in order to investigate the biological properties of the generated fusion proteins.

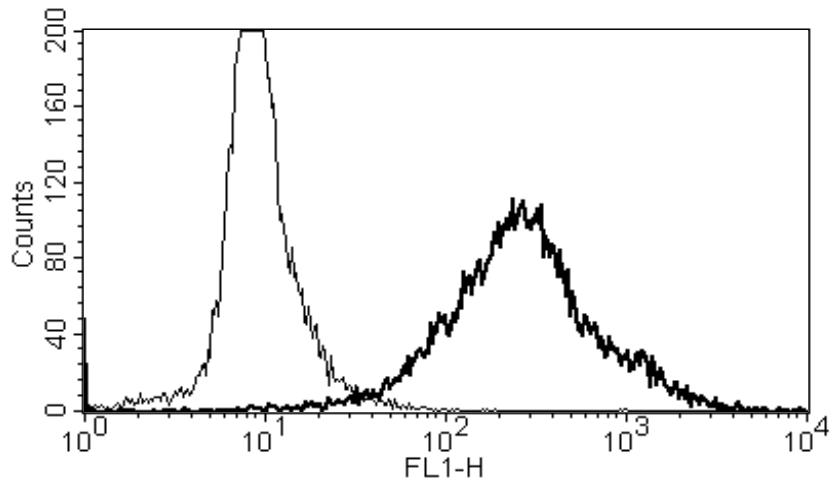
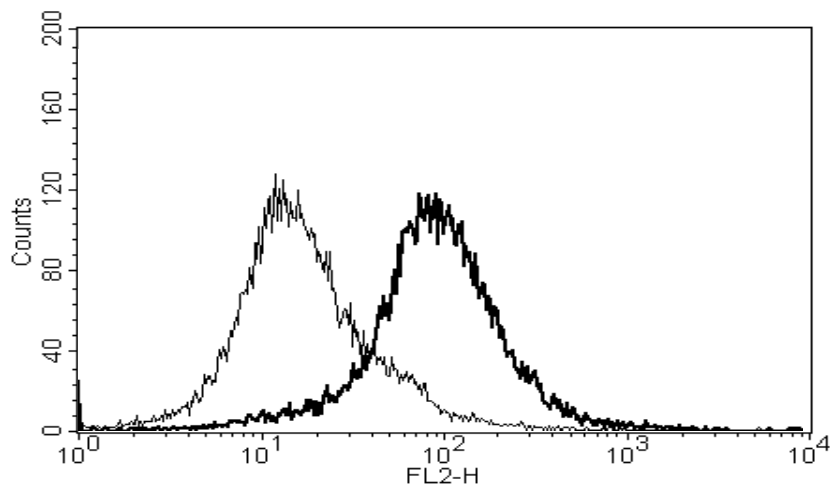


**Fig. 11.** Binding of MOGxCD3 to human T cells. Fusion protein was incubated with human CD3-positive PBMCs, and MOGxCD3 bound to T cells was detected with monoclonal anti-MOG antibody followed by FITC-labelled anti-mouse IgG1 antibody. Mean fluorescence intensity values (MFI) obtained in FACS analysis are shown.

### 5.3. Assessment of *in vitro* cytotoxicity

To test whether the potential crosslinking of target and effector cells by MOG fusion proteins is leading to elimination of MOG-reactive target cells, an *in vitro* FACS-based cytotoxicity assay<sup>54;55</sup> was developed (illustrated in Fig. 13). A major challenge of the assay was the generation of a suitable target cell line. Primary B cells from anti-MOG transgenic animals did not tolerate the assay conditions and went into apoptosis within hours post-isolation (data not shown). Due to the extremely low abundance of anti-MOG B cells in humans, patient material was not an option either. A solution was found: 8.18-C5 hybridoma cells were cultured in serum-free medium for a period of 4-5 months. Long-term culture appeared to induce the expression of high levels of cell-surface bound anti-MOG antibody (Fig. 12). This may be due to a shift in mRNA processing leading to a transcript which contains the MC exons coding for the transmembrane region of cell surface immunoglobulin.

As seen upon FACS analysis (Fig. 12A), adaptation to serum-free medium of 8.18-C5 hybridoma cells that normally secrete anti-MOG monoclonal antibody resulted in an expression of cell surface-associated murine IgG. Such hybridoma cells were capable of binding recombinant MOG on their cell surface (Fig. 12B). Thus, a stable target cell line was generated that expressed anti-MOG binding specificity on the surface. This cell line was used in conjunction with purified human PBMCs as effector cells to examine antibody-mediated cellular cytotoxicity.

**A****B**

**Fig. 12.** Flow cytometric characterization of a hybridoma line expressing MOG-reactive surface IgG. **A.** Surface expression of IgG on 8.18-C5 hybridoma cells. Hybridoma cells were cultivated in serum-free medium for 4-5 months, and cell-surface muIgG1 expression was examined with FITC-labeled goat-anti-muIgG1 antibody using flow cytometry. **B.** rMOG binding to the 8.18-C5 hybridoma line. Binding was examined with biotinylated rMOG followed by staining with streptavidin-PE. Controls show staining with the secondary labeling reagents alone.



### **5.3.1. Investigation of cytotoxicity mediated by MOG-Fc**

A FACS-based assay was developed to examine antibody-dependent cellular cytotoxicity mediated by the MOG-Fc fusion protein. This assay was based upon 1) discrimination of live and dead cells by propidium iodide (PI) and 2) identification of target cells via a specific marker (illustrated in Fig. 13). PI is a dye that stains cells having lost membrane integrity. In contrast to other systems, such as annexinV labeling, which is a marker for early apoptotic events, PI stains both apoptotic and necrotic cellular populations at a relatively advanced stage of cell death<sup>60-63</sup>. As a target cell marker, an antibody specific for mouse IgG was chosen. This assay system turned out to produce the most consistent results. Other variations of the assay, such as pre-labeling of target cells with the vital dye calcein, proved to be unreliable (data not shown). This was due to the fact that the anti-MOG target cell line was propagated in serum-free medium and did not tolerate the calcein labeling procedure. Uptake of labeled cells by macrophages, which can result in false-positive stainings, is a problem that was also occasionally encountered in this type of assay. Plotting PI on the y-axis versus anti-mouse IgG on the x-axis of a FACS dot plot, was chosen as the preferred discrimination between target and effector cells.

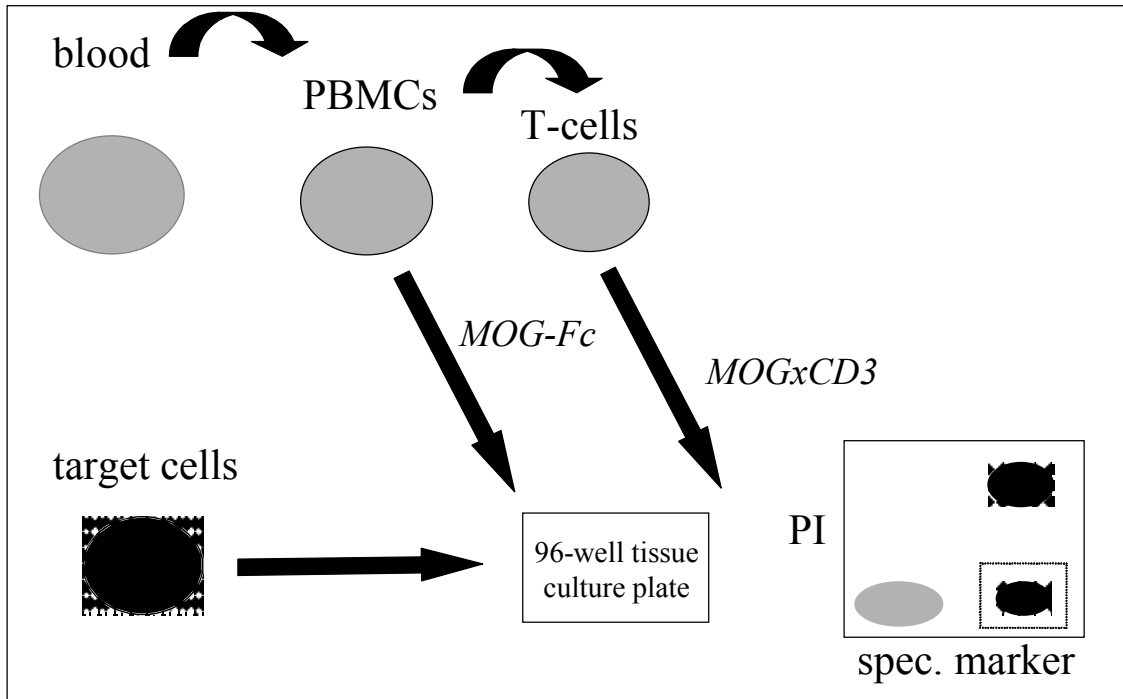


**Fig. 13.** FACS-based assay for the investigation of antibody-dependent cellular cytotoxicity (ADCC) mediated through bispecific fusion proteins. Primary blood mononuclear cells (PBMC) were extracted from buffy coats obtained from human donors. For investigation of cytotoxicity mediated by anti-CD3 fusion proteins, T cells were further enriched and used as effectors. Primary effector cells and target cells were incubated in 96-well tissue culture plates for the duration of the assay. FACS analysis (lower right) was carried out with a specific target cell marker stained against propidium iodide to discriminate between live and dead target cells.

Incubation of human PBMC as effectors and 8.18-C5 target cells at a ratio of 10:1 in the presence of MOG-Fc resulted in a complete elimination of anti-MOG target cells, as seen by the disappearance of propidium iodide-negative, anti-murine IgG-positive cells in the presence of human PBMC (Fig. 14A). No significant target cell lysis was observed in the absence of PBMCs or fusion protein (Fig. 14B). A dose-response analysis showed that half-maximal efficacy of specific target cell lysis occurred at a concentration below 100 ng/ml MOG-Fc (Fig. 14C). Complete elimination of target cells was achieved at an optimal dose of 10 µg/ml, while further increases in protein concentration up to 100 µg/ml resulted in a decrease in specific toxicity (not shown).

The specificity of MOG-Fc-mediated cell lysis in the assay was investigated by using both unrelated human IgG1 and a mouse B-cell line expressing unrelated IgG on its surface. (Figs. 14D and E). The EpCAM antigen-specific recombinant human IgG1<sup>51</sup> that can bind to human effector cells via its Fc part, but not to MOG-specific immunoglobulin on hybridoma cells, did not lead to significant redirected lysis of 8.18-C5 cells (Fig. 14D, bar 2). Likewise, the mouse B cell line TIB-208, expressing cell-surface IgG of non-MOG specificity, was not sensitive to MOG-Fc mediated lysis (Fig. 14E, bar 2). The assay was repeated 6 times. Maximum efficacy was dependent on PBMC donor and ranged from complete elimination (>98% specific lysis in 3 independent experiments) down to 44% at optimal dose. Anti-mouse IgG1 staining was not inhibited by the presence of the fusion protein.

In conclusion, the data obtained with this FACS-based ADCC assay show that the MOG-Fc fusion protein was indeed able to re-direct primary human effector cells to kill anti-MOG positive hybridoma cells. Re-directed lysis was observed in a specific dependence on the target BCR and fusion protein specificity. The outcome of the experiment was unpredictable, since coupling of B cells and FcγR<sup>+</sup> effectors through an Fc fusion protein may lead to a cell-

to-cell distance (see Fig. 2C as an illustration) that is larger than with antibodies against smaller cell-surface molecules, such as CD20. It is conceivable that a putative large distance may have prevented the effective engagement and subsequent triggering of Fc $\gamma$ R<sup>+</sup> effector cells.

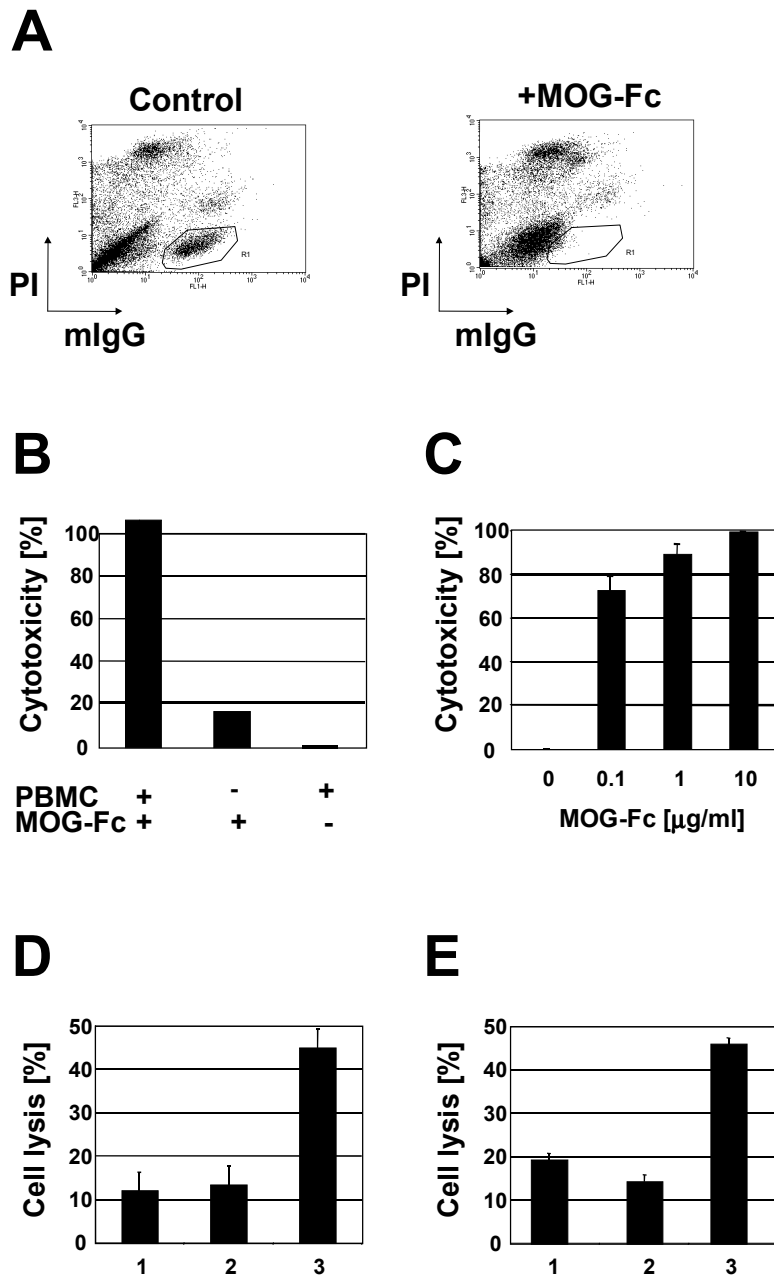


**Fig. 14.** Cytotoxic activity of MOG-Fc. 8.18-C5 target cells were incubated with human PBMCs and serial dilutions of MOG-Fc protein in RPMI/10% FCS. Incubation was performed for 16 h at 37°C/5% CO<sub>2</sub>. After incubation, target cells were labeled with anti-muIgG1 antibody (mIgG) and analyzed for viability through propidium iodide (PI) staining. **A.** Flow cytometric detection of target cell lysis. FACS scans from untreated and MOG-Fc-treated target cells on a background of PBMCs is shown. The gate used for quantitation of target cell elimination is indicated. **B.** Dependence of target cell elimination on both PBMC and MOG-Fc. As indicated, the assay was performed for 16 h in the absence or presence of PBMCs (E:T-ratio 10:1) and 10 µg/ml MOG-Fc. **C.** Dose response of the cytotoxic effect of MOG-Fc. The assay was performed at the indicated concentrations of MOG-Fc for 16 h in the presence of PBMCs (E:T ratio = 10:1). Viable mIgG-positive target cells were counted and normalized to percentage of viable target cells in the control (see Experimental Protocol). Data are representative of 3 experiments with similar results. **D.** The effect of a non-specific human IgG1. Column 1, incubation of PBMCs and target cells in the absence of isotype control and MOG-Fc. Column 2, the effect of a recombinant human IgG1 (isotype control). Column 3, the effect of MOG-Fc under identical assay conditions. **E.** The effect of MOG-Fc on an unrelated murine cell line. Mouse B cell line TIB-208 is expressing cell surface IgG1 of non-MOG specificity. Column 1, spontaneous lysis of TIB-208 cells in the presence of human PBMC. Column 2, the effect of MOG-Fc (10 µg/ml) on the viability of TIB-208 cells. Column 3, the effect of MOG-Fc (10 µg/ml) on hybridoma line 8.18-C5 under identical assay conditions. Error bars indicate S.D. values of triplicates.

### 5.3.2. Investigation of cytotoxicity mediated by MOG $\times$ CD3

The cytotoxicity mediated by the MOG $\times$ CD3 fusion protein was investigated in the FACS-based assay also used for the Fc fusion protein. The only difference was that freshly isolated human T cells rather than whole PBMCs were used as effectors. FACS analysis revealed disappearance of PI-negative, mouse-IgG positive target cells with increasing concentrations of the MOG $\times$ CD3 protein (Fig. 15A). This dose-response analysis showed half-maximal lysis at a concentration of approximately 100 ng/ ml (Fig. 15A). Maximal redirected lysis was observed at an optimal concentration of 1  $\mu$ g/ ml, translating into 80% specific toxicity after incubation for 16 h at 37°C/ 5% CO<sub>2</sub>. Thus, MOG $\times$ CD3 was produced as an active molecule capable of re-directing primary human T cells to kill anti-MOG positive target cells.

The specificity of cell-mediated toxicity was investigated as shown in Fig. 15B. MOG $\times$ CD3-mediated lysis was dependent on the presence of effector T cells (Fig. 15B, bar 2). Spontaneous lysis, measured after separate incubation of both effector and target cell populations for the duration of the assay, is shown in the last bar; here, cells were added together just prior to FACS analysis. Furthermore, incubation of cells at an effector-to-target (E:T) cell ratio of 5:1, instead of the standard 10:1 ratio, resulted in a shift of EC<sub>50</sub> of approximately a factor of 10, providing further evidence that MOG $\times$ CD3-mediated lysis is effector-cell dependent (Fig. 16).

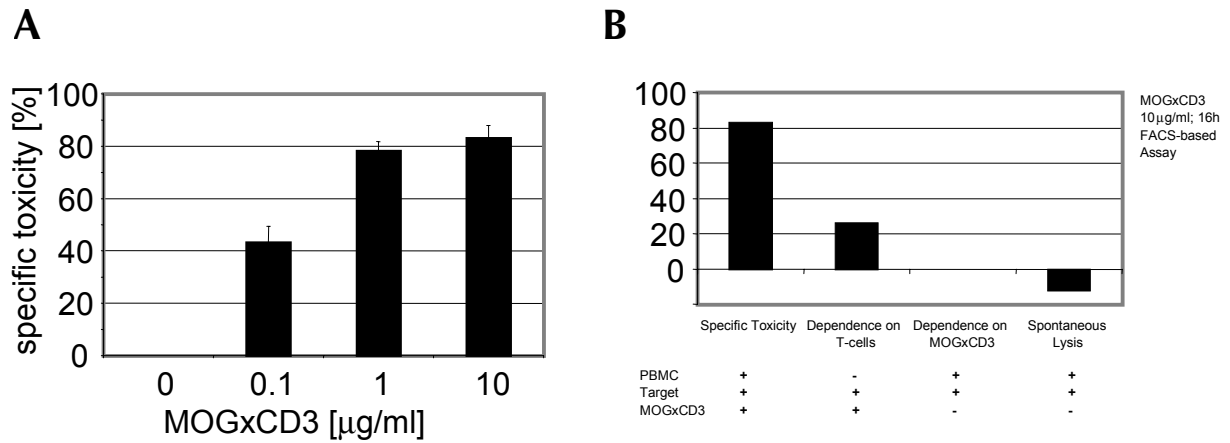


**Fig. 15.** Cytotoxic activity of MOGxCD3 fusion protein. FACS-based assay was performed. 8.18-C5 target cells were incubated with human CD3+ PBMCs and serial dilutions of the MOGxCD3 protein. Incubation was performed for 16h at 37°C/ 5% CO<sub>2</sub>. After incubation, target cells were labelled with anti-IgG1 antibody and analyzed for viability through counterstaining with propidium iodide (PI). Viable murine IgG1+ cells were counted and expressed as percentage of viable target cells in control (see materials and methods). **A.** Dose-response analysis. **B.** Specificity of lysis.

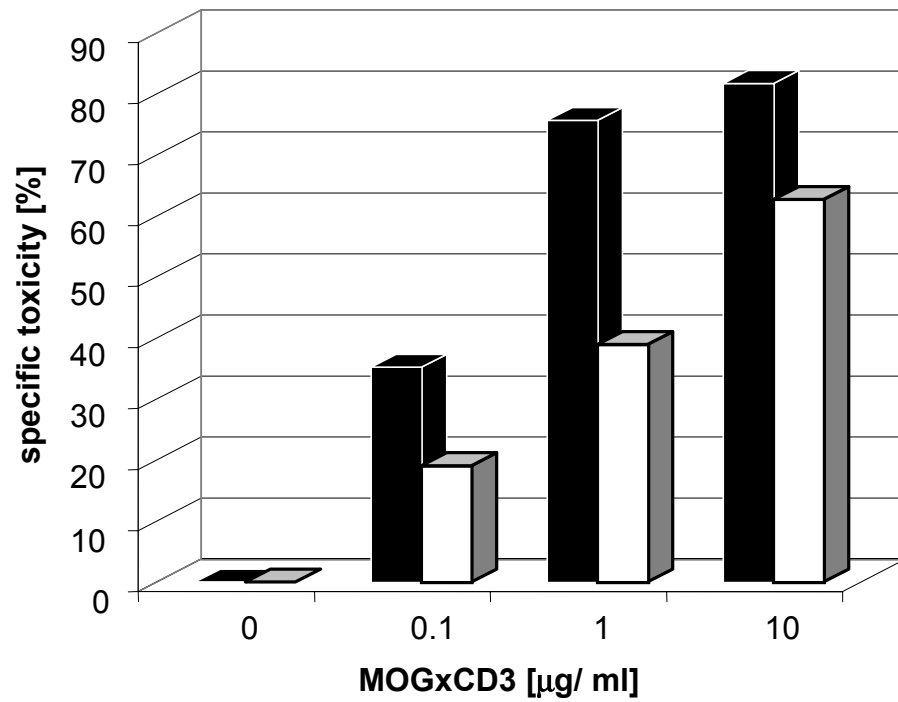


**Fig. 16.** Cytotoxic activity of MOGxCD3 is dependent on ratio of effector to target cells (E:T-ratio). Assay was performed as described for Fig. 11 with varying concentrations of effector cells and a constant number of 8.18-C5 target cells. Black bars: E:T-ratio 10:1. White bars: E:T-ratio 5:1.



In summary, these data show that MOGxCD3 exhibited cytotoxic activity against anti-MOG positive target cells. This in-vitro cytotoxicity was effector-cell dependent and specifically mediated by the fusion protein. Thus, human T cells could be re-directed and triggered to kill anti-MOG positive target cells by the novel MOGxCD3 antibody fusion protein.

#### **5.4. Investigation of MOG-Fc *in vivo* using a transgenic mouse model**

The effect of the MOG-Fc fusion protein on natural B cells was further investigated using the anti-MOG transgenic TH mouse model (illustrated in Fig. 1)<sup>11</sup>. Since human Fc $\gamma$ 1 is known to interact with murine Fc receptors, these studies were feasible<sup>42;64</sup>. This is in contrast to the MOGxCD3 molecule<sup>49</sup>, which is specific for human CD3 only and does not cross-react with the mouse TCR complex. Therefore, the following sections will deal exclusively with the characterization of the MOG-Fc fusion protein.

##### **5.4.1. Cell binding activity**

Binding of MOG-Fc to primary MOG-reactive B cells as well as primary effector cells was investigated using splenocytes from anti-MOG transgenic and wild-type mice (Fig. 16A). In these transgenic mice (designated TH), the endogenous heavy chain-J region has been replaced by the rearranged 8.18-C5 anti-MOG VDJ segment using knock-in technology (see Fig. 1)<sup>11;65</sup>. As a result, almost all B cells of transgenic mice express the MOG-specific heavy chain in combination with endogenous light chains.

It was observed in FACS analysis that >90% of all IgM-positive splenocytes from the TH knock-in mice (Fig. 17A, lower panel in bold) but not of control littermate mice (Fig. 17A, upper panel) did bind recombinant MOG-Fc. Approximately one third of IgM-positive B cells in TH mice bound MOG-Fc with high intensity while the remaining two thirds bound MOG-Fc with low intensity (Fig. 17A, lower panel). This binding pattern is reminiscent of the one reported using biotinylated, bacterially produced, recombinant rat MOG (rMOG)<sup>11;66</sup>. In this report, however, two thirds of the TH B cells did not bind rMOG at all or only poorly, and only one third of B cells bound rMOG with a broad range of intensities. Such differences are likely due to an intrinsically higher affinity of TH B cells to MOG-Fc which, in contrast to the bacterially generated rMOG, is dimeric, properly folded, N-glycosylated and has not undergone biotinylation.

Binding of MOG-Fc to wildtype splenocytes was also investigated. The upper panels of Figure 17B and 17C show FACS staining of wild-type splenocytes in the absence of MOG-Fc fusion protein. In the lower panel, wild-type splenocytes were incubated with MOG-Fc, and identical FACS stainings as in the upper panel were performed. As seen in panel 17B, MOG-Fc did bind to the Mac1<sup>high</sup> (CD11b) population, indicating a preferential binding to macrophages and myeloid CD8<sup>+</sup> DCs<sup>67;68</sup>. No binding of MOG-Fc to CD5<sup>+</sup> T cells could be detected, underscoring the selectivity for FcγR<sup>+</sup> cells. Anti-MOG (8.18-C5) positive cells in the lower quadrants most probably represented B cells binding the protein through their inhibitory Fc receptor FcγRII-B1. In contrast to panel A, stainings in the lower quadrants of Fig. 17B and 17C were performed at room temperature (see materials and methods).

In conclusion, these data show specific binding of MOG-Fc to both MOG-reactive B cells as well as Fcγ-receptor positive immune effector cells on primary mouse splenocytes.

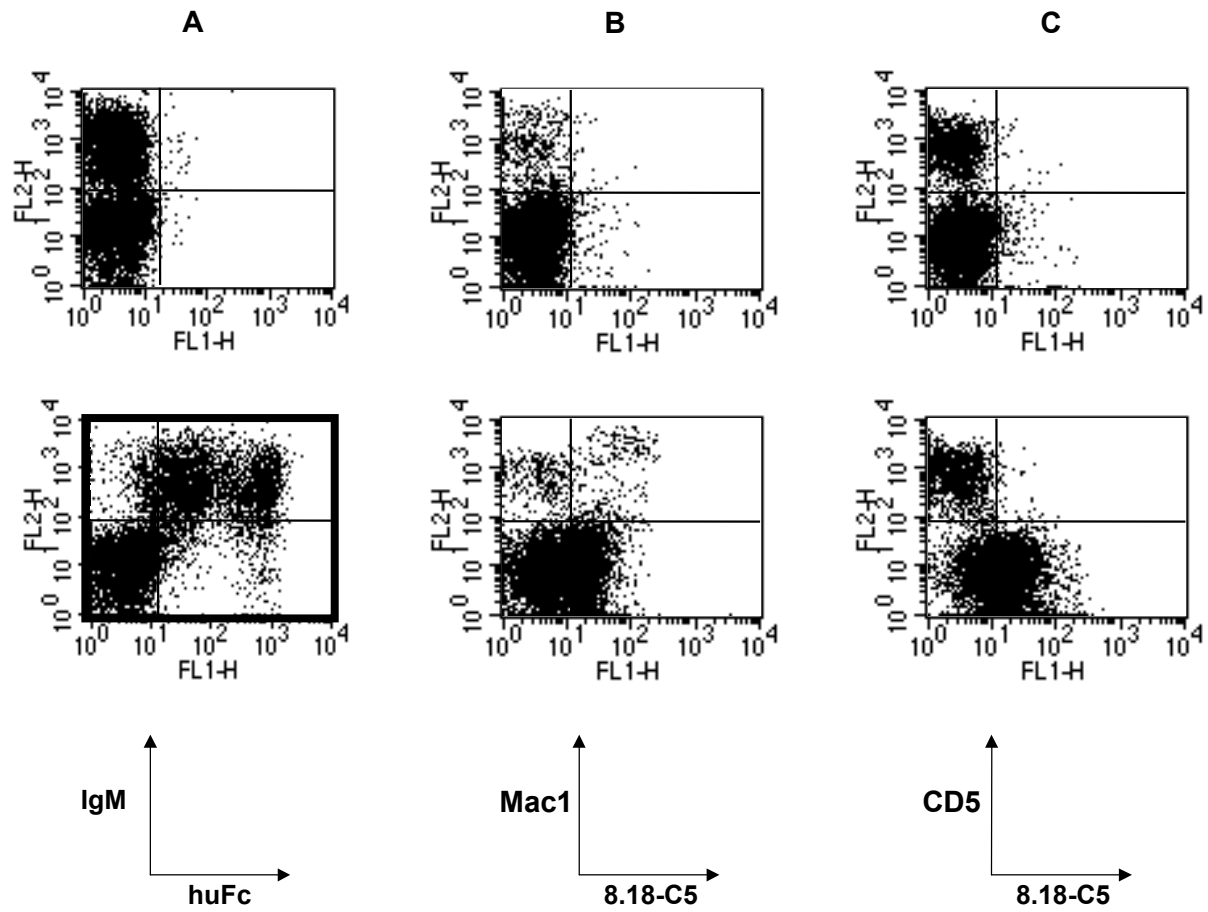


**Fig. 17.** Flow cytometric analysis of cell binding properties of MOG-Fc. **A.** Binding of MOG-Fc to B cells of Ig-MOG transgenic TH mice (bolded box). Splenocytes from wt (upper panel) and TH mice (lower panel, bold) were prepared and incubated with MOG-Fc. MOG-Fc bound to IgM-positive cells was detected by FITC-labeled human Fc $\gamma$ -specific antibody (huFc). **B, C.** Binding of MOG-Fc to Mac-1- and CD5-positive, wt mouse splenocytes. Single-cell suspensions of splenocytes were prepared. Cells were incubated with 50  $\mu$ g/ml MOG-Fc protein (lower panel) or PBS (upper panel). Cell-bound MOG-Fc was detected with biotinylated, monoclonal  $\alpha$ -MOG antibody 8.18-C5, followed by counterstaining with streptavidin-FITC, and Mac1-phycoerythrin (PE) or CD5-PE. Low-avidity binding to Mac1 and CD5 negative subpopulation in the lower panel is due to staining protocol.

## **5.4.2. *In vivo* effect of MOG-reactive B cells in transgenic and wild-type mice**

### **5.4.2.1. Antibody responses in mice treated with MOG-Fc**

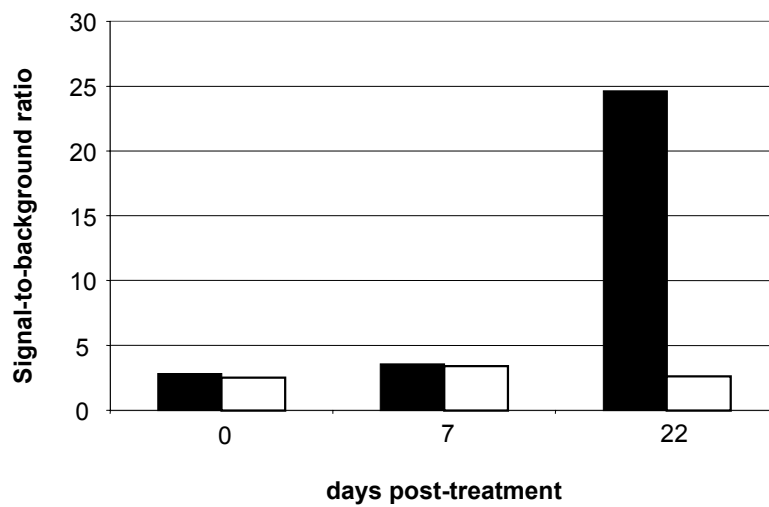
It was the aim of this study to devise new strategies aimed at targeting autoreactive B cells in the MOG-Ig model system with the potential to be used as therapeutics in autoimmune disease. Two key questions had to be answered:

- I. Does treatment with the fusion protein lead to antibodies against the two functional domains of the protein?
- II. Can one detect a B-cell depletion by MOG-Fc treatment in a "worst-case scenario" where high titers of autoreactive antibodies are present and constantly replenished?

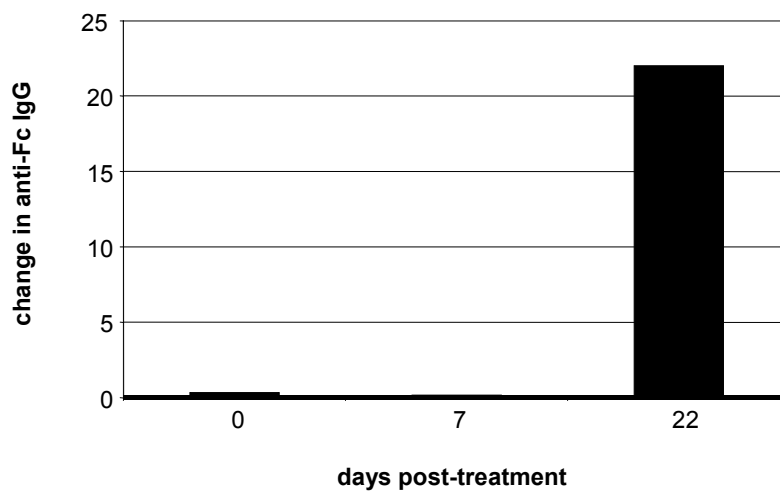
For question I., the answer was quite predictable. Indeed, human Fc is immunogenic in mice and led to formation of anti-Fc antibodies. As shown in figure 18A, wild-type mice develop anti-human Fc-specific IgG after treatment with the MOG-Fc protein. On the same note, MOG is regarded as being essentially 'foreign' by the peripheral immune system due to its CNS restriction<sup>66;69</sup>. Consequently, both anti-Fc and anti-MOG IgG antibodies were detected in wild-type mice treated with MOG-Fc fusion protein 22 days post-treatment (Fig. 18A, B).

Concerning the second question, the outcome is not easily foreseeable. Would the protein ever reach its target B cells in the presence of substantial anti-MOG Ig in the serum<sup>11</sup>? Would application of the protein lead to pathogenic phenomena, such as immune-complex deposition and renal failure, or shock syndromes? Can a depletion of MOG-reactive B cells be detected at all?

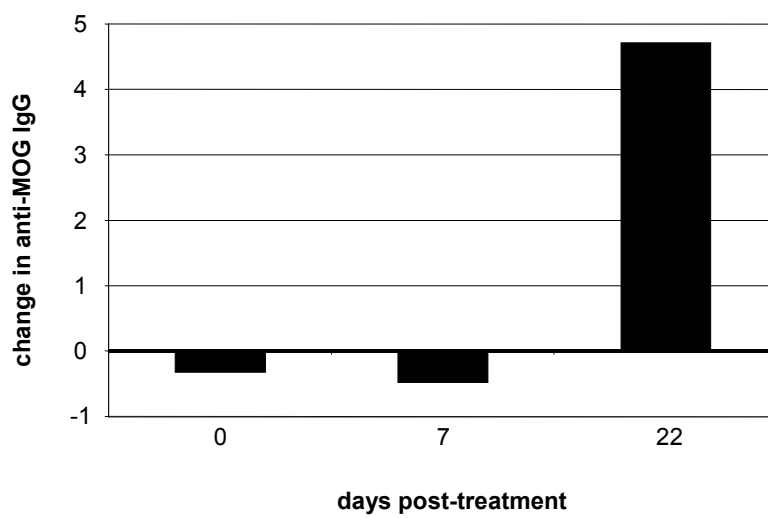
# A1



# A2



# B



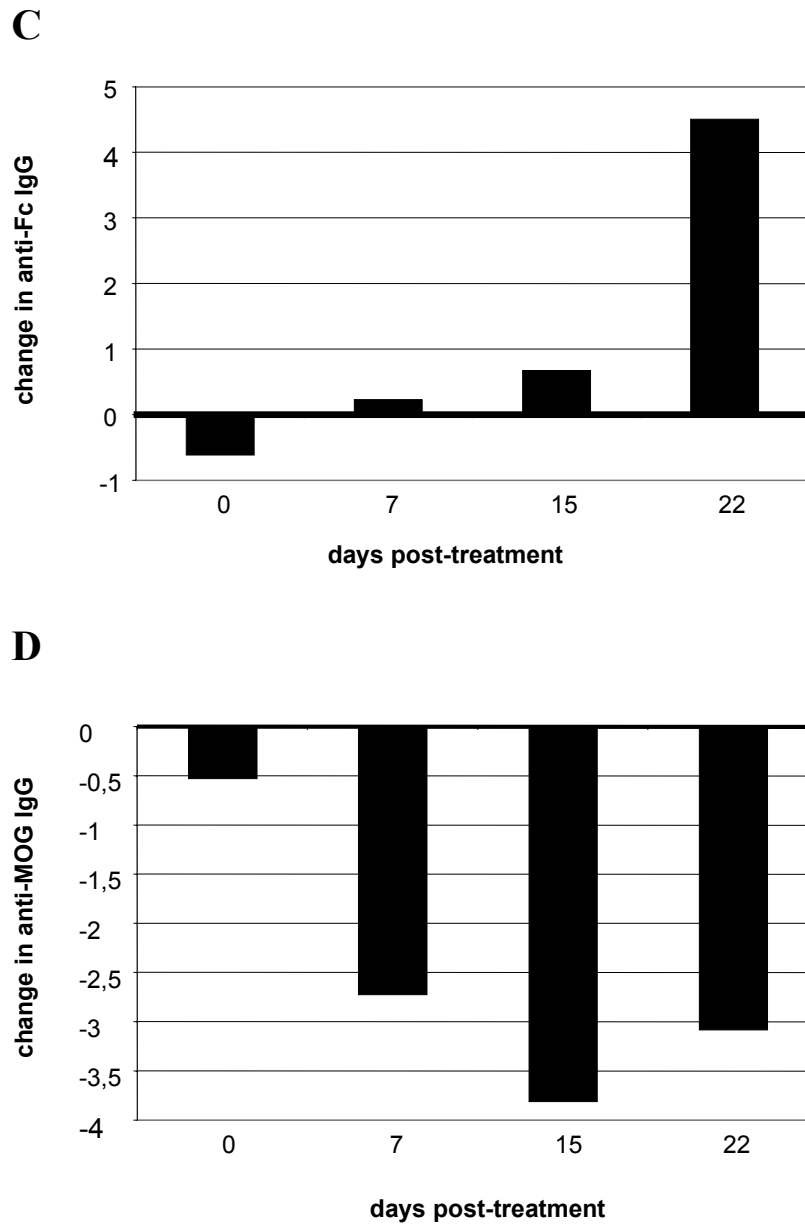


**Fig. 18.** Serum antibody titers in response to treatment with MOG-Fc. Mean values for 3-5 animals are shown. **A.** IgG response against human IgG1-Fc in wild-type (wt) mice. **A1.** Background signal of each individual sera sample against BSA was taken into account to normalize ELISA values (signal-to-background ratio). Black bars: mice treated with the fusion protein on day 1, 3 and 5. White bars: Untreated control animals. **A2.** Change of IgG response against human Fc in wt mice. Difference between values for treated vs. untreated control animals are plotted on the y-axis, obtained as illustrated in Fig. A1. **B.** Change in anti-MOG IgG response in wt mice. **C, D.** Response of TH mice post treatment with MOG-Fc. **C.** IgG titer against human Fc in MOG-Ig mice. **D.** Change in IgG titer against MOG in TH mice after treatment with the MOG-Fc fusion protein.

In fact, treatment of TH mice led to anti-human Fc titers with a kinetic profile comparable to that induced in wild-type animals (Fig. 18C). Twenty-two days post-treatment, TH mice developed anti-human Fc IgG titers (Fig. 18C). Surprisingly, anti-MOG IgG was markedly reduced in TH mice followed for 22 days after treatment (Fig. 18D). This reduction was most pronounced at day 15 post-treatment but still prominent throughout the 22-day observation period of the experiment. Evidently, treatment with MOG-Fc induced an antibody response against human Fc while, at the same time, leading to long-term reduction of anti-MOG antibody titers in TH mice. This result suggested an effect that could not simply be mediated by short-term adsorption of anti-MOG immunoglobulin and subsequent clearance of immune complexes. Thus, the cytotoxic effect of MOG-Fc on MOG-specific B cells was further investigated.

#### **5.4.2.2. *Ex vivo* cytotoxic activity of MOG-Fc**

To assess whether MOG-Fc can also eliminate natural B cells expressing MOG-reactive cell-surface immunoglobulin in a physiological environment, splenocytes from anti-MOG transgenic TH mice were isolated and tested in an *ex vivo* assay system. A special polypropylene cell culture system was established that allowed the isolated primary splenocytes to maintain viability for periods greater than 48 hours in a small medium volume of 250  $\mu$ l. In addition, recovery of lymphocytes was almost quantitative after the assay period, since the polypropylene vials did not allow macrophages or monocytes to attach to the plastic surface.

Transgenic splenocytes were prepared and incubated with 10  $\mu$ g/ml of the fusion protein for 16 hours. The endogenous Fc $\gamma$ R-bearing cells served as effectors. FACS analysis documented

a highly significant depletion of B cells, as defined by antibodies specific for the allotype-specific B cell marker IgM<sup>a</sup>, for IgD and for CD19 (Fig. 19). For all three markers, B cell depletion reached an order of 70%. The 10% increase in the percentage of Thy1<sup>+</sup> T-lymphocytes mirrored the decrease in MOG-specific B cells, representing about 10% of total live lymphocytes in the samples (Fig. 19).

Thus, the MOG-Fc protein was able to trigger mouse endogenous effector cells to specifically kill syngenic, MOG-reactive B cells in *ex vivo* splenocyte cultures from TH mice.

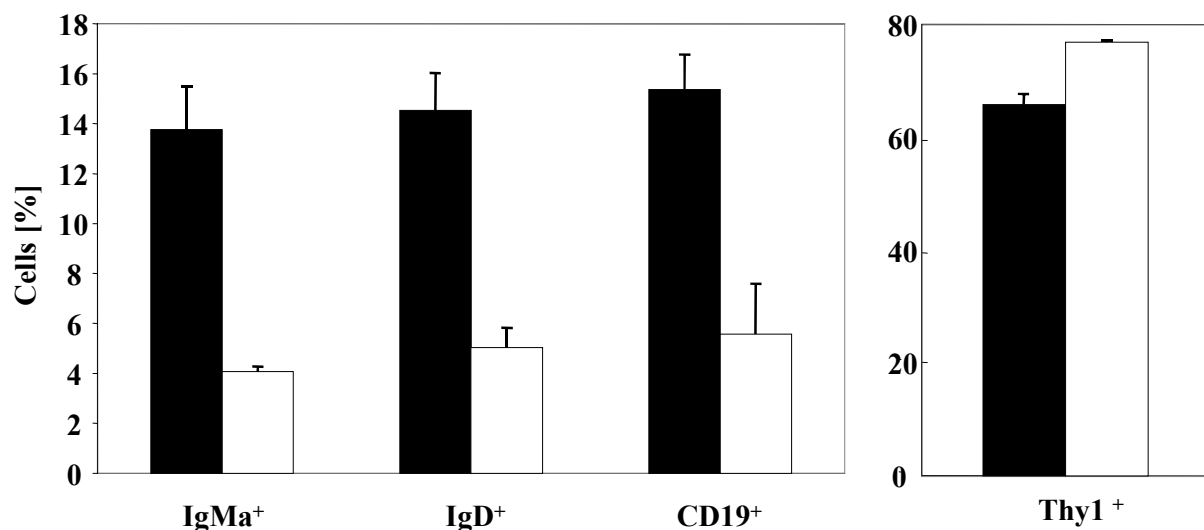


**Fig. 19.** The effect of MOG-Fc on TH splenocytes *ex vivo*. Single cell suspensions of spleens from Ig-MOG transgenic TH mice were prepared. Splenocytes were cultured in the absence (dark columns) or presence (white columns) of MOG-Fc (10  $\mu$ g/ml). After incubation, the B cell population was analyzed by flow cytometry using antibodies against the B cell markers IgM, IgD and CD19 and, as non-B cell marker, anti-Thy1. The frequency of cell populations is expressed as percentage of total live cells within the lymphocyte gate. Error bars represent S.D. values of triplicates.

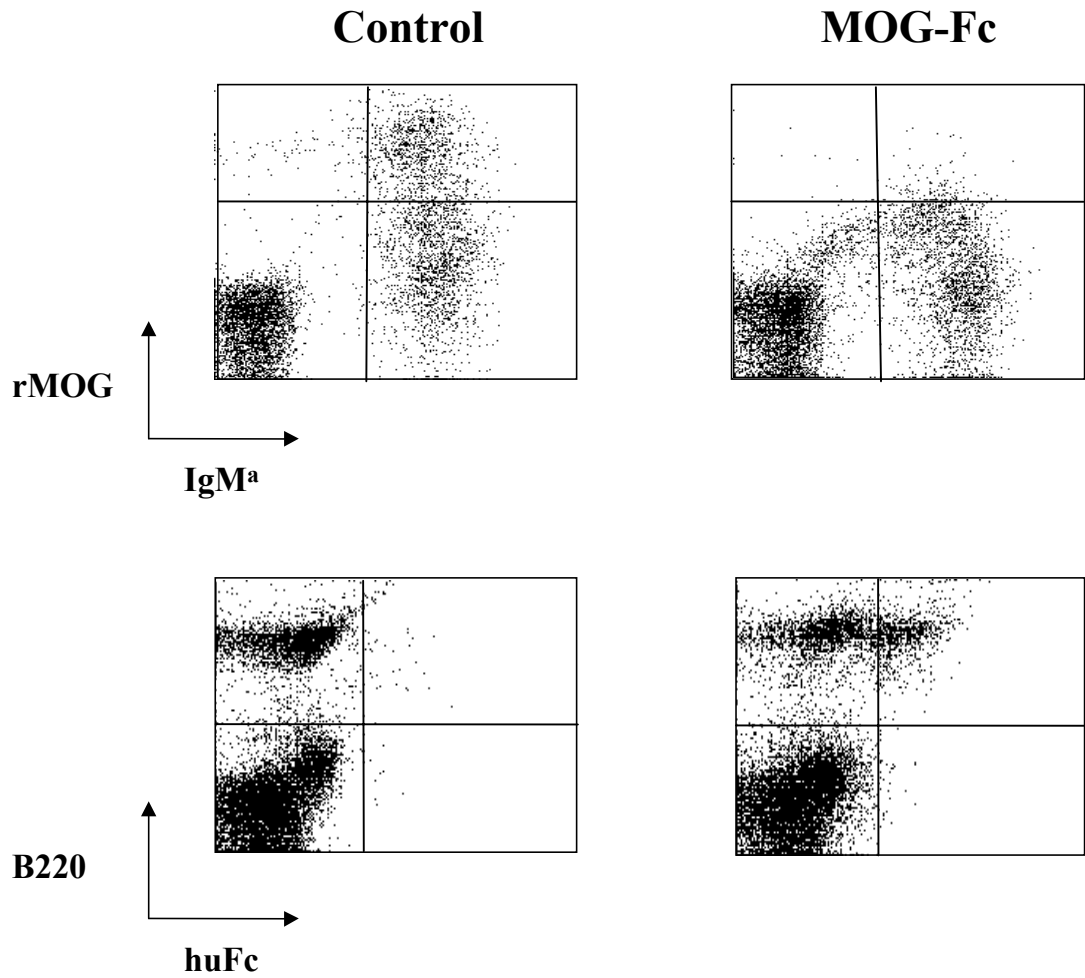
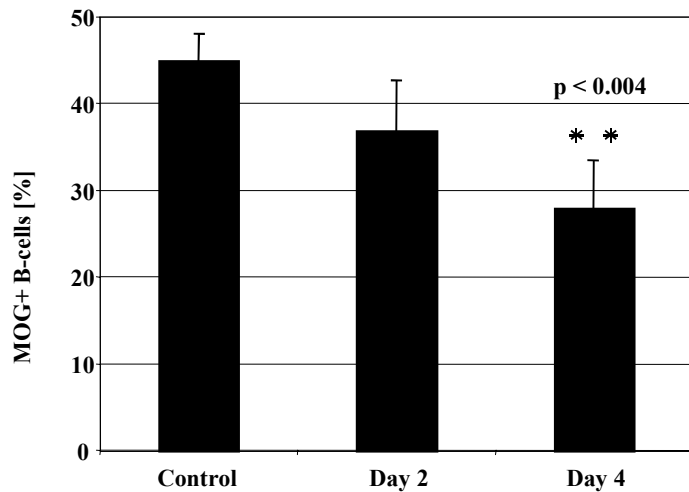


### 5.4.2.3. Effect on the B-cell population in TH mice

Having proven that MOG-Fc can deplete autoreactive B cells both *in vitro* and also *ex vivo*, the biological properties of the fusion protein were investigated in the relevant animal model. The cytotoxic efficacy of MOG-Fc was tested *in vivo* using the anti-MOG transgenic TH mouse. One hundred µg of MOG-Fc was administered intraperitoneally on days 1 and 3, and peripheral blood B lymphocyte counts were determined by FACS analysis one day post treatment. In spite of the fact that MOG-reactive B cells are generated in the bone marrow of mice on the order of  $10^7$  cells/ day (Antonio Iglesias, unpublished observation), which continuously replenishes eliminated B lymphocytes, it was found that MOG-Fc was efficient in depleting IgM-positive B cells in the fraction that strongly reacted with MOG (Fig. 20A, upper panel). MOG-Fc was still bound to B cells 24 h post-treatment (Fig. 20B), as detected by anti-human Fcγ staining of isolated B220-positive blood lymphocytes.

The percentage of MOG<sup>high</sup> B-cells decreased with statistical significance from 45% in control to less than 30% on day 4 after the first treatment (Fig. 20B). Since the number of B220-positive B cells was decreased to the same extent as the number of IgM-positive B cells (not shown), it is concluded that the reduction of B cells, as measured by flow cytometry, was due to depletion of cells and not associated with down-modulation of the B-cell receptor.

In summary, MOG-Fc was able to deplete autoreactive B cells in an *in vivo* model system. Remarkably, this result was observed in the presence of extremely high anti-MOG antibody titers and of an almost exclusively MOG-Ig positive B cell population.

**A****B**

**Fig. 20.** Effect of MOG-Fc treatment on MOG-Ig tg mice. TH mice were left untreated (Control) or treated i.p. with 100  $\mu$ g of MOG-Fc protein on days 1 and 3. **A.** Flow cytometric analysis of B cells from MOG-Fc-treated TH mice. Upper panel, the effect of MOG-Fc on IgM<sup>a</sup>-positive, rMOG-reactive B cells. Lower panel, analysis of MOG-Fc binding to B220-positive B cells as detected by an anti-human Fc $\gamma$  antibody. Peripheral blood lymphocytes (PBLs) were prepared 1 day post-treatment and their MOG<sup>high</sup> B-cell population was analyzed as indicated. Five MOG-Fc-treated and three control animals were analyzed. Representative results are shown. **B.** The effect of MOG-Fc on the MOG<sup>high</sup> B-cell population in TH mice. FACS data from five animals were quantitated and are shown as percentage of total B220<sup>+</sup> cells. Bars give S.D. values.

#### **5.4.2.4. Effect of MOG-Fc on autoreactive B cells and antibody titers in a transfer model**

The normal B-cell population in mice is naturally dominated by naive, IgM<sup>+</sup>, IgD<sup>+</sup> B lymphocytes. In MOG-Ig transgenic TH mice, B cell development follows a normal path<sup>66</sup>. Therefore, B cell depletion can be observed for the naive B-cell population only. In an autoimmune situation, however, the pathogenic cellular compartment that needs to be addressed is not that of the naive B cells, which has never encountered antigen, but it is the actively switching, proliferating B-cell blast compartment. A direct measurement of anti-MOG IgG secreted by these activated B lymphocytes, and by plasma cells, was of special interest in this context, since a marked decrease in anti-MOG IgG was observed in TH mice treated with the fusion protein. On the same note, significant changes in MOG-specific IgM titers were never encountered in TH mice. Therefore, the effect of MOG-Fc treatment on an activated B-cell population in the absence of an endogenous B-cell pool with MOG specificity was examined.

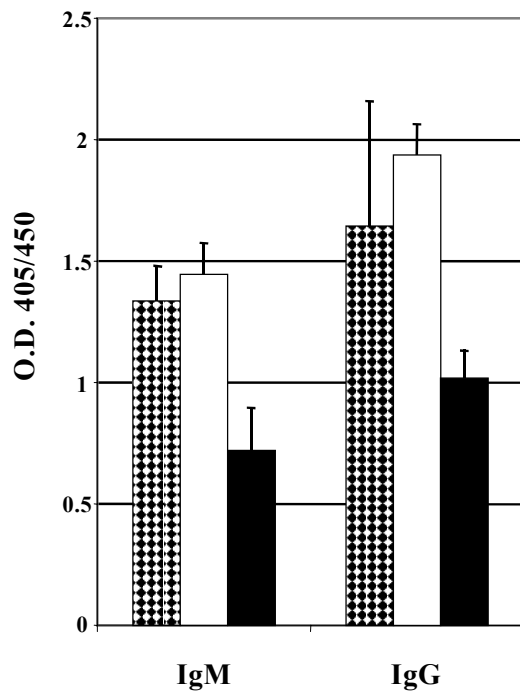
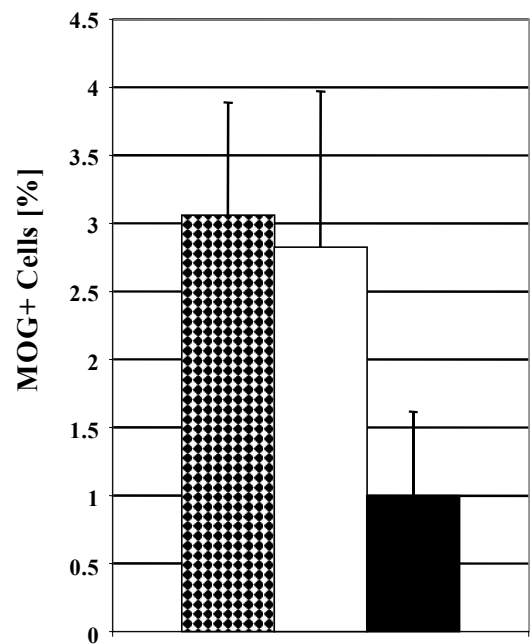
In TH mice, the number of MOG-reactive B cells is much higher than what the MOG-Fc protein would encounter in an autoimmune situation in non-transgenic mice. Nonetheless, TH mice treated with MOG-Fc showed a significant reduction in their MOG-reactive B-cell population. However, this system is rather artificial due to constant replenishment of MOG-reactive B cells from the bone marrow in high number and does not allow a fair comparison to autoimmune conditions encountered in humans, where few autoreactive B cells are present among a large background of endogenous, non-reactive B lymphocytes. To investigate a more natural situation, the capacity of MOG-Fc to deplete defined numbers of MOG-specific B cells adoptively transferred from TH mice into syngenic wild type mice was analyzed. C57BL/6 mice were first injected i.v. each with  $1.6 \times 10^7$  LPS-stimulated, purified TH B-cells

and then, on days 1, 2 and 3 after transfer, individual groups of transferred mice received 100  $\mu\text{g}$  of MOG-Fc i.p., control human IgG1 or PBS. The use of LPS-stimulated, instead of resting, B cells permitted the assessment of the effect of MOG-Fc on surface Ig<sup>+</sup> blast cells in the presence of secreted anti-MOG Abs, a situation more likely to reflect an ongoing autoimmune response in need of therapy. As shown in Fig. 21B, six days after B cell transfer, recipient mice treated with PBS or control human IgG1 Ab<sup>51</sup> consistently accumulated in their peripheral blood about 3% of MOG-binding, IgG<sup>+</sup> B cells, as well as high titers of MOG-specific IgM and IgG (Fig. 21A). In contrast, mice treated with MOG-Fc showed a strong though not complete depletion of both MOG-binding B cells and Abs (Fig. 21B, black column). MOG-Fc was detectable in serum at an average concentration of 21  $\mu\text{g}/\text{ml}$  3 days after treatment, while serum titers were below detection limit by day 10 (not shown). This is a remarkable result, since anti-MOG IgG was found to be reduced throughout the 22-day observation period in TH mice (Fig. 18D). This result shows that the reduction in autoreactive immunoglobulin titer in both the TH but also the wild-type transfer model system was caused by depletion of B cells, and not mainly through passive absorption and short-term clearance of immune complexes.

Interestingly, no pathological side effects were observed in any of the treated animals (both TH and transferred wild-type groups) followed for 2 months post-treatment. This is an interesting finding, since both MOG-Fc and MOG-specific antibodies were present at high titers in the animals that had received the fusion protein.

In final conclusion, these data demonstrate that the MOG-Fc antibody fusion protein exhibited the desired cytotoxic properties against autoreactive B cells in all systems investigated. *In vitro* analysis provided evidence that the protein was able to re-direct human Fc $\gamma$ R<sup>+</sup> effector cells to kill an anti-MOG<sup>+</sup> target cell line in a specific manner. In a syngenic *ex vivo* situation,

MOG-Fc induced the specific depletion of MOG-reactive B cells from transgenic animals. Investigation of the most relevant systems *in vivo* showed that the recombinant protein was capable of reducing anti-MOG antibody titers in an animal model. This reduction was still observed at time points when protein levels in the circulation were below detection limit, suggesting that the long-term reduction in autoreactive antibody titers was due to depletion of the autoreactive B cell compartment, and not due to short-term adsorption of MOG-Fc complexed with anti-MOG immunoglobulin. Indeed, the quantification of MOG-reactive B cells after treatment showed that those B cells were specifically depleted in the treated animals. This depletion was observed in anti-MOG transgenic TH mice and also in a wild-type mouse system transferred with syngenic MOG-reactive B cells.

**A****B**

**Fig. 21.** Depletion of MOG-reactive B cells by MOG-Fc in wt mice. BL/6 mice were transferred i.v. with purified B cells from anti-MOG transgenic TH mice. Following transfer on day 0, animals were treated with PBS (black and white bars), isotype control (human IgG1, white bars) or MOG-Fc (black bars) on days 1, 2 and 3 by i.p. injection. 5 animals were analyzed per group. **A.** Serum IgM and IgG titers against MOG on day 6 post-transfer, as determined by ELISA. **B.** FACS analysis of MOG-reactive B cells in peripheral blood.

## 5.5. Effect of MOG-Fc treatment in EAE

Experimental autoimmune encephalomyelitis is an induced autoimmune disease of the CNS and the established disease model for multiple sclerosis (MS). Pathology in EAE is mediated mainly by a Th1 response, and therefore EAE is not a prototype model for antibody-mediated autoimmunity. However, MOG-specific autoantibody responses are thought to exacerbate EAE pathology. For this reason, it was investigated whether treatment with the MOG-Fc fusion protein had an effect on EAE disease progression and severity.

The MOG M36-induced EAE was chosen as a suitable disease model<sup>70</sup>. Upon immunization with the M36 peptide, SJL/J mice develop a chronic but relatively mild CNS disease clinically characterized by episodes of recovery and relapse. It was decided that any therapeutic intervention had to be started after the first signs of disease in order to closely mimic a situation that may be encountered in human therapy. Mice were treated after cessation of the first clinical symptoms (see Fig. 22) with 3 doses of 100 µg each of MOG-Fc every other day, a dosing regimen that had shown to be effective in the depletion of B cells from transgenic TH mice.

The MOG-Fc treated animals were spared from clinical symptoms of EAE for a period of 5 days after the untreated control group presented with first signs of disease (Fig. 22). Disease scores in the non-treated control group averaged a mean of 2 (N=5), while no signs of disease whatsoever were observed in the treated animals for 23 days post immunization. However, on day 24 p.i., the MOG-Fc treated animals started to show characteristic symptoms of EAE disease. Remarkably, the disease progressed very rapidly, resulting in a clinical score >4 within 27 days post immunization. The animals had to be sacrificed at this clinical stage. The course of this delayed-type, hyperacute pathology was significantly more severe in the treated

animals than in the non-treated control group, which recovered from the second phase of M36-induced EAE within 26 days post immunization. At that time point, the MOG-Fc treated animals presented with an average score > 3.5.

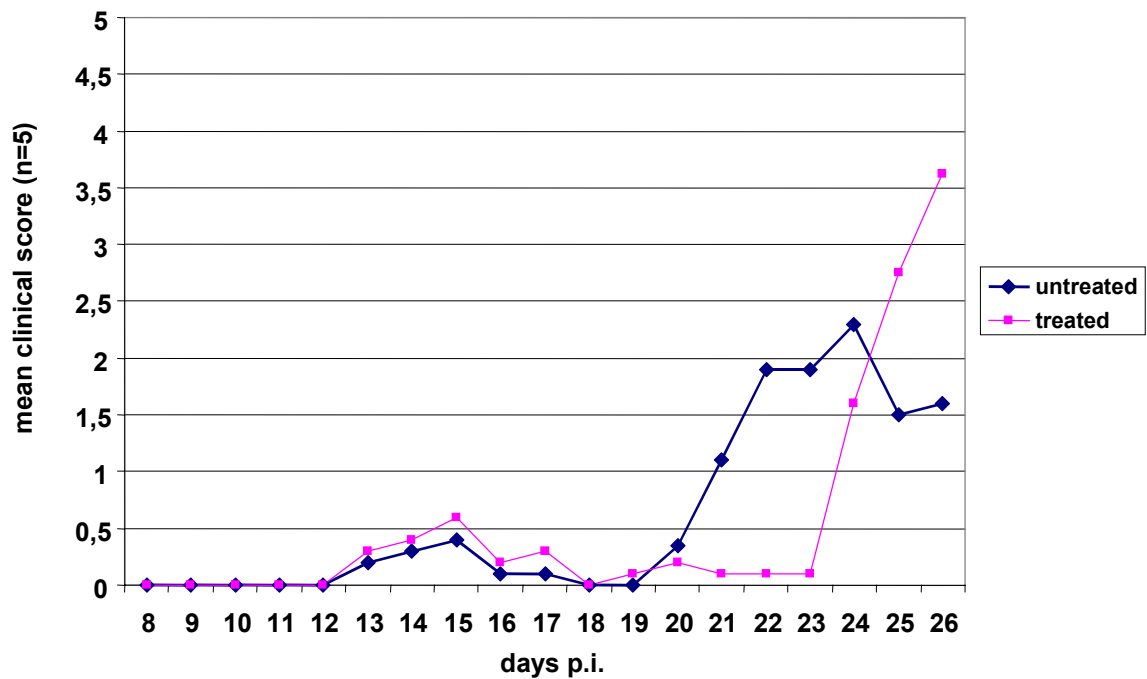


**Fig. 22.** Effect of MOG-Fc treatment on EAE. SJL/J mice were immunized with M36 peptide on day 0. On days 17, 19 and 21, animals were treated with 100  $\mu$ g of MOG-Fc protein in PBS via i.p. injection. No clinical signs of disease were observed for the MOG-Fc treated group (red) until day 24 post-immunization, whereas the untreated control group developed EAE by day 21. At day 24, treated animals presented with first signs of clinical EAE. Rapid disease progression was observed in the treated group.



## **5.6. Fine specificity of the T-cell response in SJL/J mice**

Due to the severe exacerbation of EAE observed after MOG-Fc treatment, it was hypothesized that treatment must have induced a highly pathogenic, MOG-specific T-helper response, much like the one seen with animals immunized with bacterially produced, recombinant MOG in CFA<sup>69</sup>. Responses versus MOG in the SJL/J mouse system are always directed against a single epitope contained within the extracellular domain of the MOG protein, however. Therefore, it was decided to further analyze the specificity of the SJL/J T-cell response against this epitope, designated M36, with the aim of discovering mutations within the epitope that would abolish recognition by M36-specific T cells, and thereby prevent undesired activation of MOG-specific T cells.

### **5.6.1. Alanine scan of M36 epitope**

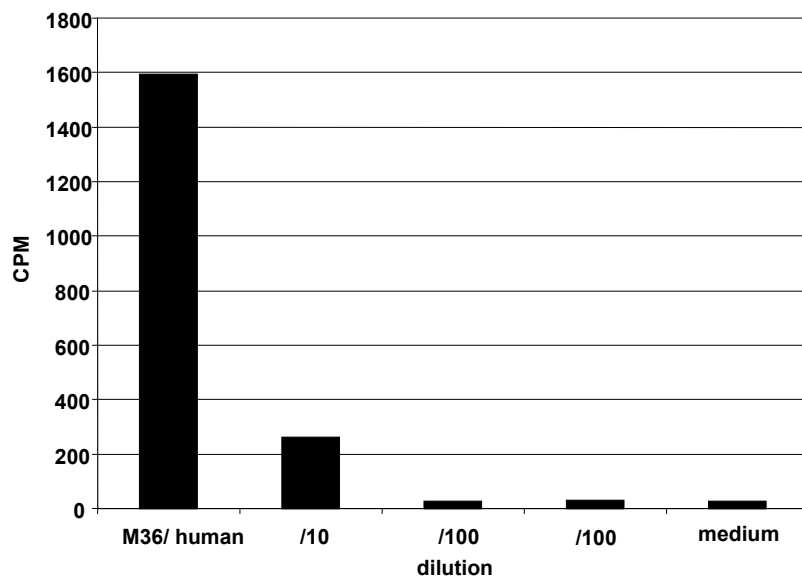
In the chosen SJL/J mouse model system, immunization with MOG induces a T-cell response against two main regions: sequence 1-22 and 92-106 (M36) of the MOG extracellular domain<sup>70</sup>. While clones against 1-22 are incapable of inducing disease, clones versus M36 are encephalitogenic and induce EAE upon transfer into recipient animals<sup>70</sup>. Therefore, the M36 region was analyzed for TCR contact residues via alanine scanning.

A panel of 17 peptides was synthesized. These included human and mouse M36 wild-type peptide, which differ at position 5 (Y in mouse, F in human). It was of importance to verify that mouse T cells would also recognize the human peptide, since the MOG-Fc protein contains the extracellular domain of human MOG. Stimulation of the mouse M36-specific T cell line with human M36 peptide resulted in similar proliferative responses, as measured by

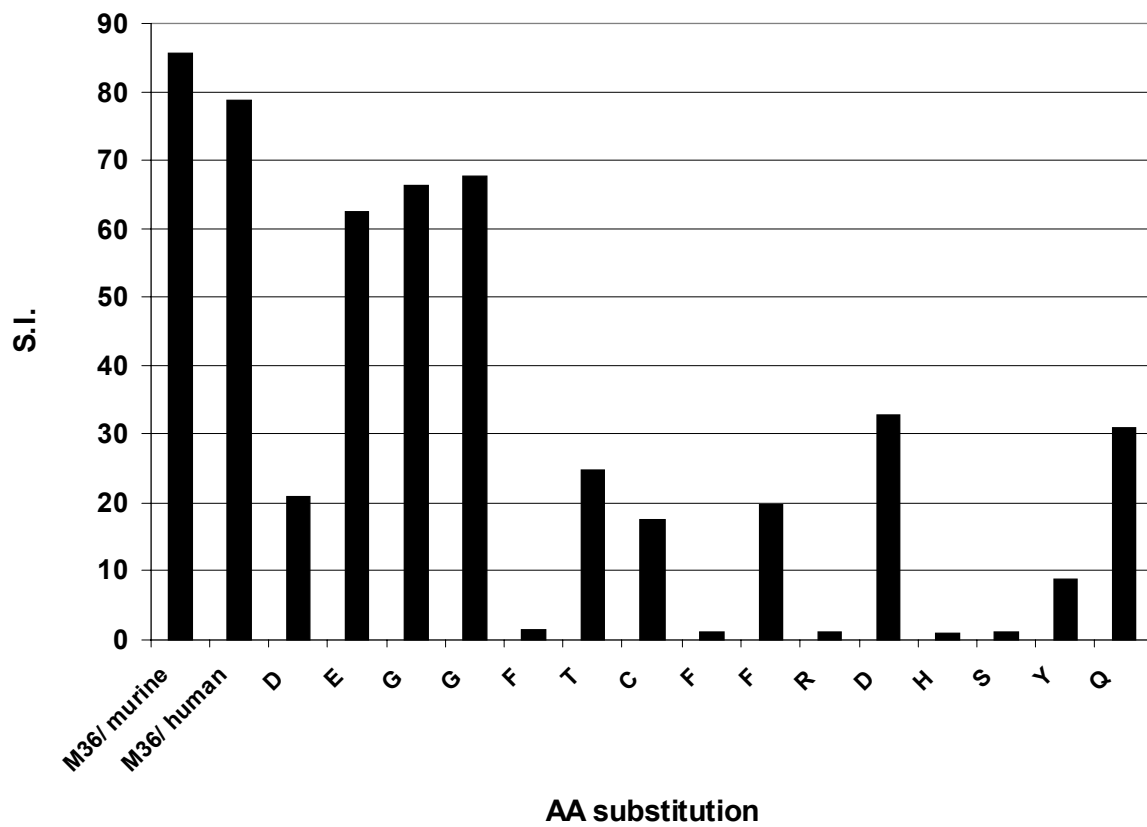
<sup>3</sup>H incorporation assay (see Fig. 23B). On the same note, T-cell proliferation induced by human M36 was dose-dependent (Fig. 23A), providing further evidence that T-cell stimulation induced with the human M36 wild-type peptide was peptide-specific. Under the same experimental conditions, a set of single alanine-substituted peptides was tested for their potential to induce proliferation of the M36-responsive T cells. Various alterations in stimulation potential were discovered (see Fig. 23B), ranging from a stimulation index (S.I.) comparable to wild-type (alanine substitution for G at position 4) down to an almost complete lack of stimulation, at the level of the medium control (S.I. = 1). The peptides found to induce the lowest S.I. values (alanine substitutions at positions 5, 8, 10, 12 and 13) were further tested for their ability to prevent proliferation induced by wild-type M36 peptide.

In a peptide competition experiment, SJL/J antigen-presenting cells (APCs) were pre-pulsed with human M36 peptide for 2 hours. After a washing step with medium, substituted peptides were added at equal concentrations, and proliferation was assessed by standard <sup>3</sup>H incorporation assay. It was found that peptides substituted at positions 10, 12 and 13 were able to completely suppress proliferation induced by the wild-type peptide (Fig. 23C). Taking into account a recent report that predicted the ligand motif of the MHC class II molecule H2-A<sup>S</sup> expressed in the SLJ/J mouse strain<sup>71</sup>, amino acids 10 (R) and 13 (S) are likely MHC class II anchor amino acids. In order to generate mutant MOG proteins with reduced T-cell activation capacity, each mutation was separately introduced into the wild-type MOG-Fc protein.

**A**



**B**



C

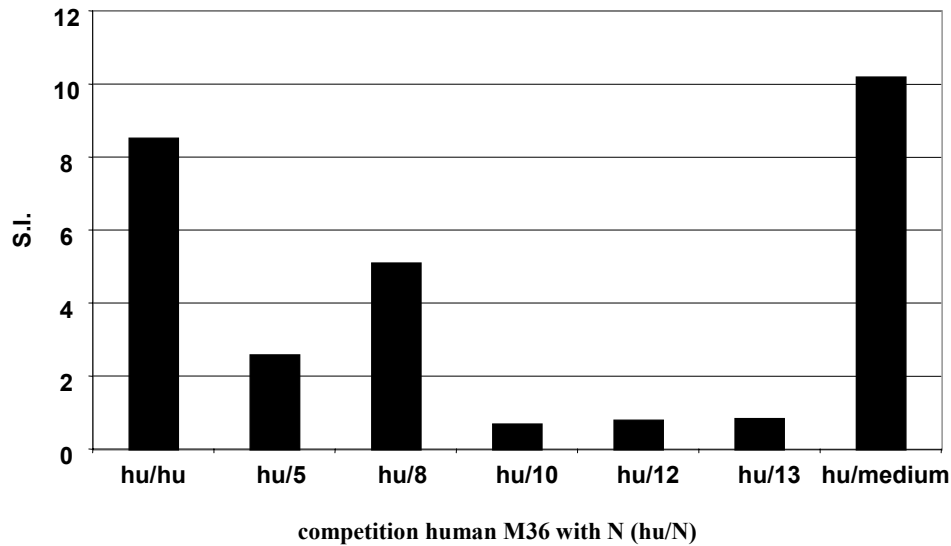


**Fig. 23. A.** Dose response of M36 T-cell line to M36 peptide. M36-specific mouse T cell line was stimulated with SJL APCs loaded with human M36 peptide in decreasing concentrations. Proliferation was assessed in a dose response experiment by standard  $^3\text{H}$ -thymidine incorporation assay. **B.** Proliferation of M36 T-cell line to mutated M36 peptides. Mutated versions of M36 peptide were synthesized. A panel of 15 peptides was generated, each carrying a single amino acid point mutation to alanine (ala-scanning). Proliferation of M36-responsive T-cell line to peptide stimulation was assessed by  $^3\text{H}$ -thymidine incorporation assay. Stimulation index was calculated as  $\text{S.I.} = (\text{cpm}) / (\text{cpm medium control})$ . **C.** T-cell antagonist assay using mutated M36 peptides. Peptides identified as non-stimulatory for M36 T cells were further tested for their ability to compete with wt M36 peptide. Irradiated SJL splenocytes were used as APCs and loaded with wt M36 peptide. After 2 h of incubation, APCs were washed with medium, and alanine-substituted peptide variants were added as well as M36 T cells. Peptides substituted at positions 10, 12 or 13 of the M36 region were able to inhibit proliferation of M36 T cells to wt peptide.

### **5.7. Generation of mutated MOG-Fc proteins (R-MOG, S-MOG)**

Mutated MOG-Fc proteins carrying a single amino acid substitution to alanine at position 10 (R replaced by A, designated R-MOG) and 13 (S replaced by A, designated S-MOG) of the MOG extracellular domain were generated. Constructs encoding the desired nucleotide exchanges were generated by site-directed mutagenesis. The encoded proteins were generated and purified exactly as previously described for the wild-type MOG-Fc protein. As shown in Fig. 24 for the S-MOG protein, binding of the mutated extracellular domain of MOG to MOG-specific TH B cells in isolated splenocytes was still intact. Panel A shows selective binding to transgenic (lower panel) but not to wild-type splenocytes (upper panel). No binding to CD5-positive T cells was evident (panel B). In panel C, binding to B220+ anti-MOG transgenic TH B cells is shown in the absence of binding to wt B cells. Panel D shows the secondary antibody control stainings without prior incubation with Fc fusion protein. Therefore, mutated proteins were generated that retained specific binding activity to their target B cells.

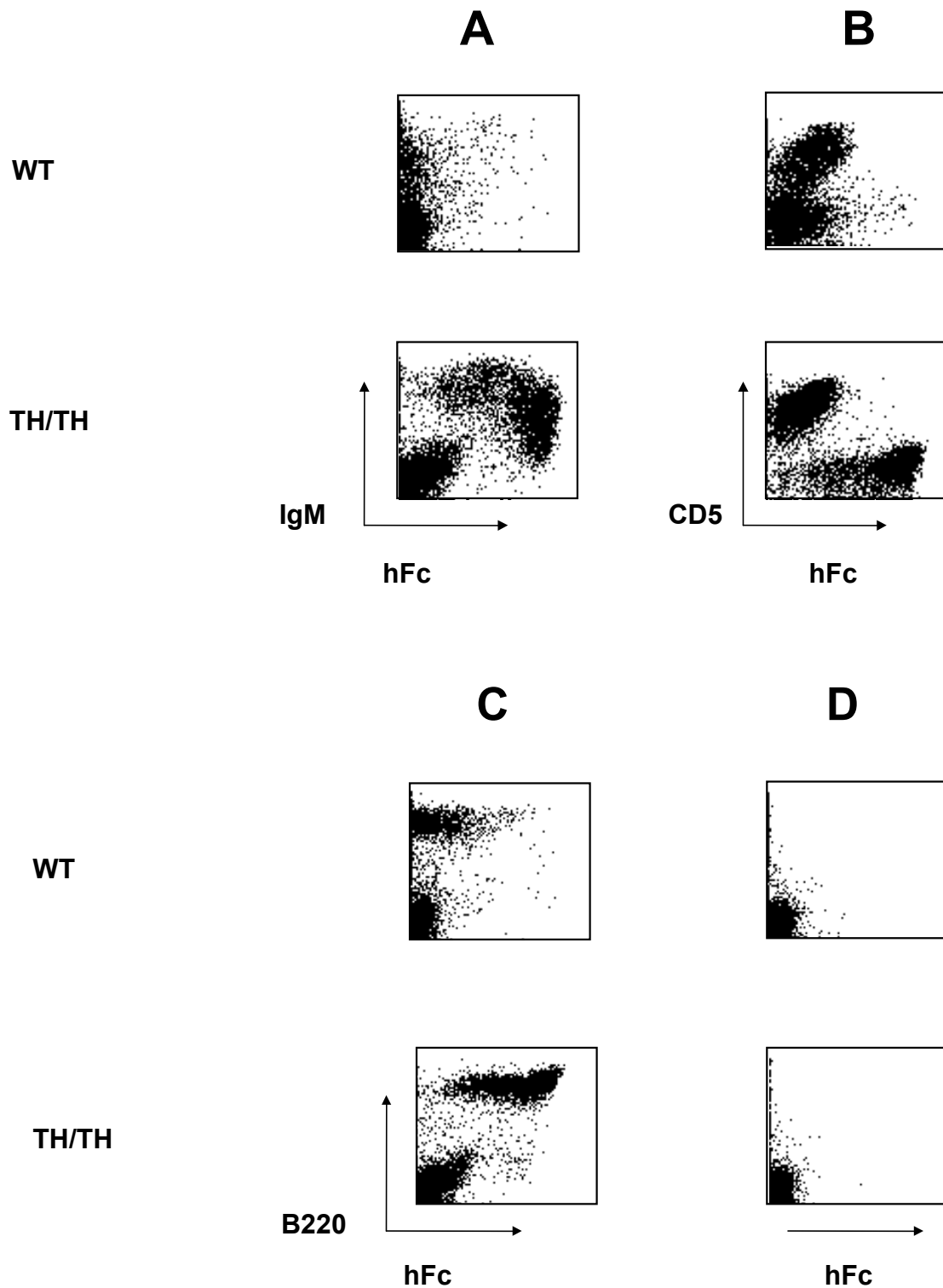


**Fig. 24.** Binding of S-MOG protein to splenocytes from TH mice vs. negative wt controls. Flow cytometric analysis of cell binding properties. Binding of Fc fusion protein to B cells of Ig-MOG transgenic TH mice. Splenocytes from wt (upper panel) and TH mice (lower panel) were prepared and incubated with mutated MOG-Fc protein. MOG-Fc bound to IgM-positive cells was detected by FITC-labeled human Fc $\gamma$ -specific antibody (huFc). Stainings show selective binding to transgenic B cells (panel **A**, **C**) in the absence of unselective binding to T cells, as detected through the marker CD5 (panel **B**). No staining was detected with the secondary anti-Fc antibody alone in the absence of MOG fusion protein (**D**).

## 5.8. Treatment of PLPs-immunized animals transferred with TH B cells

The central question that had to be answered regarding the mutated MOG-Fc proteins is whether they induce a MOG-specific T-cell response. Since the SJL/J M36-specific T-cell line used for the investigation of peptide-induced proliferation was insensitive to MOG protein-induced stimulation, it was decided to employ the most relevant *in vivo* model for obtaining therapeutic efficacy, e.g., clinical disease score. An EAE model was chosen that did not rely on immunization with the MOG antigen, but one that rested on immunization with PLPs peptide and transfer of MOG-specific TH B cells as an exacerbating factor. The TH transfer model had shown to be responsive to MOG-Fc induced depletion of B cells (compare section 5.4.2.4.) and permitted the investigation of immunopathology induced by treatment. This was achieved in the absence of pre-sensitization to MOG, due to the MOG-independent immunization regimen used to induce EAE.

The disease progression in the PLPs transfer model can be seen in Figure 25. Animals were treated via i.p. injection on days 7, 8 and 9 after PLPs immunization with 3 times 100 µg of protein for each treatment cycle. While the untreated control group showed an average score of 1 by day 15, the group treated with wild-type MOG-Fc protein presented with a rapidly progressive, monophasic disease course that culminated in a score > 4 by day 24 post immunization. Animals treated with both R-MOG or S-MOG variants showed no significant difference in clinical score compared to the wild-type MOG-Fc treated group. Very clearly, all 3 treatment regimens induced an exacerbated EAE progression that resulted in a disease that was significantly more severe than in the untreated control animals. Thus, no clinical benefit could be observed by treating EAE with MOG-Fc, or one of the mutated MOG-Fc variants, designed to minimize T-cell stimulation induced by the MOG domain of the protein.

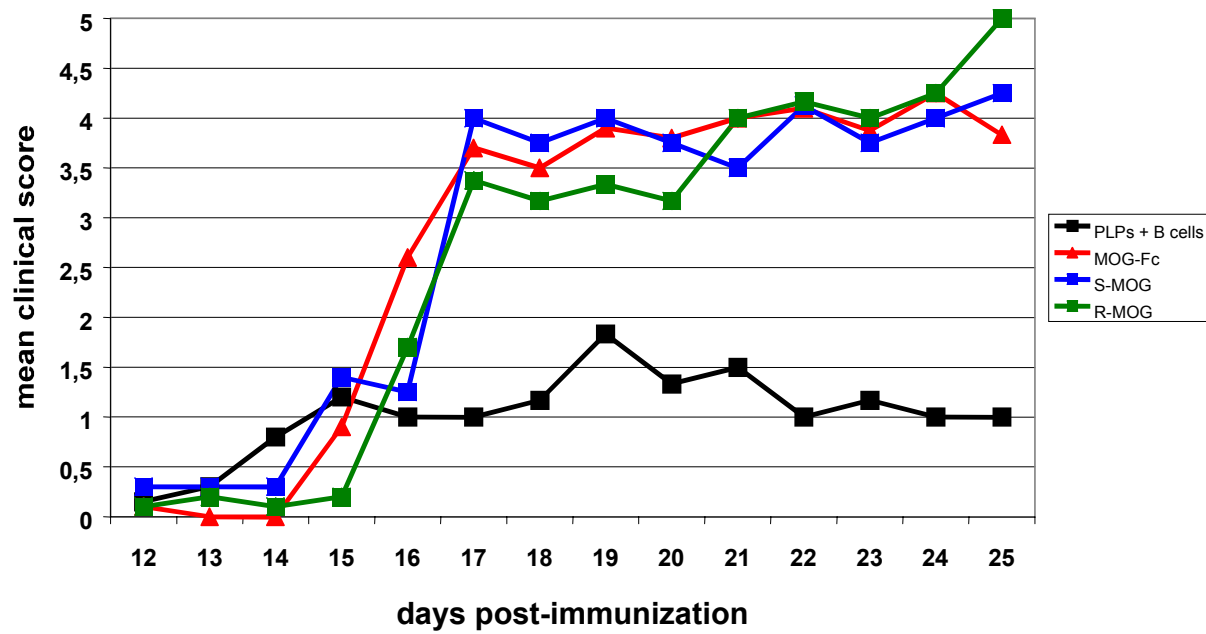


**Fig. 25.** Modified MOG-Fc proteins exacerbate EAE. Animals were immunized on day 0 with PLPs and transferred with TH B cells on day 1. On days 7, 8 and 9, mice were treated with 100 $\mu$ g of recombinant protein via i.p. injection. Untreated control animals present with mild clinical symptoms of EAE, not exceeding a maximum score of 2. All animals treated with MOG-Fc (red), S-MOG (blue), or R-MOG (green) develop hyperacute EAE by day 17 post immunization.



## 6. Discussion

### 6.1. *In vitro* properties of MOGxCD3 fusion protein

Bispecific antibodies have been investigated since the mid-1980s<sup>72-74</sup>. In these early reports, it was shown that bispecific antibodies (bsAbs) could override the natural specificity of an effector cell for its target and 're-direct' the effector to kill a target cell that it would otherwise ignore. In order to mediate re-directed lysis, a bsAb must bind directly to a triggering molecule on the effector cell<sup>74;75</sup> while simultaneously cross-linking target and effector cells for specific killing. By varying the specificities of the anti-effector and anti-target domains of the bsAb, a range of effector functions can be recruited against a variety of target cells. In fact, the early 1990s saw the first clinical investigations evaluating bsAbs as therapeutic agents, mainly in cancer therapy<sup>76;76-83</sup>. However, a major obstacle in using bispecific antibodies harnessing the potential of T cells irrespective of their MHC restriction, was encountered in the strict requirement of T-cell responses for costimulatory or regulatory molecules<sup>84</sup>. As a consequence, investigators have used approaches for the simultaneous engagement of co-stimulatory molecules, such as CD28, while at the same time cross-linking an activating receptor with the same molecule<sup>85</sup>, or T cell mitogens such as IL-2 were chosen as co-medication<sup>84</sup>. For instance, bispecific antibodies triggering CD3 have been applied in combination with anti-CD28 Abs<sup>86-88</sup>. Characteristic outcomes of these trials included serious side effect profiles and low efficacy of bsAb treatment<sup>84</sup>. In order to overcome these limitations, it was chosen to incorporate the anti-CD3 moiety as described by Löffler et al<sup>49</sup>. In contrast to a diabody format, which possesses a rather rigid structure, the use of flexible serine-glycine linkers provides for a bispecific scFv-format that reduces the distance from target cell to effector to a minimum<sup>89</sup>. This format has proven to be highly potent in recruiting

T-cells for re-directed lysis of target cells in the absence of simultaneous engagement of accessory molecules on T cells by additional agents (Dreier et al., submitted)<sup>49;90</sup>.

In order to extend the concept of bispecific antibodies to the targeting of autoreactive B cells, a protein was designed that incorporated the extracellular domain of the auto-antigen MOG at the N-terminus fused to the heavy chain Fv fragment of a C-terminally attached anti-CD3 scFv<sup>49</sup> directed against human CD3ε. The MOGxCD3 protein was expressed in CHO cells and purified using a His-6 tag at the C-terminus. Expression in CHO cells has proven to be superior for the generation of correctly folded, active bispecific scFv antibodies.

ELISA and Western blot analysis (see Figures 8 and 9) revealed that the MOGxCD3 fusion protein was produced as an intact molecule of the predicted size. Using the conformation-dependent anti-MOG monoclonal antibody 8.18-C5<sup>52</sup> for capture in ELISA, it was shown that the extracellular domain of human MOG was indeed correctly folded. FACS analysis of purified human T cells incubated with the fusion protein (Fig. 11) showed that incorporation of a non-immunoglobulin domain into the scFv format at the N-terminus did not abrogate its binding to human CD3 on T cells. Other groups have used single chain fusion proteins for the targeting of tumor cells over-expressing growth factor receptors via anti-CD3 or anti-CD64 scFv Abs<sup>91;92</sup>. Effector targeting domains were generally attached at the N-terminus, which can be a limitation with regard to the ligand, which then needs to be fused in a C-terminal position. Thus, the MOGxCD3 molecule provides for a versatile immunoligand platform due to its incorporation of a functional anti-CD3 domain at the C-terminus.

Employing a FACS-based cytotoxicity assay<sup>54;55</sup> using a hybridoma cell line selected for expression of cell-surface bound anti-MOG antibody, it could be shown that MOGxCD3 mediated re-directed lysis of MOG-reactive hybridoma cells (Fig. 15, Fig. 16). Complete

elimination of target cells was observed with freshly isolated human CD3-positive cells without prior stimulation with T-cell mitogens, such as IL-2.

A dose-response analysis showed that an optimal concentration of MOG $\times$ CD3 fusion protein was reached at 10  $\mu$ g/ml, leading to elimination of >80% of target cells (Fig. 15A). Lysis was dependent on the presence of effector cells (Fig. 15B, 2<sup>nd</sup> bar) and on the effector-to-target cell ratio (Fig. 16), as well as on the presence of the MOG $\times$ CD3 protein (Fig. 15B, 3<sup>rd</sup> bar).

Taken together, the data obtained for the MOG $\times$ CD3 bispecific molecule show that unstimulated human T cells can be re-directed to induce the specific lysis of hybridoma cells carrying autoreactive cell-surface immunoglobulin. *In vivo* studies of the bispecific T-cell recruiting MOG $\times$ CD3 molecule in rodents or primates could not be performed due to the specificity of the scFv targeting domain for human CD3 $\epsilon$ . For the investigation of targeting autoreactive B cells in a physiological situation, a fusion protein composed of an Fc effector domain and the MOG targeting moiety, designated MOG-Fc, was generated and studied in the MOG-Ig transgenic TH mouse system.

## **6.2. Rationale for construction of Fc fusion protein**

Therapeutic options for the treatment of antibody-mediated autoimmune diseases are very limited and dissatisfactory. Treatment regimens include immunosuppressive drugs, corticosteroids or plasmapheresis, which generally act only in a transient fashion, or may lead to a general immunodeficiency. In search for a more specific approach, it was attempted to selectively deplete autoantibody-producing B cells through targeted lysis by immune effector cells, employing the bispecific fusion protein MOG-Fc. The intention was to combine human

MOG for the specific targeting of MOG-reactive B cells with an immune effector mechanism leading to an efficient and at the same time well-tolerated elimination of target cells. Other approaches were disregarded, such as bacterial toxin fusions, because of their relatively small therapeutic window and high immunogenicity<sup>93;94</sup>. Because of its high tolerability, the Fc part of human IgG1 was employed instead. This immunoglobulin (Ig) isotype is well-suited for induction of antibody-dependent cellular cytotoxicity (ADCC) and complement-dependent cytotoxicity (CDC) and is validated for the efficient elimination of tumor cells by the marketed antibody therapeutics trastuzumab<sup>48</sup> and rituximab<sup>40</sup>. Another potential advantage is the dimerization of the CH2 and CH3 domains in the human IgG heavy chain that increases the avidity of target cell binding by linking two MOG molecules. In addition, human Fc $\gamma$ 1 can efficiently bind murine Fc $\gamma$  receptors (see Fig. 17B)<sup>64</sup> thus facilitating functional studies with the MOG-Fc protein in transgenic mice expressing anti-MOG Abs<sup>95</sup>.

The choice of the most suitable Fc effector domain was a consideration of central importance. A number of previous studies have shed light on the interaction of Ig isotypes and Fc receptors<sup>42;96-98</sup>. It has become clear that IgG Fc contains distinct Fc receptor (FcR) binding sites<sup>96;99</sup>. These are different from the ones recognized by neonatal FcR<sup>100;101</sup> or staphylococcus protein A. In fact, whereas the CH2-CH3 interface of the IgG Fc domain contains the binding site for the neonatal Fc receptor (FcRn), protein A and the low-affinity Fc $\gamma$ RIII<sup>102</sup> (CD16), the binding sites for the Fc $\gamma$ RII family and Fc $\gamma$ RI differ. Being expressed on neutrophils and macrophages, Fc $\gamma$  receptors of type IIa (CD32) and Fc $\gamma$ RI (CD64) possess important functions in cellular immunity, however<sup>2</sup>. Therefore, fusion proteins aimed at harnessing the potential of cells positive for either Fc $\gamma$ R must encompass the critical binding residues (Fig. 23). For this reason, the lower hinge and adjacent CH2 domain were incorporated into the MOG-Fc fusion protein. These domains were found to be critical for interaction between Fc $\gamma$ RIIa, Fc $\gamma$ RI and human IgG by mutational studies<sup>96;103</sup>.

As glycosylation of the CH2 domain is thought to be required for efficient binding to Fc receptors<sup>96</sup> as well as for 'recycling' of IgG through the neonatal Fc receptor<sup>64;97;98</sup>, the choice of an appropriate eucaryotic expression system is also an important consideration. Therefore, the dhfr-deficient chinese hamster ovary (CHO) cell line<sup>49</sup> was chosen as an eucaryotic system for expression of the recombinant MOG-Fc protein.

### **6.3. Investigation of targeting autoreactive B cells with Fc fusion protein**

The MOG-Fc protein was expressed and purified as a disulfide-linked dimer in CHO-cells and was shown to bind to both MOG-reactive B lymphocytes, B cell hybridoma cells and to FcγR<sup>+</sup> phagocytes. MOG-Fc treatment resulted in effective and specific effector cell-dependent lysis of MOG-specific hybridoma cells. To explore the cytotoxic potential of MOG-Fc on regular B cells *in vivo*, the fusion protein was studied in transgenic knock-in mice (TH mice). These mice possess large numbers of MOG-specific B cells, and correspondingly high titers of anti-MOG Abs, due to the site-directed targeting of a MOG specific Ig V<sub>H</sub> gene (Fig. 1)<sup>95</sup>. A marked decrease in anti-MOG IgG titers was observed throughout the observation period (Fig. 18D), even though human Fc proved to be immunogenic in the animals (Fig. 18C). This result shows that the effect of MOG-Fc on B cells, e.g. autoantibody titers, outweighed a potential induction of anti-MOG antibodies in the course of treatment. As shown in Fig. 18A and 18B, wild-type mice do develop an antibody titer to both the human Fc part as well as the MOG domain of the fusion protein 22 days after being treated, which is not surprising considering the immunological unique expression profile of MOG<sup>69</sup>.

Having observed that MOG-Fc lowered autoantibody titers *in vivo*, it was investigated whether the fusion protein exhibited cytotoxic activity against the autoreactive B-cell population in anti-MOG transgenic mice. In fact, MOG-Fc had the ability to deplete primary anti-MOG-positive B cells from TH mice *ex vivo* and *in vivo*. Elimination of MOG-reactive B cells *ex vivo* was efficient (on the order of 70% within 16 hours, Fig. 19), while *in vivo* it was lower but still significant among the population of highly MOG-reactive B cells in TH mice (Fig. 20). This result can be explained as follows:

First, it should be noted that TH mice have an extremely high titer of circulating MOG-reactive antibodies<sup>95</sup>, which interferes with the binding of MOG-Fc to MOG-specific B cells. Second, the large pool of continuously replenished, MOG-specific B lymphocytes in TH mice represents an exaggerated large target cell population which may partly resist specific drug depletion *in vivo*. In contrast, the frequency of autoreactive B cells in human autoimmune disease is much lower<sup>8;104</sup>.

To study the effect of MOG-Fc on a limited number of autoreactive B cells among a high background of normal B cells from the endogenous B-cell pool, a wild-type transfer model was established. The model consisted of purified B cells obtained from TH mice that were transferred into syngenic wild-type recipient animals by intravenous injection. In this TH transfer model, the treatment of transferred mice with MOG-Fc resulted in efficient depletion of about 70% of all MOG-reactive B cells, as detectable 6 days after B-cell transfer and 2 days after the last treatment (Fig. 21A). Four to six days after transfer, most TH-derived B cells detected were actively switching, IgM<sup>-</sup> MOG<sup>+</sup> IgG<sup>+</sup> B-cell blasts. In MOG-Fc-treated mice, but not in control mice, serum titers of MOG-binding Abs were reduced, despite the

presence of actively secreting plasma cells, which cannot be targeted via ADCC by MOG-Fc. Thus, the action of MOG-Fc on autoreactive B-cells is not restricted to resting B cells (Fig. 19, 20) but includes also the active elimination of activated B-cells and the reduction of circulating Abs (see Fig. 21).

The ability of MOG-Fc to bind and eliminate autoreactive B cells even in the presence of high anti-MOG antibody titers *in vivo* demonstrate its utility for a novel therapy of antibody-mediated autoimmune diseases. While bone marrow-resident plasma cells, which carry little if any Ig on their surface, cannot be eliminated by the described approach, the introduction of recombinant antigen into circulation by the fusion protein could prove to be of additional therapeutic benefit. MOG-Fc could bind pathogenic autoantibodies and route them to clearance. Theoretically, the formation of such immune complexes might recall pathogenic pathways, such as glomerulonephritis. However, signs of clinical immune complex disease in TH mice monitored for more than two months following treatment with MOG-Fc were not encountered. Anaphylactic reactions were not seen either. Sustained elimination of MOG-reactive, resting, activated and possibly also memory B cells may, in the long run, lead to a depletion of MOG-secreting plasma cells as well. This is underscored by the long-term reduction in anti-MOG IgG in TH mice treated with MOG-Fc (see Fig. 18D).

It has to be noted that MOG is a strictly CNS-specific auto-antigen that is neither expressed in the thymus nor in the periphery, which sets it apart from other CNS constituents like myelin basic protein (MBP)<sup>9</sup> or other target antigens of B-cell mediated autoimmune attack in indications like pemphigus vulgaris and myasthenia gravis<sup>3;105</sup>. Thus, MOG-specific clones are not subject to clonal deletion or peripheral tolerance induction, making MOG a potent encephalitogen<sup>11</sup>. It should be emphasized that MOG was chosen mainly as a suitable model

antigen for the study of B-cell depletion in the absence of an inflammatory context, as would be encountered in EAE or MS. In the case of Th2-dominated and truly B-cell mediated autoimmune indications, the respective antigen is usually expressed in thymus and periphery, and thus participates in the generation of tolerance. In summary, the present data demonstrate the potential of MOG-Fc-based compounds in the attenuation of autoreactive B-cell responses *in vivo*.

#### **6.4. Effect of MOG-Fc treatment in EAE**

MOG is an important auto-antigen involved in the pathogenesis of multiple sclerosis, and MOG-induced EAE is the only model of MS to evoke both encephalitogenic T cells as well as demyelinating autoantibodies<sup>69</sup>. Due to the highly encephalitogenic potential of MOG when it is used in a CFA emulsion to immunize experimental animals for the induction of EAE, it was clear from the beginning that one might encounter limitations when using this format as a therapeutic modality in EAE. In addition, EAE is a classical Th1-mediated autoimmune disease where autoantibodies may have an exacerbating function, but B cells are not required for disease development. In fact, EAE can even be induced in B-cell deficient mice<sup>106;107</sup>. On the other hand, tolerization regimens with high-dose antigen therapy of MOG-induced EAE have been described for the marmoset primate model<sup>108</sup>. In this model, the induction of MOG-EAE could be prevented by giving repeated high doses of the soluble antigen. In the long run, the treatment failed, due to the appearance of a pathogenic, MOG-specific humoral response after cessation of treatment. However, this report showed that MOG-EAE can be positively modulated by high doses of the antigen itself, which led to the decision to investigate the effect of MOG-Fc treatment in EAE.



The M36-induced EAE model was chosen as a first *in vivo* system to investigate therapeutic efficacy (see Fig. 22). Surprisingly, treated animals showed no clinical signs of disease for a period of 4 to 5 days after the non-treated group had developed the first clinical features of EAE. Thereafter, however, disease progression was rapid and clearly more severe than in the untreated control group. Due to the rapid onset and hyperacute profile of disease, reminiscent of rMOG-induced EAE, it was hypothesized that the treatment had induced a MOG-specific T-helper response. However, alterations of the immunodominant, encephalitogenic MHC class II epitope within the MOG-Fc protein (Fig. 23), introduced in order to prevent T-cell stimulation by the MOG fusion protein, did not result in a measurable change in clinical outcome after treatment, as investigated in the PLPs-induced EAE transfer model (see Fig. 25). There may be a number of reasons for the failure of the modified proteins to positively modulate the course of EAE. First, the immunodominant epitope within the MOG extracellular domain was characterized using a monoclonal T-cell line selected for responsiveness to M36 stimulation. Clearly, the MOG-specific T-cell response *in vivo* is oligoclonal, even though sequencing of TCR variable genes has shown that just a few T cell clones dominate the response (A. Iglesias, personal communication). The M36 T-cell line may have been too much of an artificial system, not representative of the *in vivo* situation. Secondly, the appearance of subdominant MOG-specific clones even after a possible elimination of the dominant T-cell response is possible, and these clones may be of equally pathogenic potential. Thirdly, it has to be remembered that MOG-Fc is a fully human protein. Therefore, the Fc part is immunogenic in mice, as proven by the detection of mouse antibody titers against human Fc in the treated animals. Thus, a B cell that has bound MOG-Fc via the protein's MOG part will still be able to present immunogenic epitopes contained within the Fc portion, and will receive help from Fc-specific T helper cells. This could lead to the long-term induction of a MOG-specific Ig response, even in the absence of encephalitogenic, MOG-specific MHC class II epitopes contained within the MOG domain of the protein. Clearly,

using MOG-Fc to positively modulate immunopathology in EAE or even MS is not feasible. The MOG system should be regarded as purely a model system suitable for the investigation of B-cell targeting strategies, which may then be transferred to other, possibly less potent target auto-antigens involved in truly B-cell mediated autoimmunity.

## 6.5. Perspectives

In the work presented here, novel recombinant proteins aimed at specifically targeting autoreactive B cells were generated. These bispecific antibody fusion proteins were shown to induce re-directed lysis of autoreactive B cells, thus reducing the number of potentially pathogenic B cells and corresponding autoantibody titers *in vivo*. These findings constitute core requirements for the specific immunotherapy of antibody-mediated autoimmune diseases.

On the basis of data obtained from MOG-Fc in the MOG-Ig model system, informed choices can be made in order to engineer refined recombinant proteins for application in B-cell mediated autoimmunity. These proteins should fulfill several requirements:

1. Maximum induction of re-directed lysis through engagement of effector cells.
2. Minimal binding to antigen-presenting cells.
3. Long serum half-life with low side effect profile.
4. Low immunogenicity of the auto-antigen domain.

For the general format used for engagement of Fc $\gamma$ R<sup>+</sup> effector cells, further adjustments to the Fc effector domain can be considered in addition to those already outlined and incorporated in

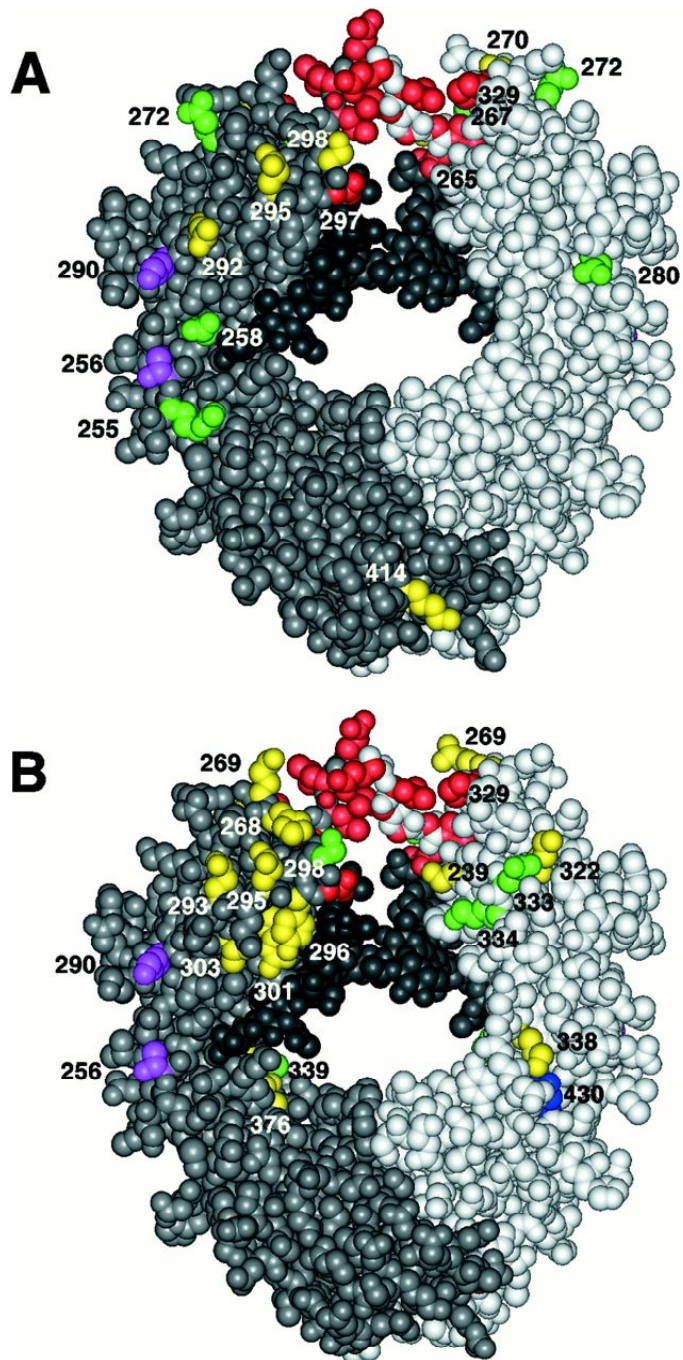


**Fig. 26.** Binding sites of human IgG1 for FcR. **A.** IgG1 residues comprising the binding site for FcRI and FcRII. The two Fc heavy chains are in light and medium gray; carbohydrate is in dark gray. Residues that affected binding to all FcR are in red; the FcRI binding site is composed only of red residues. Residues that showed improved binding to FcRII and FcRIIIA are in magenta. Residues that showed reduced binding only to FcRII are in yellow. Residues that showed 50% improved binding only to FcRII are in green. **B.** IgG1 residues comprising the binding site for FcRI and FcRIIIA. The two Fc heavy chains are in light and medium gray; carbohydrate is in dark gray. Residues that affected binding to all FcR are in red; the FcRI binding site is composed only of red residues. Residues that showed improved binding to FcRII and FcRIIIA are in magenta. Residues that showed reduced binding only to FcRIIIA are in yellow. Residues that showed 25% improved binding only to FcRIIIA are in green. Glu430, involved in a salt-bridge with Lys338, is shown in blue. From Shields 2001.

the general considerations in section 6.2. In tables II and III, the binding of mutated human IgG1 Fc regions to Fc receptors is characterized<sup>99</sup>. It would be tempting to investigate the potential of mutated Fc fusion proteins designed to maximize the engagement of FcγRIIIA while reducing the binding to the FcγRII family. Accordingly, the hope would be that proteins engineered in this way would lead to increased triggering of NK cells through the low-affinity FcγRIIIA while reducing the binding to APCs carrying FcγRII in the absence of CD16. Thus, presentation of auto-antigen should be reduced, leading to reduced immunogenicity. Also, serum half-life may be prolonged in the absence of high-affinity binding to FcγRI.

Notably, the mutation of S298 to alanine is characterized by an increase in CD16 binding, even in combination with other mutations in its vicinity (table III). K334A exhibited a significant increase in ADCC when incorporated into anti-HER2 IgG1 variants. This increase was additive when K334A was present with S298A, and was even further enhanced when E333A was present<sup>99</sup>. Thus, modifications of the Fc region may lead to a bispecific protein with optimized effector function.

In spite of the importance of the general protein format, attention must be given to the investigated target indication and the corresponding auto-antigen. Promising antigens involved in B-cell mediated autoimmunity could be the desmogleins 3 and 1, well-defined targets for pathogenic antibodies in pemphigus vulgaris<sup>109</sup>, or the extracellular part of the alpha chain of the acetylcholine receptor, the main auto-antibody target structure in myasthenia gravis<sup>110</sup>.

For pemphigus vulgaris, fusion proteins could be envisioned that accompany two B-cell target specificities into a single Fc molecule. This could be accomplished by using a heterodimerization domain in the IgG1 heavy chain, engineered for directed dimerization

through additional disulfide bonds in combination with "knobs-into-holes" mutations<sup>111</sup>. This modified IgG1 Fc backbone could be used for expression of the Dsg-1 and Dsg-3 extracellular domain, each fused to a separate heavy chain, resulting in a molecule with both specificities. A fusion protein of this kind may lead to depletion of both Dsg-1 as well as Dsg-3 specific B cells.

Myasthenia Gravis (MG) constitutes another example of a truly B-cell mediated autoimmune disease. MG is a T-cell dependent, antibody-mediated autoimmune disease of the neuromuscular junction, in which the nicotinic acetylcholine receptor (AChR) is the major autoantigen. Autoantibodies to the alpha-chain of the nicotinic acetylcholine receptor present at the neuromuscular junction block neuromuscular transmission. MG is a fatal affliction; patients affected with this disease develop progressive weakness potentially leading to death. Experimental autoimmune MG (EAMG), inducible in various animal species by immunization with AChR or by passive transfer of anti-AChR antibodies, is a reliable model of the human disease, suitable for the investigation of therapeutic strategies<sup>112-114</sup>. MG is currently treated mainly by acetylcholinesterase inhibitors and by generalized immunosuppression. These treatments have been effective for both MG and EAMG but are often associated with severe side effects. Ideally, the treatment should be specific and should suppress selectively the immunological reactivity that leads to the neuromuscular disorder without impairing the entire immune system. The immune response to AChR is highly heterogeneous<sup>115-118</sup> and a wide variety of T- and B-cell epitopes have been defined in MG and EAMG. Thus, the search for new molecules suitable for treatment of MG should deal with this heterogeneity. Candidate molecules for antigen-specific immunotherapy of MG should share specificities with the native antigen without being pathogenic and should be available in sufficient amounts.

The extracellular portion of the AchR alpha-subunit is the target for the majority of the anti-AchR antibodies in MG sera<sup>119</sup>. Recombinant proteins corresponding to this region encompass T and B cell epitopes and can be prepared in large amounts. They therefore represent a potential substitute for the entire antigen for immunotherapy studies. These recombinant fragments were able to attenuate EAMG passively transferred by pathogenic monoclonal anti-AchR antibodies<sup>120;121</sup>. While passive adsorption of pathogenic antibodies by recombinant autoantigen fragments has already proven successful in treatment regimens of EAMG<sup>122;123</sup>, the autoreactive B cell as origin of these pathogenic antibodies is not addressed. Therefore, the extracellular domain from amino acids 1-210 of the human AchR alpha chain could be combined with an effector domain for the recruitment of immune effector cells, thus leading to depletion of autoreactive B cells and attenuation of disease.

The work presented here describes novel recombinant proteins with the proven ability to deplete autoreactive B cells as the root cause of pathogenic autoantibodies. The concept of targeting B cells specific for autoantigens for elimination through immune-effector mechanisms is a novel and provocative one. Applying the platform format generated using the MOG model system to B-cell mediated autoimmune disease models will show whether the antigen-specific modulation of the B cell response in humoral autoimmunity results in a clinical benefit. This could lead to antigen-specific therapy of B-cell mediated autoimmune diseases, an ultimate goal of applied immunology.

**Table II****Binding of human IgG1 non-Ala variants to human FcRII and FcRIIIA**

---

Variant <sup>a</sup>	FcRIIAb mean (S.D.)	FcRIIB mean (S.D.)	FcRIIIA mean (S.D.) n <sup>c</sup>
D265N	0.02 (0.01)	0.03 (0.01)	0.02 (0.01) 3
D265E	0.11 (0.04)	0.03 (0.01)	0.02 (0.01) 3
S267G	1.18 (0.10)	0.95 (0.14)	0.08 (0.02) 4
S267T	0.42 (0.10)	0.45 (0.01)	0.05 (0.05) 3
D270N	0.03 (0.02)	0.05 (0.05)	0.04 (0.03) 5
D270E	0.08 (0.01)	0.06 (0.01)	0.90 (0.17) 3
D280N	1.07 (0.18)	1.22 (0.19)	1.16 (0.21) 6
E293D	0.90 (0.02)	0.88 (0.07)	0.37 (0.07) 3
S298T	0.29 (0.19)	0.27 (0.19)	0.73 (0.21) 6
S298N	0.05 (0.03)	0.08 (0.08)	0.06 (0.03) 5
R301M	1.29 (0.17)	1.56 (0.12)	0.48 (0.21) 4
P331S	0.91 (0.08)	0.78 (0.07)	0.58 (0.19) 4
E333Q	0.70 (0.05)	0.64 (0.09)	1.05 (0.09) 3
E333N	0.59 (0.04)	0.52 (0.07)	0.56 (0.10) 4
E333D			1.26 (0.04) 3
K334R	1.15 (0.09)	1.33 (0.18)	0.68 (0.07) 5
K334Q	1.08 (0.11)	1.10 (0.21)	1.23 (0.08) 7
K334N	1.16 (0.11)	1.29 (0.30)	1.11 (0.12) 8
K334E	0.74 (0.15)	0.72 (0.12)	1.30 (0.09) 6
K334V	1.13 (0.11)	1.09 (0.15)	1.34 (0.18) 3
K338M	0.99 (0.13)	0.93 (0.15)	0.49 (0.04) 2

---

<sup>a</sup> Residue numbers are according to the Eu numbering system.

<sup>b</sup> Values are the ratio of binding of the variant to that of native IgG1 at 0.33 or 1 µg/ml. A value greater than 1 denotes binding of the variant was improved compared with native IgG1, whereas a ratio less than 1 denotes reduced binding compared to native IgG1.

<sup>c</sup> Number of independent assays for FcRIIA, FcRIIB, and FcRIIIA. At least two separately expressed and purified lots of each variant were assayed.

Table adapted from Shields 2001.

**Table III****Binding of human IgG1 combination variants to human FcRn and FcR**

Variant <sup>a</sup>	FcRn <sup>b</sup> mean (S.D.) n	FcRIIA <sup>c</sup>	FcRIIB	FcRIIIA
S267A		1.41 (0.00) 2	1.56 (0.16) 2	0.96 (0.12) 2
H268A				
S267A		1.62 (0.15) 2	2.01 (0.45) 2	1.04 (0.12) 2
E258A				
S267A		1.60 (0.18) 3	1.72 (0.13) 3	0.88 (0.07) 3
R255A				
S267A		1.51 (0.13) 3	1.82 (0.32) 3	0.95 (0.05) 3
E272A				
T256A		0.44 (0.03) 2	0.22 (0.04) 2	1.41 (0.06) 2
S298A				
S298A		0.34 (0.05) 5	0.16 (0.08) 5	1.53 (0.24) 5
E333A				
S298A		0.41 (0.07) 6	0.19 (0.08) 6	1.62 (0.34) 6
K334A				
S298A		0.34 (0.15) 10	0.15 (0.06) 10	1.51 (0.31) 10
E333A				
K334A				
E380A	8.0 (1.0) 6	1.02 (0.07) 2	1.05 (0.11) 2	1.02 1
N434A				
T307A	11.8 (1.5) 5	0.99 (0.06) 2	0.99 (0.11) 2	0.96 1
E380A				
N434A				
L309A	0.9 (0.1) 4	0.98 1	1.04 1	0.92 1
E380A				
K288A	2.9 (0.4) 4	0.94 (0.11) 2	0.96 (0.17) 2	0.88 1
N434A				

<sup>a</sup> Residue numbers are according to the Eu numbering system.

<sup>b</sup> Values are the ratio of binding of the variant to that of native IgG1 at pH 6.0.

<sup>c</sup> Values are the ratio of binding of the variant to that of native IgG1 at 0.33 or 1 µg/ml. A value greater than 1 denotes binding of the variant was improved compared with native IgG1, whereas a ratio less than 1 denotes reduced binding compared with native IgG1.

Table adapted from Shields 2001.





## **7. Acknowledgements**

This work was performed at Micromet AG and the Max-Planck-Institute of Neurobiology in Martinsried. I am indebted to Prof. Patrick Baeuerle for his longstanding support, the truly creative atmosphere and stimulating discussions.

I wish to thank PD Dr. Antonio Iglesias for a wonderful cooperation and his passion for immunology.

Thanks to Dr. Torsten Dreier, Dr. Robert Hofmeister and Dr. Andreas Wolf for their help and support at Micromet AG.

Ute Sukop has been an expert capacity in experimental mouse work at the Max-Planck-Institute and deserves a special 'thank you'.

I also wish to thank Prof. Hans-Georg Rammensee for supporting this thesis at the Eberhard-Karls-Universität, Tübingen.

## 8. Publications

Portions of this thesis have been submitted for publication as below:

Zocher M, Baeuerle PA, Dreier T, Iglesias A. Specific Depletion of Autoreactive B Lymphocytes by a Recombinant Fusion Protein *in vitro* and *in vivo* (submitted).

Other publications:

Zocher M, Czub S, Schulte-Monting J, de La Torre JC, Sauder C (2000). Alterations in neurotrophin and neurotrophin receptor gene expression patterns in the rat central nervous system following perinatal Borna disease virus infection. *J Neurovirol.* **6**:462-77.

Hallensleben W, Zocher M, Staeheli P (1997). Borna disease virus is not sensitive to amantadine. *Arch Virol.* **142**:2043-8.

## 9. Abbreviations

8.18-C5	anti-MOG monoclonal antibody
ag	antigen
APC	antigen-presenting cell
bp	base pair
BSA	bovine serum albumine
cDNA	complementary DNA
CFA	complete Freund's adjuvant
CH50	total hemolytic complement activity
CHO cells	chinese hamster ovary cells
CNS	central nervous system
DMEM	Dulbecco's modified eagle's medium
E. coli	Escherichia coli
EAE	experimental autoimmune encephalomyelitis
ELISA	enzyme-linked immunosorbant assay
FACS	fluorescence activated cell sorter
Fc	immunoglobulin Fragment crystallizable
FcR	Fc receptor
FCS	fetal calf serum
FITC	fluorescein isothiocyanate
Ig	immunoglobulin
kb	kilobase pairs
kDa	kilo Dalton
KO	knock out
MBP	myelin basic protein

MEM- $\alpha$	modified eagle's medium alpha
MHC	major histocompatibility complex
MOG	myelin oligodendrocyte glycoprotein
MOG-Ig	anti-MOG immunoglobulin
mRNA	messenger RNA
PCR	polymerase chain reaction
PLP	proteolipid protein
rpm	revolutions per minute
RT	room temperature
scFv	single chain Fv fragment
SDS	sodium dodecylsulfate
TCR	T-cell receptor
tg	transgenic
Th	T-helper lymphocyte
Th1	T helper cell of type 1
Th2	T helper cell of type 2
Tween 20	polyoxyethylene sorbitane monolaurate
wt	wild type

## 10. Reference List

1. Hohlfeld, R. 1997. Biotechnological agents for the immunotherapy of multiple sclerosis. Principles, problems and perspectives. *Brain*. 120:865-916.
2. Janeway, C. A. and Travers, P. Immunobiology. The Immune System in Health and Disease. 2nd edition. 1996. Current Biology Ltd.  
Ref Type: Serial (Book, Monograph)
3. Padberg, F., M. Matsuda, R. Fenk, N. Patenge, B. Kubuschok, R. Hohlfeld, H. Wekerle, and S. Spuler. 1999. Myasthenia gravis: selective enrichment of antiacetylcholine receptor antibody production in untransformed human B cell cultures. *Eur.J.Immunol.* 29:3538-3548.
4. Link, H., O. Olsson, J. Sun, W. Z. Wang, G. Andersson, H. P. Ekre, T. Brenner, O. Abramsky, and T. Olsson. 1991. Acetylcholine receptor-reactive T and B cells in myasthenia gravis and controls. *J.Clin.Invest.* 87:2191-2195.
5. Amagai, M. 1999. Autoimmunity against desmosomal cadherins in pemphigus. *J.Dermatol.Sci.* 20:92-102.
6. Nguyen, V. T., A. Ndoeye, and S. A. Grand. 2000. Pemphigus vulgaris antibody identifies pemphaxin. A novel keratinocyte annexin-like molecule binding acetylcholine. *J.Biol.Chem.* 275:29466-29476.

7. Tournadre, A., M. D'Incan, J. J. Dubost, F. Franck, P. Dechelotte, P. Souteyrand, and M. Soubrier. 2001. Cutaneous lymphoma associated with Epstein-Barr virus infection in 2 patients treated with methotrexate. *Mayo.Clin.Proc.* 76:845-848.
8. Nishifuji, K., M. Amagai, M. Kuwana, T. Iwasaki, and T. Nishikawa. 2000. Detection of antigen-specific B cells in patients with pemphigus vulgaris by enzyme-linked immunospot assay: requirement of T cell collaboration for autoantibody production. *J.Invest.Dermatol.* 114:88-94.
9. Iglesias, A. 2001. Maintenance and loss of self-tolerance in B cells. *Springer.Semin.Immunopathol.* 23:351-366.
10. Battegay, M., P. Fiedler, U. Kalinke, F. Brombacher, R. M. Zinkernagel, H. H. Peter, G. Kohler, and H. Eibel. 1996. Non-tolerant B cells cause autoimmunity in anti-CD8 IgG2a-transgenic mice. *Eur.J.Immunol.* 26:250-258.
11. Litzemberger, T., R. Fassler, J. Bauer, H. Lassmann, C. Linington, H. Wekerle, and A. Iglesias. 1998. B lymphocytes producing demyelinating autoantibodies: development and function in gene-targeted transgenic mice. *J.Exp.Med.* 188:169-180.
12. Boccaccio, G. L. and L. Steinman. 1996. Multiple sclerosis: from a myelin point of view. *J.Neurosci.Res.* 45:647-654.
13. Steinman, L. 1996. Multiple sclerosis: a coordinated immunological attack against myelin in the central nervous system. *Cell.* 85:299-302.

14. Ebers, G. C., A. D. Sadovnick, and N. J. Risch. 1995. A genetic basis for familial aggregation in multiple sclerosis. Canadian Collaborative Study Group. *Nature*. 377:150-151.
15. Sadovnick, A. D. and G. C. Ebers. 1995. Genetics of multiple sclerosis. *Neurol.Clin.* 13:99-118.
16. Oksenberg, J. R., A. B. Begovich, H. A. Erlich, and L. Steinman. 1993. Genetic factors in multiple sclerosis. *JAMA*. 270:2362-2369.
17. Olsson, T. 1992. Immunology of multiple sclerosis. *Curr.Opin.Neurol.Neurosurg.* 5:195-202.
18. Ben Nun, A., H. Wekerle, and I. R. Cohen. 1981. The rapid isolation of clonable antigen-specific T lymphocyte lines capable of mediating autoimmune encephalomyelitis. *Eur.J.Immunol.* 11:195-199.
19. Lassmann, H., F. Zimprich, K. Rossler, and K. Vass. 1991. Inflammation in the nervous system. Basic mechanisms and immunological concepts. *Rev.Neurol.(Paris.)* 147:763-781.
20. Lassmann, H. 1991. Inflammation and the blood-brain barrier. *Brain.Pathol.* 1:88.
21. Raine, C. S. 1991. Multiple sclerosis: a pivotal role for the T cell in lesion development. *Neuropathol.Appl.Neurobiol.* 17:265-274.



22. Martin, R., H. F. McFarland, and D. E. McFarlin. 1992. Immunological aspects of demyelinating diseases. *Annu.Rev.Immunol.* 10:153-87.:153-187.
23. Genain, C. P., B. Cannella, S. L. Hauser, and C. S. Raine. 1999. Identification of autoantibodies associated with myelin damage in multiple sclerosis. *Nat.Med.* 5:170-175.
24. Genain, C. P., M. H. Nguyen, N. L. Letvin, R. Pearl, R. L. Davis, M. Adelman, M. B. Lees, C. Linington, and S. L. Hauser. 1995. Antibody facilitation of multiple sclerosis-like lesions in a nonhuman primate. *J.Clin.Invest.* 96:2966-2974.
25. Raine, C. S., B. Cannella, S. L. Hauser, and C. P. Genain. 1999. Demyelination in primate autoimmune encephalomyelitis and acute multiple sclerosis lesions: a case for antigen-specific antibody mediation. *Ann.Neurol.* 46:144-160.
26. Linington, C., B. Engelhardt, G. Kapocs, and H. Lassman. 1992. Induction of persistently demyelinated lesions in the rat following the repeated adoptive transfer of encephalitogenic T cells and demyelinating antibody. *J.Neuroimmunol.* 40:219-224.
27. Sun, J. B., T. Olsson, W. Z. Wang, B. G. Xiao, V. Kostulas, S. Fredrikson, H. P. Ekre, and H. Link. 1991. Autoreactive T and B cells responding to myelin proteolipid protein in multiple sclerosis and controls. *Eur.J.Immunol.* 21:1461-1468.
28. Hahne, M., D. Rimoldi, M. Schroter, P. Romero, M. Schreier, L. E. French, P. Schneider, T. Bornand, A. Fontana, D. Lienard, J. Cerottini, and J. Tschopp. 1996. Melanoma cell expression of Fas(Apo-1/CD95) ligand: implications for tumor immune escape. *Science.* 274:1363-1366.

29. Andreola, G., L. Rivoltini, C. Castelli, V. Huber, P. Perego, P. Deho, P. Squarcina, P. Accornero, F. Lozupone, L. Lugini, A. Stringaro, A. Molinari, G. Arancia, M. Gentile, G. Parmiani, and S. Fais. 2002. Induction of Lymphocyte Apoptosis by Tumor Cell Secretion of FasL-bearing Microvesicles. *The Journal of Experimental Medicine* 195:1303-1316.
30. Chappell, D. B., T. Z. Zaks, S. A. Rosenberg, and N. P. Restifo. 1999. Human melanoma cells do not express Fas (Apo-1/CD95) ligand. *Cancer.Res.* 59:59-62.
31. Ferrone, S., J. F. Finerty, E. M. Jaffee, and G. J. Nabel. 2000. How much longer will tumour cells fool the immune system? *Immunol.Today.* 21:70-72.
32. Finke, J., S. Ferrone, A. Frey, A. Mufson, and A. Ochoa. 1999. Where have all the T cells gone? Mechanisms of immune evasion by tumors. *Immunol.Today.* 20:158-160.
33. Wang, E., G. Q. Phan, and F. M. Marincola. 2001. T-cell-directed cancer vaccines: the melanoma model. *Expert.Opin.Biol.Ther.* 1:277-290.
34. Schiller, J. T. and D. R. Lowy. 2001. Papillomavirus-like particle based vaccines: cervical cancer and beyond. *Expert.Opin.Biol.Ther.* 1:571-581.
35. Sun, Y., A. Paschen, and D. Schadendorf. 1999. Cell-based vaccination against melanoma--background, preliminary results, and perspective. *J.Mol.Med.* 77:593-608.
36. Zauner, W., K. Lingnau, F. Mattner, A. von Gabain, and M. Buschle. 2001. Defined synthetic vaccines. *Biol.Chem.* 382:581-595.

37. Hallek, M. and C. M. Wendtner. 1996. Recombinant adeno-associated virus (rAAV) vectors for somatic gene therapy: recent advances and potential clinical applications. *Cytokines.Mol.Ther.* 2:69-79.
38. Dietrich, G., A. Bubert, I. Gentschev, Z. Sokolovic, A. Simm, A. Catic, S. H. Kaufmann, J. Hess, A. A. Szalay, and W. Goebel. 1998. Delivery of antigen-encoding plasmid DNA into the cytosol of macrophages by attenuated suicide *Listeria monocytogenes*. *Nat.Biotechnol.* 16:181-185.
39. Holliger, P. and H. Hoogenboom. 1998. Antibodies come back from the brink. *Nat.Biotechnol.* 16:1015-1016.
40. Hainsworth, J. D. 2000. Rituximab as first-line systemic therapy for patients with low-grade lymphoma. *Semin.Oncol.* 27:25-29.
41. Hainsworth, J. D. 2000. Monoclonal antibody therapy in lymphoid malignancies. *Oncologist.* 5:376-384.
42. Clynes, R. A., T. L. Towers, L. G. Presta, and J. V. Ravetch. 2000. Inhibitory Fc receptors modulate in vivo cytotoxicity against tumor targets. *Nat.Med.* 6:443-446.
43. Rammensee, H. G., M. H. Julius, D. Nemazee, J. Langhorne, R. Lamers, and G. Kohler. 1987. Targeting cytotoxic T cells to antigen-specific B lymphocytes. *Eur.J.Immunol.* 17:433-436.
44. Ong, G. L. and M. J. Mattes. 1989. Mouse strains with typical mammalian levels of complement activity. *J.Immunol.Methods.* 125:147-158.

45. Loibner, H., R. Plot, A. Rot, G. Werner, M. Wrann, H. Samonigg, M. Schmid, H. Stoger, M. Truschnig, D. Herlyn, and . 1990. Immunoreactivity of patient with colorectal cancer metastasis after immunisation with anti-idiotypes. *Lancet.* %20;335:171.
46. Samonigg, H., M. Wilders-Truschnig, H. Loibner, R. Plot, A. Rot, I. Kuss, G. Werner, H. Stoger, M. Wrann, D. Herlyn, and . 1992. Immune response to tumor antigens in a patient with colorectal cancer after immunization with anti-idiotypic antibody. *Clin.Immunol.Immunopathol.* 65:271-277.
47. Samonigg, H., M. Wilders-Truschnig, I. Kuss, R. Plot, H. Stoger, M. Schmid, T. Bauernhofer, A. Tiran, T. Pieber, L. Havelec, and H. Loibner. 1999. A double-blind randomized-phase II trial comparing immunization with antiidiotypic goat antibody vaccine SCV 106 versus unspecific goat antibodies in patients with metastatic colorectal cancer. *J.Immunother.* 22:481-488.
48. Baselga, J., L. Norton, J. Albanell, Y. M. Kim, and J. Mendelsohn. 1998. Recombinant humanized anti-HER2 antibody (Herceptin) enhances the antitumor activity of paclitaxel and doxorubicin against HER2/neu overexpressing human breast cancer xenografts. *Cancer.Res.* 58:2825-2831.
49. Loffler, A., P. Kufer, R. Lutterbuse, F. Zettl, P. T. Daniel, J. M. Schwenkenbecher, G. Riethmuller, B. Dorken, and R. C. Bargou. 2000. A recombinant bispecific single-chain antibody, CD19 x CD3, induces rapid and high lymphoma-directed cytotoxicity by unstimulated T lymphocytes. *Blood.* 95:2098-2103.

50. Canfield, S. M. and S. L. Morrison. 1991. The binding affinity of human IgG for its high affinity Fc receptor is determined by multiple amino acids in the CH2 domain and is modulated by the hinge region. *J.Exp.Med.* 173:1483-1491.
51. Raum, T., R. Gruber, G. Riethmuller, and P. Kufer. 2001. Anti-self antibodies selected from a human IgD heavy chain repertoire: a novel approach to generate therapeutic human antibodies against tumor-associated differentiation antigens. *Cancer.Immunol.Immunother.* 50:141-150.
52. Schluesener, H. J., R. A. Sobel, C. Linington, and H. L. Weiner. 1987. A monoclonal antibody against a myelin oligodendrocyte glycoprotein induces relapses and demyelination in central nervous system autoimmune disease. *J.Immunol.* 139:4016-4021.
53. Goodell, E. M., S. Bilgin, and R. A. Carchman. 1978. Biochemical characteristics of phagocytosis in the P388 D1 cell. *Exp.Cell.Res.* 114:57-62.
54. Zarcone, D., A. B. Tilden, G. Cloud, H. M. Friedman, A. Landay, and C. E. Grossi. 1986. Flow cytometry evaluation of cell-mediated cytotoxicity. *J.Immunol.Methods.* %20;94:247-255.
55. Jacobs, D. B. and C. Pipho. 1983. Use of propidium iodide staining and flow cytometry to measure anti-mediated cytotoxicity: resolution of complement-sensitive and resistant target cells. *J.Immunol.Methods.* 62:101-108.

56. Windhagen, A., C. Scholz, P. Hollsberg, H. Fukaura, A. Sette, and D. A. Hafler. 1995. Modulation of cytokine patterns of human autoreactive T cell clones by a single amino acid substitution of their peptide ligand. *Immunity*. 2:373-380.
57. De Magistris, M. T., J. Alexander, M. Coggeshall, A. Altman, F. C. Gaeta, H. M. Grey, and A. Sette. 1992. Antigen analog-major histocompatibility complexes act as antagonists of the T cell receptor. *Cell*. 68:625-634.
58. Ashkenazi, A. and S. M. Chamow. 1997. Immunoadhesins as research tools and therapeutic agents. *Curr.Opin.Immunol*. 9:195-200.
59. Chamow, S. M. and A. Ashkenazi. 1996. Immunoadhesins: principles and applications. *Trends.Biotechnol*. 14:52-60.
60. Moore, A., C. J. Donahue, K. D. Bauer, and J. P. Mather. 1998. Simultaneous measurement of cell cycle and apoptotic cell death. *Methods.Cell.Biol*. 57:265-78.:265-278.
61. Idink-Mecking, C. A., D. J. Richel, I. Vermes, M. R. Schaafsma, C. Reutelingsperger, and C. Haanen. 1998. Ex vivo evidence of lymphocyte apoptosis in hairy cell leukemia, induced by 2-chlorodeoxyadenosine treatment. *Ann.Hematol*. 76:25-29.
62. Vermes, I., C. Haanen, H. Steffens-Nakken, and C. Reutelingsperger. 1995. A novel assay for apoptosis. Flow cytometric detection of phosphatidylserine expression on early apoptotic cells using fluorescein labelled Annexin V. *J.Immunol.Methods*. 184:39-51.

63. Vermes, I., C. Haanen, D. J. Richel, M. R. Schaafsma, E. Kalsbeek-Batenburg, and C. P. Reutelingsperger. 1997. Apoptosis and secondary necrosis of lymphocytes in culture. *Acta.Haematol.* 98:8-13.
64. Ober, R. J., C. G. Radu, V. Ghetie, and E. S. Ward. 2001. Differences in promiscuity for antibody-FcRn interactions across species: implications for therapeutic antibodies. *Int.Immunol.* 13:1551-1559.
65. Fassler, R., K. Martin, E. Forsberg, T. Litzemberger, and A. Iglesias. 1995. Knockout mice: how to make them and why. The immunological approach. *Int.Arch.Allergy.Immunol.* 106:323-334.
66. Litzemberger, T., H. Bluthmann, P. Morales, D. Pham-Dinh, A. Dautigny, H. Wekerle, and A. Iglesias. 2000. Development of myelin oligodendrocyte glycoprotein autoreactive transgenic B lymphocytes: receptor editing in vivo after encounter of a self-antigen distinct from myelin oligodendrocyte glycoprotein. *J.Immunol.* 165:5360-5366.
67. Maldonado-Lopez, R., T. De Smedt, B. Pajak, C. Heirman, K. Thielemans, O. Leo, J. Urbain, C. R. Maliszewski, and M. Moser. 1999. Role of CD8alpha+ and CD8alpha-dendritic cells in the induction of primary immune responses in vivo. *J.Leukoc.Biol.* 66:242-246.
68. Maldonado-Lopez, R., T. De Smedt, P. Michel, J. Godfroid, B. Pajak, C. Heirman, K. Thielemans, O. Leo, J. Urbain, and M. Moser. 1999. CD8alpha+ and CD8alpha-subclasses of dendritic cells direct the development of distinct T helper cells in vivo. *J.Exp.Med.* 189:587-592.

69. Iglesias, A., J. Bauer, T. Litzemberger, A. Schubart, and C. Linington. 2001. T- and B-cell responses to myelin oligodendrocyte glycoprotein in experimental autoimmune encephalomyelitis and multiple sclerosis. *Glia*. 36:220-234.
70. Amor, S., N. Groome, C. Linington, M. M. Morris, K. Dornmair, M. V. Gardinier, J. M. Matthieu, and D. Baker. 1994. Identification of epitopes of myelin oligodendrocyte glycoprotein for the induction of experimental allergic encephalomyelitis in SJL and Biozzi AB/H mice. *J.Immunol.* 153:4349-4356.
71. Kalbus, M., B. T. Fleckenstein, M. Offenhausser, M. Bluggel, A. Melms, H. E. Meyer, H. G. Rammensee, R. Martin, G. Jung, and N. Sommer. 2001. Ligand motif of the autoimmune disease-associated mouse MHC class II molecule H2-A(s). *Eur.J.Immunol.* 31:551-562.
72. Karpovsky, B., J. A. Titus, D. A. Stephany, and D. M. Segal. 1984. Production of target-specific effector cells using hetero-cross-linked aggregates containing anti-target cell and anti-Fc gamma receptor antibodies. *J.Exp.Med.* 160:1686-1701.
73. Staerz, U. D. and M. J. Bevan. 1985. Cytotoxic T lymphocyte-mediated lysis via the Fc receptor of target cells. *Eur.J.Immunol.* 15:1172-1177.
74. Staerz, U. D., O. Kanagawa, and M. J. Bevan. 1985. Hybrid antibodies can target sites for attack by T cells. *Nature*. 314:628-631.
75. Valerius, T., B. Stockmeyer, A. B. van Spriel, R. F. Graziano, van den Herik-Oudijk IE, R. Repp, Y. M. Deo, J. Lund, J. R. Kalden, M. Gramatzki, and J. G. van De



- Winkel. 1997. Fc $\alpha$ RI (CD89) as a novel trigger molecule for bispecific antibody therapy. *Blood*. 90:4485-4492.
76. Segal, D. M., G. J. Weiner, and L. M. Weiner. 1999. Bispecific antibodies in cancer therapy. *Curr.Opin.Immunol*. 11:558-562.
77. Withoff, S., W. Helfrich, L. F. de Leij, and G. Molema. 2001. Bi-specific antibody therapy for the treatment of cancer. *Curr.Opin.Mol.Ther*. 3:53-62.
78. Todorovska, A., R. C. Roovers, O. Dolezal, A. A. Kortt, H. R. Hoogenboom, and P. J. Hudson. 2001. Design and application of diabodies, triabodies and tetrabodies for cancer targeting. *J.Immunol.Methods*. 248:47-66.
79. Weiner, L. M. 2000. Bispecific antibodies in cancer therapy. *Cancer.J.Sci.Am*. 6 Suppl 3:S265-71.:S265-S271.
80. de Leij, L., G. Molema, W. Helfrich, and B. J. Kroesen. 1998. Bispecific antibodies for treatment of cancer in experimental animal models and man. *Adv.Drug.Deliv.Rev*. 31:105-129.
81. Wang, H., Y. Liu, L. Wei, and Y. Guo. 2000. Bi-specific antibodies in cancer therapy. *Adv.Exp.Med.Biol*. 465:369-80.:369-380.
82. Koelemij, R., P. J. Kuppen, C. J. van de Velde, G. J. Fleuren, M. Hagens, and A. M. Eggermont. 1999. Bispecific antibodies in cancer therapy, from the laboratory to the clinic. *J.Immunother*. 22:514-524.

83. de Gast, G. C., J. G. van De Winkel, and B. E. Bast. 1997. Clinical perspectives of bispecific antibodies in cancer. *Cancer.Immunol.Immunother.* 45:121-123.
84. van Spriël, A. B., H. H. van Ojik, and J. G. van De Winkel. 2000. Immunotherapeutic perspective for bispecific antibodies. *Immunol.Today.* 21:391-397.
85. De Jonge, J., C. Heirman, M. de Veerman, S. Van Meirvenne, M. Moser, O. Leo, and K. Thielemans. 1998. In vivo retargeting of T cell effector function by recombinant bispecific single chain Fv (anti-CD3 x anti-idiotypic) induces long-term survival in the murine BCL1 lymphoma model. *J.Immunol.* 161:1454-1461.
86. Cochlovius, B., S. M. Kipriyanov, M. J. Stassar, J. Schuhmacher, A. Benner, G. Moldenhauer, and M. Little. 2000. Cure of Burkitt's lymphoma in severe combined immunodeficiency mice by T cells, tetravalent CD3 x CD19 tandem diabody, and CD28 costimulation. *Cancer.Res.* 60:4336-4341.
87. Cochlovius, B., S. M. Kipriyanov, M. J. Stassar, O. Christ, J. Schuhmacher, G. Strauss, G. Moldenhauer, and M. Little. 2000. Treatment of human B cell lymphoma xenografts with a CD3 x CD19 diabody and T cells. *J.Immunol.* 165:888-895.
88. Kipriyanov, S. M., G. Moldenhauer, J. Schuhmacher, B. Cochlovius, C. W. der Lieth, E. R. Matys, and M. Little. 1999. Bispecific tandem diabody for tumor therapy with improved antigen binding and pharmacokinetics. *J.Mol.Biol.* 293:41-56.
89. Keck, P. C. and J. S. Huston. 1996. Symmetry of Fv architecture is conducive to grafting a second antibody binding site in the Fv region. *Biophys.J.* 71:2002-2011.

90. Mack, M., G. Riethmuller, and P. Kufer. 1995. A small bispecific antibody construct expressed as a functional single-chain molecule with high tumor cell cytotoxicity. *Proc.Natl.Acad.Sci.U.S.A.* 92:7021-7025.
91. Goldstein, J., R. F. Graziano, K. Sundarapandiyam, C. Somasundaram, and Y. M. Deo. 1997. Cytolytic and cytostatic properties of an anti-human Fc gammaRI (CD64) x epidermal growth factor bispecific fusion protein. *J.Immunol.* 158:872-879.
92. Graziano, R. F., J. Goldstein, K. Sundarapandiyam, C. Somasundaram, T. Keler, and Y. M. Deo. 1997. Targeting tumor cell destruction with CD64-directed bispecific fusion proteins. *Cancer.Immunol.Immunother.* 45:124-127.
93. Kreitman, R. J. 1999. Immunotoxins in cancer therapy. *Curr.Opin.Immunol.* 11:570-578.
94. Vallera, D. A., S. Y. Seo, A. Panoskaltis-Mortari, J. D. Griffin, and B. R. Blazar. 1999. Targeting myeloid leukemia with a DT(390)-mIL-3 fusion immunotoxin: ex vivo and in vivo studies in mice. *Protein.Eng.* 12:779-785.
95. Litzemberger, T., R. Fassler, J. Bauer, H. Lassmann, C. Linington, H. Wekerle, and A. Iglesias. 1998. B lymphocytes producing demyelinating autoantibodies: development and function in gene-targeted transgenic mice. *J.Exp.Med.* 188:169-180.
96. Wines, B. D., M. S. Powell, P. W. Parren, N. Barnes, and P. M. Hogarth. 2000. The IgG Fc contains distinct Fc receptor (FcR) binding sites: the leukocyte receptors Fc gamma RI and Fc gamma RIIa bind to a region in the Fc distinct from that recognized by neonatal FcR and protein A. *J.Immunol.* 164:5313-5318.

97. Williams, T. E., S. Nagarajan, P. Selvaraj, and C. Zhu. 2000. Concurrent and independent binding of Fc $\gamma$  receptors IIa and IIIb to surface-bound IgG. *Biophys.J.* 79:1867-1875.
98. Williams, T. E., P. Selvaraj, and C. Zhu. 2000. Concurrent binding to multiple ligands: kinetic rates of CD16b for membrane-bound IgG1 and IgG2. *Biophys.J.* 79:1858-1866.
99. Shields, R. L., A. K. Namenuk, K. Hong, Y. G. Meng, J. Rae, J. Briggs, D. Xie, J. Lai, A. Stadlen, B. Li, J. A. Fox, and L. G. Presta. 2001. High resolution mapping of the binding site on human IgG1 for Fc $\gamma$  RI, Fc $\gamma$  RII, Fc $\gamma$  RIII, and FcRn and design of IgG1 variants with improved binding to the Fc $\gamma$  R. *J.Biol.Chem.* 276:6591-6604.
100. Ghetie, V. and E. S. Ward. 2000. Multiple roles for the major histocompatibility complex class I-related receptor FcRn. *Annu.Rev.Immunol.* 18:739-66.:739-766.
101. Medesan, C., P. Cianga, M. Mummert, D. Stanescu, V. Ghetie, and E. S. Ward. 1998. Comparative studies of rat IgG to further delineate the Fc:FcRn interaction site. *Eur.J.Immunol.* 28:2092-2100.
102. Gergely, J. and G. Sarmay. 1990. The two binding-site models of human IgG binding Fc $\gamma$  receptors. *FASEB.J.* 4:3275-3283.
103. Jefferis, R., J. Lund, and J. D. Pound. 1998. IgG-Fc-mediated effector functions: molecular definition of interaction sites for effector ligands and the role of glycosylation. *Immunol.Rev.* 163:59-76.:59-76.

104. Link, H., O. Olsson, J. Sun, W. Z. Wang, G. Andersson, H. P. Ekre, T. Brenner, O. Abramsky, and T. Olsson. 1991. Acetylcholine receptor-reactive T and B cells in myasthenia gravis and controls. *J.Clin.Invest.* 87:2191-2195.
105. Stanley, J. R. 1997. Update: structure and function of pemphigus vulgaris antigen. *J.Dermatol.* 24:741-743.
106. Hjelmstrom, P., A. E. Juedes, J. Fjell, and N. H. Ruddle. 1998. B-cell-deficient mice develop experimental allergic encephalomyelitis with demyelination after myelin oligodendrocyte glycoprotein sensitization. *J.Immunol.* 161:4480-4483.
107. Dittel, B. N., T. H. Urbania, and C. A. Janeway, Jr. 2000. Relapsing and remitting experimental autoimmune encephalomyelitis in B cell deficient mice. *J.Autoimmun.* 14:311-318.
108. Genain, C. P., K. Abel, N. Belmar, F. Villinger, D. P. Rosenberg, C. Linington, C. S. Raine, and S. L. Hauser. 1996. Late complications of immune deviation therapy in a nonhuman primate. *Science.* %20;274:2054-2057.
109. Amagai, M. 1999. Autoimmunity against desmosomal cadherins in pemphigus. *J.Dermatol.Sci.* 20:92-102.
110. Zisman, E., Y. Katz-Levy, M. Dayan, S. L. Kirshner, M. Paas-Rozner, A. Karni, O. Abramsky, C. Brautbar, M. Fridkin, M. Sela, and E. Mozes. 1996. Peptide analogs to pathogenic epitopes of the human acetylcholine receptor alpha ásubunit as potential modulators of myasthenia gravis. *PNAS* 93:4492-4497.

111. Merchant, A. M., Z. Zhu, J. Q. Yuan, A. Goddard, C. W. Adams, L. G. Presta, and P. Carter. 1998. An efficient route to human bispecific IgG. *Nat.Biotechnol.* 16:677-681.
112. Fuchs, S. 1979. Immunology of the nicotinic acetylcholine receptor. *Curr.Top.Microbiol.Immunol.* 85:1-29.:1-29.
113. Drachman, D. B. 1996. Immunotherapy in neuromuscular disorders: current and future strategies. *Muscle.Nerve.* 19:1239-1251.
114. Drachman, D. B., S. Okumura, R. N. Adams, and K. R. McIntosh. 1996. Oral tolerance in myasthenia gravis. *Ann.N.Y.Acad.Sci.* 778:258-72.:258-272.
115. Manfredi, A. A., M. P. Protti, M. W. Dalton, J. F. Howard, Jr., and B. M. Conti-Tronconi. 1993. T helper cell recognition of muscle acetylcholine receptor in myasthenia gravis. Epitopes on the gamma and delta subunits. *J.Clin.Invest.* 92:1055-1067.
116. Moiola, L., M. P. Protti, A. A. Manfredi, M. H. Yuen, J. F. Howard, Jr., and B. M. Conti-Tronconi. 1993. T-helper epitopes on human nicotinic acetylcholine receptor in myasthenia gravis. *Ann.N.Y.Acad.Sci.* 681:198-218.:198-218.
117. Protti, M. P., A. A. Manfredi, R. M. Horton, M. Bellone, and B. M. Conti-Tronconi. 1993. Myasthenia gravis: recognition of a human autoantigen at the molecular level. *Immunol.Today.* 14:363-368.

118. Hawke, S., H. Matsuo, M. Nicolle, G. Malcherek, A. Melms, and N. Willcox. 1996. Autoimmune T cells in myasthenia gravis: heterogeneity and potential for specific immunotargeting. *Immunol.Today*. 17:307-311.
119. Tzartos, S. J., M. E. Seybold, and J. M. Lindstrom. 1982. Specificities of antibodies to acetylcholine receptors in sera from myasthenia gravis patients measured by monoclonal antibodies. *Proc.Natl.Acad.Sci.U.S.A.* 79:188-192.
120. Barchan, D., M. C. Souroujon, S. H. Im, C. Antozzi, and S. Fuchs. 1999. Antigen-specific modulation of experimental myasthenia gravis: nasal tolerization with recombinant fragments of the human acetylcholine receptor alpha-subunit. *Proc.Natl.Acad.Sci.U.S.A.* 96:8086-8091.
121. Im, S. H., D. Barchan, S. Fuchs, and M. C. Souroujon. 1999. Suppression of ongoing experimental myasthenia by oral treatment with an acetylcholine receptor recombinant fragment. *J.Clin.Invest.* 104:1723-1730.
122. Barchan, D., O. Asher, S. J. Tzartos, S. Fuchs, and M. C. Souroujon. 1998. Modulation of the anti-acetylcholine receptor response and experimental autoimmune myasthenia gravis by recombinant fragments of the acetylcholine receptor. *Eur.J.Immunol.* 28:616-624.
123. Souroujon, M. C., D. Barchan, and S. Fuchs. 1998. Modulation of experimental autoimmune myasthenia gravis by recombinant fragments of the human acetylcholine receptor. *Ann.N.Y.Acad.Sci.* 841:572-5.:572-575.





## 11. Curriculum vitae

S. Marcel Zocher, geboren am 21. Januar 1974 in Korbach, Deutschland

Universität Tübingen und Micromet AG, Martinsried

Nov. 1999 bis Juni 2002

*Promotionsarbeit*

angefertigt am Max-Planck-Institut für Neurobiologie und in der Micromet AG

Betreuer: Prof. Patrick A. Baeuerle

Betreuer an der Universität Tübingen: Prof. Hans-Georg Rammensee

Universität Freiburg und MPI für Immunbiologie, Deutschland

1994 bis Okt. 1999

*Diplom in Biologie (Hauptfach: Molekulare Immunologie)*

Foothill College, Los Altos Hills, California, USA

Jan. 1992 - Dez. 1993

*Associate in Science Degree (A.S.) mit Auszeichnung (Honors). Hauptfach: Physik*

Mountain View High School, California, USA

Feb. 1991 - Jan. 1992

Andreae - Gymnasium, Herrenberg, Germany

1984 - 1991

Im Selbstverlag herausgegeben von:

Zoher, Marcel

Ludwigstr. 2

82110 Germering

